Quantum-corrected rotating black holes and naked singularities in (2 + 1) dimensions

Marc Casals,[1,2,*] Alessandro Fabbri,[3,†] Cristián Martínez,[4,‡] and Jorge Zanelli[4,§]

[1]Centro Brasileiro de Pesquisas Físicas (CBPF), Rio de Janeiro, CEP 22290-180, Brazil
[2]School of Mathematics and Statistics, University College Dublin, Belfield, Dublin 4, Ireland
[3]Departamento de Física Teórica and IFIC, Universidad de Valencia-CSIC, C. Dr. Moliner 50, 46100 Burjassot, Spain
[4]Centro de Estudios Científicos (CECs), Arturo Prat 514, Valdivia 5110466, Chile

(Received 15 February 2019; published 13 May 2019)

We analytically investigate the perturbative effects of a quantum conformally coupled scalar field on rotating (2 + 1)-dimensional black holes and naked singularities. In both cases we obtain the quantum-backreacted metric analytically. In the black hole case, we explore the quantum corrections on different regions of relevance for a rotating black hole geometry. We find that the quantum effects lead to a growth of both the event horizon and the ergosphere, as well as to a reduction of the angular velocity compared to their corresponding unperturbed values. Quantum corrections also give rise to the formation of a curvature singularity at the Cauchy horizon and show no evidence of the appearance of a superradiant instability. In the naked singularity case, quantum effects lead to the formation of a horizon that hides the conical defect, thus turning it into a black hole. The fact that these effects occur not only for static but also for spinning geometries makes a strong case for the role of quantum mechanics as a cosmic censor in Nature.

DOI: 10.1103/PhysRevD.99.104023

I. INTRODUCTION

The quantum regime of gravitation has been one of the outstanding conundrums of theoretical physics for almost a century. Even the perturbative semiclassical framework, where the matter fields are quantized while the quantum nature of a background geometry is ignored, is a difficult problem, both technically and conceptually. Yet, important results have been shown within the semiclassical framework. For example, in the presence of a black hole (BH), it has been shown that quantum effects give rise to Hawking radiation [1]. Such a semiclassical framework is possibly a good approximation for astronomical BHs, but probably too crude for a microscopic BH near the end of the evaporation process.

In this paper we focus in particular on a different question of interest within the semiclassical framework: the fate of timelike singularities as solutions of the classical Einstein field equations when quantum matter effects are taken into account. Timelike space-time singularities appear in various settings. For example, rotating BHs possess a hypersurface, called the Cauchy horizon, inside the event horizon, beyond which there is a timelike singularity. Such a singularity, while not visible to observers outside the black hole, may be visible to observers that fall inside the BH. This can be seen in Fig. 1(b), where $r = 0$, r_- and r_+ are the radii of, respectively, the singularity, Cauchy horizon and event horizon. Nonrotating but electrically charged black hole solutions also possess a Cauchy horizon with a timelike singularity lying beyond it. Another example is that of space-time solutions (rotating or not) possessing timelike singularities but no event horizon; such "naked" singularities (NSs) would thus be visible even to far-away observers.

The presence of a generic (timelike) singularity is an undesirable feature from a physical point of view, since it signifies the breakdown of predictability: Cauchy data on an initial hypersurface does not have a unique evolution; heuristically: we do not know what may "come out" of such a singularity. Therefore, Penrose formulated a cosmic censorship hypothesis (CCH)[2]. The weak version of CCH [3,4] essentially states that if a singularity forms from the gravitational collapse of matter, then it will be surrounded by an event horizon—thus, it will not be visible to far-away observers. In its turn, the strong version of CCH [5] essentially states that if a singularity forms from the gravitational collapse of matter, then it will generically be spacelike or null (not timelike)—thus, the singularity will

*mcasals@cbpf.br,marc.casals@ucd.ie
†afabbri@ific.uv.es
‡martinez@cecs.cl
§z@cecs.cl

not be visible to any observers at all (although they may crash into it).

Given that there exist exact space-time solutions of the classical Einstein equations which contain timelike singularities, it is important to investigate whether they *generically* form under gravitational collapse. Investigating whether singularities are stable under field perturbations will help ascertain whether they are generic singularities or not.

In $(3+1)$-dimensions, it has been shown that classical field perturbations lead to a curvature (nontimelike) singularity at the Cauchy horizon in the case of spherically symmetric and electrically charged (Reissner-Nordström) BHs, with [6,7] or without [8–11] a positive cosmological constant, as well as in the case of rotating (Kerr) BHs [12,13]. These results are in support of strong CCH.[1] In space-times with a number of dimensions other than four, on the other hand, violation of strong CCH has been found in, e.g., [14,15], as due to the Gregory-Laflamme instability [16].

As for weak CCH, recent work [17] has shown that a Kerr BH or a Kerr-Newman (i.e., electrically-charged Kerr) BH cannot be turned into a NS by throwing matter into it, as long as its stress-energy tensor satisfies the null energy condition. However, in the specific case of $(3+1)$-D anti–de Sitter (AdS) space-time (i.e., a Universe with a negative cosmological constant), Ref. [18] has shown that weak CCH may be violated.

The above examples deal with the *classical* stability of space-times possessing timelike singularities. It is also important to investigate their stability properties under *quantum* field perturbations. This can be achieved via the semiclassical Einstein equations, in which the classical stress energy tensor is supplemented with the renormalized expectation value of the quantum stress-energy tensor (RSET) calculated on a fixed, classical background space-time.

In the quantum case, the results for timelike singularities in $(3+1)$-dimensions are very scarce. One of the very few results is the argument in [19–21] that the RSET calculated on Reissner-Nordström or Kerr(-Newman) background space-time diverges on (at least a part of) the CH; there is also the recent [22], which contains an exact calculation of the renormalized expectation value of the square of the field on the Cauchy horizon of Reissner-Nordström and is found to be regular there, while the trace of the RSET diverges. We note, however, that the RSET was not obtained explicitly in these works and, therefore, the space-time resulting from the quantum perturbations of the Reissner-Nordström or Kerr(-Newman) background could not be obtained. In order to understand the full structure of the backreacted space-time, resulting from quantum field perturbations, one should solve the semiclassical Einstein equations. To the best of our knowledge, this has not been achieved exactly[2] for any $(3+1)$-D BH space-time. There already exist some works in the literature where the quantum-backreacted metric has been obtained in $(1+1)$-dimensions (see e.g., [24] and references therein) as well as in $(2+1)$-dimensions. We next review quantum-backreaction results on a specific $(2+1)$-D case: the so-called Bañados-Teitelboim-Zanelli (BTZ) geometries, which include both BHs [25,26] and NSs [27].

Semiclassical backreaction on *static* BTZ space-times has been studied in the following works. References [28,29] showed that the horizon of a static BTZ BH is "pushed out" due to backreaction and that a curvature singularity forms at the center of the BH (although this region where the curvature singularity forms is in principle beyond the regime of validity of the semiclassical approximation). Also in the case of a static BTZ BH, [30] found that the contribution of the backreaction to the gravitational force on a static particle may be positive or negative depending on the radius.

These works are for the case that the background space-time is that of a static BTZ BH, which does not possess a timelike singularity. In the case of a static (timelike) BTZ NS, we showed in [31] that backreaction creates an event horizon and forms a curvature singularity at its center (although, again, this region inside the BH in principle lies beyond the regime of validity of the semiclassical approximation).

In the important case of nonzero rotation, to the best of our knowledge, the only work up until recently which aimed at investigating quantum-backreaction was that of Steif in [32]. Steif found that, in the case of a rotating BTZ BH, the RSET diverges as the inner horizon is approached from its inside. In the paper [33] we went further and we presented results for the backreacted metric, both in the case of a rotating BTZ BH and a rotating BTZ NS. In this paper we provide the full details of the calculation presented in [33]. We analytically obtain the quantum-backreacted metric everywhere for these two background space-times. This enables us to thoroughly study the effect of quantum corrections on rotating geometries describing both BHs and naked conical singularities in $2+1$ dimensions. In particular, we study the quantum stability of such space-times in relation to CCH. We also investigate the effects of quantum backreaction on other interesting regions of the space-times. For example, in the case of the rotating BH space-time, we determine the quantum backreaction on the event horizon and on the ergosphere (region outside the rotating horizon where observers cannot remain static). Our results show that, in the BH case, the event horizon is pushed out (as in the static case) and the

[1]There are different versions of strong CCH. These results are in support of some version or other of strong CCH: they show varying degrees of "irregularity" of the field perturbation on the Cauchy horizon depending on the specific physical setting, while the C^0 character is preserved in all settings studied.

[2]See [23], where an *approximation* for the RSET was used in $(3+1)$-D Schwarzschild space-time.

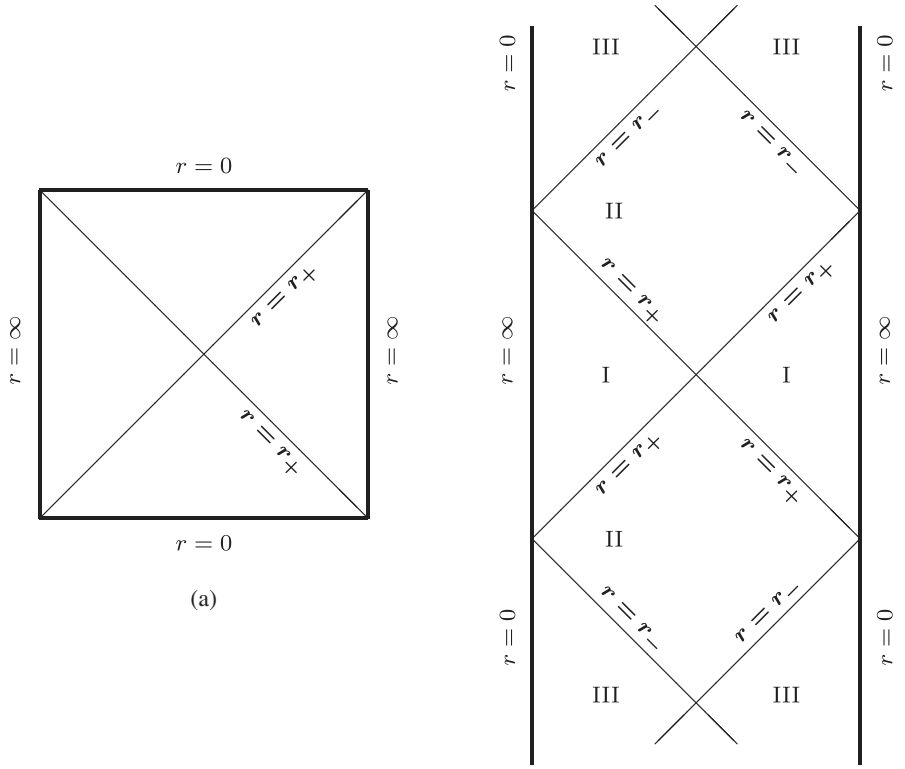

FIG. 1. Penrose diagrams for BTZ black holes: static black hole in panel (a) and rotating, nonextremal black hole in panel (b).

inner horizon develops a *curvature* singularity. This singularity in the backreacted spacetime may be spacelike or timelike, depending on the values of the mass and angular momentum of the black hole; when it is spacelike, strong CCH is enforced. In the NS case, we find that an event horizon forms and shields the singularity, which becomes a spacelike curvature singularity (as in the static case of [31]). Quantum effects on the NS thus act to enforce strong CCH.

There is an issue worth mentioning regarding our space-time setting and evolution of initial data. Our BTZ geometries are asymptotically AdS. Therefore, they are not globally-hyperbolic and the Cauchy value problem is, in principle, not well posed. It is known, however, that this issue may be resolved by imposing specific boundary conditions for the matter field on the AdS boundary [34]—see $r = \infty$ in Fig. 1. We specifically impose the so-called transparent boundary conditions [34] on the AdS boundary. Furthermore, we are dealing with regions of space-time which possess a timelike singularity. This is true, of course, for the NS case, but also for the region inside the Cauchy horizon of the rotating BH case (which is the region that we need to deal with in order to find the instability of the Cauchy horizon). Similarly to the AdS boundary, the field effectively satisfies some specific boundary conditions on the timelike singularity, so that unique evolution of initial data is restored.

Another point worth mentioning is that the singularity on the Cauchy horizon that we find appears in the limit as we approach the Cauchy horizon from its *inside*. However, as opposed to Kerr, in the rotating BTZ geometry there exist no closed timelike curves. Therefore, we are not faced with the issues that such curves cause in relation to the initial value problem in the region inside the Cauchy horizon in Kerr.

An important point of our results is that they show that the quantum effects on black holes and naked singularities found in the static case [28,29,31] are rather generic. They do not require the geometry to be static, but they are also present in many of the spinning cases.

Finally, we note that, since three-dimensional gravity has no local dynamical degrees of freedom (d.o.f.), the quantum effects can only be due to the quantized matter source, which in our case is provided by a (conformally coupled[3]) scalar field. As mentioned, the quantum fluctuations of the scalar field vacuum on a fixed background geometry give rise to a RSET which is of $O(\hbar)$ and acts as a source of Einstein's equations. These corrected equations give rise to a one-loop correction on the geometry (backreaction). In principle, one could go on to compute the second order correction to the RSET by recalculating it, this time, on the backreacted geometry. However, those would in principle

[3]The choice of conformal coupling is motivated by simplicity: because AdS space-time is conformal to Minkowski space-time, the quantum propagator in AdS is then obtained directly from its expression in flat space-time.

be corrections of $O(\hbar^2)$ and we choose not to continue in this direction.

The paper is organized as follows. In Sec. II we review the classical rotating BTZ geometries, both for black holes and for naked singularities. In that section we also review an exact black hole solution of the Einstein equations with a source given by a particular classical scalar field configuration. In Sec. III we consider a quantum scalar field on a rotating BTZ geometry and calculate the two-point function and the RSET. We analytically solve the semiclassical Einstein equations in Sec. IV. We analyze in depth the physical features of these quantum-backreacted geometries in Sec. V. We finish the main body of the paper with a discussion in Sec. VI, where we summarize our results and point to open questions. After the main body there are three Appendixes: in Appendix A we present the background BTZ geometries as the result of identifying points in the embedding space $\mathbb{R}^{2,2}$; in Appendix B we review the two-point function in (the covering space of) AdS_3; in the last Appendix C, we (re)derive the two-point function in a static naked singularity space-time via the alternative method of mode sums.

We use units such that the cosmological constant is $\Lambda = -\ell^{-2}$ and the Planck length is $l_P = \hbar\kappa/(8\pi)$, where ℓ is the radius of curvature and κ is the $(2+1)$-dimensional gravitational constant. We choose metric signature $(-++)$.

II. REVIEW OF BTZ GEOMETRIES: BLACK HOLES AND CONICAL SINGULARITIES

Three-dimensional BTZ BH and NS space-times are exact solutions of the vacuum Einstein field equations with a negative cosmological constant "$-\ell^{-2}$", described by the line element

$$ds^2 = \left(M - \frac{r^2}{\ell^2}\right)dt^2 - Jdtd\theta + \left(\frac{r^2}{\ell^2} - M + \frac{J^2}{4r^2}\right)^{-1} dr^2 + r^2 d\theta^2, \tag{2.1}$$

where $-\infty < t < +\infty$, $0 < r < \infty$, $0 \le \theta < 2\pi$ (periodic). The constants M and J are, respectively, the mass[4] and angular momentum of these space-times. In this section we review in some detail these classical solutions. For further details, we refer the reader to the original papers [25,26] in the BH case, and [27] in the NS case.

A. Black hole

The metric (2.1) describes a spinning black hole provided $M\ell \ge |J| > 0$. In this case, the space-time possesses a Cauchy horizon at $r = r_- > 0$ and an event horizon at $r = r_+ \ge r_-$, where

$$r_\pm \equiv \frac{\ell|\alpha_\pm|}{2}, \qquad \alpha_\pm \equiv \sqrt{M + \frac{J}{\ell}} \pm \sqrt{M - \frac{J}{\ell}}. \tag{2.2}$$

Note that

$$M = \frac{\alpha_+^2 + \alpha_-^2}{4} > 0 \quad \text{and} \quad J = \frac{\ell\alpha_+\alpha_-}{2}, \tag{2.3}$$

with $\alpha_+ > 0$, $\alpha_+ \ge \alpha_-$, and $\alpha_+^2 - \alpha_-^2 = 4\sqrt{M^2 - J^2/\ell^2}$. The static BH is obtained for $J = 0$, where $\alpha_+ = 2\sqrt{M} > 0$, $\alpha_- = 0$, and there is no Cauchy horizon.

The coordinates in Eq. (2.1) do not cover the maximal analytical extension of the rotating BTZ BH space-time. The maximal analytical extension is represented in Fig. 1 by means of a Carter-Penrose diagram.

Clearly, the extremal (i.e., maximally rotating) BH corresponds to $M\ell = |J|$. See Eq. (A2) for an expression of the subextremal line-element (2.1) in terms of $\alpha_\pm$ and Eq. (A12) for the line-element for the extremal BTZ BH.

The inner horizon is classically unstable [35,36] in a similar manner to that of Kerr or Reissner-Nordström space-times [11,13,37]. Unlike the $(3+1)$-D Kerr geometry, however, the $(2+1)$-D BH possesses no curvature singularities—instead, it possesses a *causal* singularity at $r = 0$[5]: there exist inextendible incomplete geodesics that hit $r = 0$ [25,26]. Like the singularity in Kerr, the singularity of the BTZ BH is timelike. The past boundary of the causal future of the timelike singularity is the (future) Cauchy horizon. The name of "Cauchy" given to this horizon is because the Cauchy problem the[6] is not well-posed to its future. In Kerr, the situation is even worse since there exist closed timelike curves near its singularity [38]. In the rotating BTZ space-time, on the other hand, there exist no closed timelike curves *by construction* of the space-time.

Conformal infinity $\mathcal{I}$ for null geodesics corresponds to the so-called AdS boundary at $r = \infty$. This boundary is a *timelike* hypersurface and so the space-time is not globally hyperbolic. Figure 1 shows the causal structure that gives the defining characters to the event and Cauchy horizons, as well as to the AdS boundary.

The metric in Eq. (2.1) is stationary and axially symmetric, with associated Killing vectors $\partial/\partial t$ and $\partial/\partial\theta$, respectively. The Killing vector $\partial/\partial t$ is timelike for $r > r_{\rm SL} \equiv \sqrt{M}\ell$, it is null at $r = r_{\rm SL}$ and it is spacelike for $r_+ < r < r_{\rm SL}$. This means that no static observers can lie in the region $r < r_{\rm SL}$. The hypersurface $r = r_{\rm SL}$ is called

[4]The Hamiltonian mass and angular momentum of the BTZ space-time are, in fact, $M\pi/\kappa$ and $J\pi/\kappa$, respectively, but we shall just refer to M and J as the mass and angular momentum.

[5]In a slight abuse of language, we refer to $r = 0$ although, this singularity is, strictly speaking, not a point of the space-time.

[6]The Cauchy problem is the initial value problem when the field data is given on a certain constant-coordinate hypersurface.

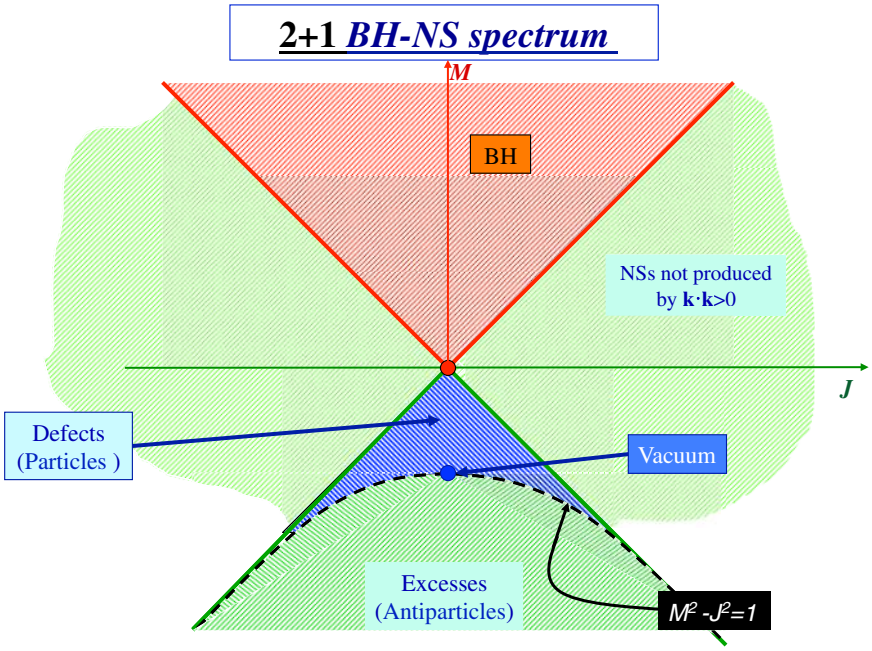

FIG. 2. Schematic representation of BTZ black hole and naked singularity states for different values of M and J.

the static limit surface and the region $r \in (r_+, r_{\rm SL})$ is called the ergosphere. The existence of an ergosphere allows for the Penrose process, whereby particles (only massless ones in the BTZ case) can extract rotational energy from the BH (see [3] in Kerr and [39] in rotating BTZ). The ergosphere also allows for the wave-equivalent of the Penrose process, the so-called phenomenon of superradiance, whereby boson field waves can extract rotational energy from the BH. For superradiance, see [40,41] in Kerr and [42] in asymptotically-AdS Kerr. In BTZ, on the other hand, a massless scalar field obeying Dirichlet boundary conditions does not exhibit superradiance [43], although the specific case of a massive scalar field obeying certain Robin boundary conditions does exhibit superradiance [44].

In its turn, the Killing vector $\chi \equiv \partial/\partial t + \Omega\partial/\partial\theta$, where $\Omega \equiv J/(2r_+^2)$ is the angular velocity of the event horizon, is the generator of the event horizon. The vector χ is null at the event horizon and, in the nonextremal case, it is timelike for $r > r_+$. This means that, in the nonextremal case, timelike observers that rigidly rotate at the angular velocity of the BH can lie anywhere outside the event horizon, i.e., there is no speed-of-light surface as in Kerr. In the extremal case, on the other hand, the Killing vector χ is null everywhere.

Spinning BHs can also be obtained by boosting a static BH of a given mass M_0, yielding a new BH state of mass M and angular momentum J, with

$$M = \frac{M_0(1+\omega^2)}{(1-\omega^2)}, \qquad J = \frac{2\omega M_0 \ell}{(1-\omega^2)}, \tag{2.4}$$

where ω is the boost parameter in the Lorentz transformation and it satisfies $|\omega| < 1$. In this way, all BH states with M and J lying on the hyperbola $M^2 - J^2/\ell^2 =$ const on the M-J plane—see Fig. 2—are connected by boosts [45].

B. Naked singularity

If the mass in the BTZ metric (2.1) is continued to negative values, the geometry then becomes a conical NS (there is a curvature singularity at $r = 0$) [27], with the single exception of nonrotating AdS_3 space-time ($M = -1, J = 0$). For $-M\ell > |J|$, we define

$$\beta_\pm \equiv \sqrt{-M + J/\ell} \pm \sqrt{-M - J/\ell} \in \mathbb{R}, \tag{2.5}$$

so that

$$M = -\frac{\beta_+^2 + \beta_-^2}{4} < 0 \quad \text{and} \quad J = \frac{\ell\beta_+\beta_-}{2}, \tag{2.6}$$

with $\beta_+ \geq |\beta_-| \geq 0$ and $\beta_+^2 - \beta_-^2 = 4\sqrt{M^2 - J^2/\ell^2}$.

It follows from the line element (2.1) [see Eq. (A21) for the NS line element in terms of $\beta_\pm$] with mass $M < 0$ that its metric components are well-defined everywhere for $r \neq 0$, which means that there is no horizon and it therefore describes a NS. Its conformal structure at infinity is as in the BH case and so it also possesses a (timelike) AdS boundary at $r = \infty$.

The spinless (i.e., $J = 0$) states in the range $-1 < M < 0$ correspond to conical space-times with angular defects $\Delta = 2\pi(1 - \sqrt{-M})$ (particles), while those with $M < -1$ are conical excesses (antiparticles). The dividing case, $M = -1$, corresponds to AdS_3 vacuum space-time.

TABLE I. Identification vector $\mathbf{k}$ for the nonextremal ($M^2\ell^2 > J^2$) and extremal ($M^2\ell^2 = J^2$) BH and NS geometries in terms of the $so(2,2)$ generators J_{ab} (see Appendix A).

	$M^2\ell^2 > J^2$	$M^2\ell^2 = J^2$	Type of Killing vector $\mathbf{k}$
$M > 0$	$\frac{1}{2}(\alpha_+ J_{01} + \alpha_- J_{23})$	$\alpha(J_{01} + J_{23}) + \frac{1}{2}(J_{02} + J_{03} + J_{12} + J_{13})$	Spacelike, no fixed points
$M < 0$	$\frac{1}{2}(\beta_+ J_{21} + \beta_- J_{30})$	$\beta(J_{03} - J_{12}) - \frac{1}{2}(J_{01} + J_{03} + J_{12} - J_{23})$	Spacelike, $r = 0$ fixed point

The static conical singularities can also be boosted to obtain spinning (anti)particles, in the same manner as for BHs. All of these states are described by the same BTZ metric, Eq. (2.1), with $M\ell \leq -|J|$.

Like the BH metric, the NS metric is also stationary and axially symmetric, with the same associated Killing vectors $\partial/\partial t$ and $\partial/\partial\theta$, respectively. In this geometry, $\partial/\partial t$ is always timelike and there is no ergosphere. The extremal NS case corresponds to maximal rotation, $M\ell = -|J|$, and its metric is given in Eq. (A29).

The spectrum of BHs and NSs can thus be summarized as follows:

$M > 0 \quad \& \quad 0 \leq M^2\ell^2 - J^2 < \infty$: Black holes

$M < 0 \quad \& \quad 0 \leq M^2\ell^2 - J^2 < 1$: Particles

$M < 0 \quad \& \quad J \neq 0 \quad \& \quad 1 = M^2\ell^2 - J^2$: Rotating AdS_3

$M = -1 \quad \& \quad J = 0$: Nonrotating AdS_3(vacuum)

$M < 0 \quad \& \quad 1 < M^2\ell^2 - J^2 < \infty$: Antiparticles

This spectrum is represented schematically in the M-J plane in Fig. 2. The case $M = J = 0$ is known as the "zero-mass black hole" or the maximum-deficit conical singularity.

C. Construction of the classical BTZ geometries

In order to construct the BTZ geometries, we first consider flat $\mathbb{R}^{(2,2)}$ with coordinates X^0, X^1, X^2, $X^3 \in \mathbb{R}$ and metric

$$ds^2 = -(dX^0)^2 + (dX^1)^2 + (dX^2)^2 - (dX^3)^2. \tag{2.7}$$

We can then think of AdS_3 as the pseudosphere

$$-(X^0)^2 + (X^1)^2 + (X^2)^2 - (X^3)^2 = -\ell^2 \tag{2.8}$$

embedded in $\mathbb{R}^{(2,2)}$. However, the topology of AdS_3 is $S^1(\text{time}) \times \mathbb{R}^2(\text{space})$ and so the space-time contains closed timelike curves. The covering of AdS_3, denoted by CAdS_3, is obtained by "unwrapping" the S^1, so that the resulting space-time does not contain closed timelike curves. We can now obtain BHs and NSs in $(2+1)$-dimensions as locally negative constant curvature geometries by identifying points in the covering space CAdS_3, which is represented by its embedding in flat $\mathbb{R}^{2,2}$. The identification is a quotient of CAdS_3 by a Killing vector $\mathbf{k}$ in the algebra $so(2,2)$ of global isometries of the pseudosphere.

In the **BH** case ($M \geq |J| \geq 0$), $\mathbf{k}$ is a Killing vector that acts transitively, that is, leaving no fixed points on CAdS_3. The region where the Killing vector is spacelike ($\mathbf{k}^2 > 0$) is identified as $r > 0$ in the resulting manifold, while the region where $\mathbf{k}$ is timelike ($\mathbf{k}^2 = r^2 < 0$) is removed in order to avoid traversable closed timelike curves [26]. Thus $r = 0$ is a causal singularity. The specific form of $\mathbf{k}$ depends on the mass M and angular momentum J of the BH, with $M \geq |J|/\ell$.

In the **NS** case, the Killing vector for the identification is a spacelike rotation that keeps $r = 0$ fixed. The manifold $\mathrm{CAdS}_3/\mathbf{k}(M,J)$ then has a conical NS at the fixed point of $\mathbf{k}$ (i.e., $r = 0$), where the curvature has a Dirac-δ singularity. The corresponding identification is along the compact coordinate θ.

These identifications can also be expressed as the action of a matrix $H(\mathbf{k})$ that maps every point in $\mathbb{R}^{2,2}$ to its image under $\mathbf{k}$, given in Table I. The identification matrices in $\mathbb{R}^{2,2}$ corresponding to the different BHs and conical singularities are given explicitly in Appendix A.

D. Black hole solutions with a scalar field

We complete the discussion of the classical system by reviewing an exact solution of Einstein equations in the presence of a source given by a massless and conformally-coupled real scalar field ϕ [46]. The action in three space-time dimensions reads

$$I = \int d^3x\sqrt{-g}\left[\frac{R + 2\ell^{-2}}{2\kappa} - \frac{1}{2}g^{\mu\nu}\nabla_\mu\phi\nabla_\nu\phi - \frac{1}{16}R\phi^2\right], \tag{2.9}$$

which provides the following field equations:

$$G_{\mu\nu} - \ell^{-2}g_{\mu\nu} = \kappa T_{\mu\nu}, \qquad \Box\phi - \frac{1}{8}R\phi = 0, \tag{2.10}$$

where the stress-energy tensor is given by

$$T_{\mu\nu} = \nabla_\mu\phi\nabla_\nu\phi - \frac{1}{2}g_{\mu\nu}g^{\alpha\beta}\nabla_\alpha\phi\nabla_\beta\phi + \frac{1}{8}(g_{\mu\nu}\Box - \nabla_\mu\nabla_\nu + G_{\mu\nu})\phi^2. \tag{2.11}$$

It is straightforward to check that this stress-energy tensor is conserved and traceless, which in turn implies that the geometry has a constant Ricci scalar,

$$R = -6\ell^{-2}. \tag{2.12}$$

An exact static, circularly-symmetric solution was found in [46]. Its line element is given by

$$ds^2 = -f(r)dt^2 + f^{-1}(r)dr^2 + r^2 d\theta^2, \tag{2.13}$$

where

$$f(r) \equiv \frac{1}{\ell^2}\left(r^2 - 3C^2 - \frac{2C^3}{r}\right) = \frac{(r+C)^2(r-2C)}{\ell^2 r}, \tag{2.14}$$

is the lapse function, C is an arbitrary integration constant and the corresponding scalar field is given by

$$\phi(r) = \sqrt{\frac{8C}{\kappa(r+C)}}. \tag{2.15}$$

This exact solution describes a BH with an event horizon at $r_+ = 2C$ provided $C > 0$. In that case, the event horizon surrounds a single curvature singularity at $r = 0$, as can be shown by calculating the Kretschmann scalar,

$$R^{\mu\nu\lambda\rho}R_{\mu\nu\lambda\rho} = \frac{12(r^6 + 2C^6)}{\ell^4 r^6}. \tag{2.16}$$

For $C = 0$ the solution reduces to the massless BTZ spacetime with a vanishing scalar field. The on-shell stress-energy tensor is given by

$$T^{\mu}{}_{\nu} = \frac{C^3}{\kappa\ell^2 r^3}\,\mathrm{diag}(1, 1, -2), \tag{2.17}$$

which is consistently traceless. It should be noted that, except for the constant factor $C^3/(\kappa\ell^2)$, the rest in the expression in (2.17) coincides exactly with the renormalized stress-energy tensor (3.43) to be presented in the next section.

III. QUANTUM SCALAR FIELD

The semiclassical Einstein equations are obtained by replacing the classical stress-energy of the matter field(s) by the renormalized expectation value of the quantum stress-energy tensor operator (RSET). In the presence of a cosmological constant $\Lambda = -\ell^{-2}$, the semiclassical Einstein equations are

$$G_{\mu\nu} - \frac{g_{\mu\nu}}{\ell^2} = \kappa\langle\psi|T_{\mu\nu}|\psi\rangle_{\mathrm{ren}}, \tag{3.1}$$

where $\langle\psi|T_{\mu\nu}|\psi\rangle_{\mathrm{ren}}$ is the RSET for a quantum field in a state $|\psi\rangle$. For ease of notation, we henceforth drop the subindex "ren" as well as the symbol for the quantum state in the RSET, and we thus denote it by $\langle T_{\mu\nu}\rangle$.

A. Two-point functions

From now on we shall consider a massless, conformally coupled scalar field ϕ (conformal coupling in three dimensions corresponds to a coupling constant $\xi = 1/8$ [47]). In this case, the (Klein-Gordon) field equation is

$$\left(\Box + \frac{3}{4\ell^2}\right)\phi(x) = 0. \tag{3.2}$$

As opposed to Eq. (2.10), the d'Alembertian $\Box = g^{\mu\nu}\nabla_\mu\nabla_\nu$ here is with respect to a *background* metric $g_{\mu\nu}$ (i.e., it is a solution of the classical *vacuum* Einstein equations) which, in our case, we shall take to be a BTZ geometry.

The RSET for the quantum scalar field ϕ in a state $|\psi\rangle$ is typically constructed from a geometric differential operator acting on the Hadamard elementary two-point function, which is the anticommutator $G^{(1)}(x,x') = \langle\psi|\{\phi(x),\phi(x')\}|\psi\rangle$ [48], where x and x' are space-time points. The anticommutator is related to the Feynman Green function $G_F(x,x')$ and to the Wightman function $G^+(x,x') = \langle\psi|\phi(x)\phi(x')|\psi\rangle$ as [47,49]:

$$G^{(1)}(x,x') = 2\,\mathrm{Im}(G_F(x,x')) = 2\,\mathrm{Re}(G^+(x,x')). \tag{3.3}$$

Clearly from their definitions, both the anticommutator and the Wightman function satisfy (with respect to either x or x') the homogeneous scalar field equation (3.2). In its turn, the Feynman Green function satisfies the Green function equation

$$\left(\Box + \frac{3}{4\ell^2}\right)G_F(x,x') = -\frac{\delta^{(3)}(x-x')}{\sqrt{-g}}, \tag{3.4}$$

where $g \equiv det(g_{\mu\nu})$ and $\delta^{(3)}$ is the Dirac-δ distribution in three dimensions.

1. Locally AdS_3 space-time

In principle, there are two possible approaches to compute the two-point function in the BTZ geometries. The first one is to expand this function in terms of elementary modes of the wave equation (3.2) satisfying appropriate boundary conditions. The second approach is to use the fact that these geometries can be obtained by an appropriate identification in the covering AdS_3 geometry. This second approach is the one followed by [28,29,32,50] and the one that we shall follow here—except in Appendix C, where we follow the first approach.

Within the second approach, the two-point function in BTZ can be readily obtained from the two-point function in the embedding space $CAdS_3$ [28,32]. As mentioned in Sec. II, the BTZ space-times are not globally hyperbolic.

For the Cauchy problem to be well-defined in these space-times, one must impose boundary conditions on the timelike AdS boundary [34] (as well as on the timelike singularity in the NS case). The field may obey different boundary conditions on the AdS boundary. We choose transparent boundary conditions, which correspond to defining the field modes that are smooth on the entire Einstein static universe to which the AdS geometry can be conformally mapped [28,34]. Taking advantage of the fact that AdS_3 is a maximally symmetric space-time, the anticommutator in $CAdS_3$ corresponding to these boundary conditions can be found to be [32,34,50–52]

$$G_A^{(1)}(x,x') = \frac{1}{2\sqrt{2}\pi}\frac{\Theta(\sigma(x,x'))}{\sqrt{\sigma(x,x')}}, \tag{3.5}$$

where Θ is the Heaviside step function,

$$\sigma(x,x') \equiv (-(X^0-X'^0)^2+(X^1-X'^1)^2+(X^2-X'^2)^2 - (X^3-X'^3)^2)/2, \tag{3.6}$$

and x and x' are points in AdS_3. Here, X^a and X'^a, with $a=0,1,2,3$, are the coordinates in the embedding space $\mathbb{R}^{(2,2)}$ of the points x and x', respectively. We note that $\sigma(x,x')$ is equal to one-half of the square of the geodesic distance between the two points X^a and X'^a in flat $\mathbb{R}^{(2,2)}$ (this is Synge's world function in $\mathbb{R}^{(2,2)}$, not in $CAdS_3$). Since X^a and X'^a belong to the pseudosphere, $\sigma(x,x')$ is the chordal distance between x and x'. Throughout the paper, we use Latin letters (such as a and b) for indices of coordinates of points in $\mathbb{R}^{2,2}$ and Greek letters (such as μ and ν) for indices of coordinates of points in $CAdS_3$ and BTZ geometries. See Appendix B for further details and an explicit coordinate expression for $G_A^{(1)}(x,x')$.

2. Multiply connected spaces

Let us now turn to the calculation of the two-point function and the RSET specifically in the BTZ geometries. Applying the method of images—according to which one must sum over all distinct images of a point obtained by the identification in the embedding space—it readily follows that the anticommutator both for the BH and NS geometries reads

$$G^{(1)}(x,x') = \sum_{n\in I} G_A^{(1)}(x,H^n x'), \tag{3.7}$$

where H is the identification matrix in $\mathbb{R}^{2,2}$ introduced in Sec. II C[7] and the range I is described below. In the case of transparent boundary conditions, the two-point function can be written as

$$G^{(1)}(x,x') = \frac{1}{2\sqrt{2}\pi}\sum_{n\in I}\frac{\Theta(\sigma(x,H^n x'))}{\sqrt{\sigma(x,H^n x')}}. \tag{3.8}$$

This expression applies to the case that the field obeys specific boundary conditions on the AdS boundary ($r=\infty$) and, if the spacetime possesses one (which is the case for all BTZ geometries except for the static BH), also on the timelike singularity ($r=0$). In the case of a static NS, we (re)derive the expression (3.8) in Appendix C using the alternative method of mode sums, and we see explicitly that the boundary conditions satisfied at the timelike singularity are square-integrability.

In the expressions above, $I \subset \mathbb{Z}$ is a summation range over all the various distinct images (see Appendix C where, in the static NS case, the "sum over images" arises as a "sum over caustics"). The identification matrices for the BH and NS cases are different and we give them explicitly in Appendix A; the ranges I are also different in each case and we describe them next.

Black hole.—The Green function for the three-dimensional BTZ BH was discussed in [28,32,50]. Since the identification matrix H acts transitively on $\mathbb{R}^{2,2}$, the sum in Eq. (3.7) includes an infinite countable number of images: $n \in I = \mathbb{Z}$. As is shown in Appendix A, the H matrix for the rotating black hole is given by

$$H = \begin{pmatrix} \cosh(\pi\alpha_+) & \sinh(\pi\alpha_+) & 0 & 0 \\ \sinh(\pi\alpha_+) & \cosh(\pi\alpha_+) & 0 & 0 \\ 0 & 0 & \cosh(\pi\alpha_-) & -\sinh(\pi\alpha_-) \\ 0 & 0 & -\sinh(\pi\alpha_-) & \cosh(\pi\alpha_-) \end{pmatrix}. \tag{3.9}$$

Conical singularity.—In the case of a conical singularity, the method of images does not reproduce the mode expansion for the two-point function for *arbitrary* values of M and J. Let us for now focus on the static case. If the deficit angle Δ is of the form $2\pi(k-1)/k$, $k \in \mathbb{Z}^+$, the angular identification produces a finite number of images.[8] On the other hand, for arbitrary real values of Δ the sum in Eq. (3.7) must be replaced by an integral since the associated eigenfunctions acquire a continuous degree and order [53]. The integral expressions, however, interpolate between the discrete sums that occur for consecutive deficit angles, $2\pi(k-1)/k$ and $2\pi k/(k+1)$.

The rationale that explains the difference between the BH case NS cases is as in electrostatics: the method of images between two parallel conducting plates generates a

[7] Strictly speaking, H is meant to act on a point in $\mathbb{R}^{2,2}$. As a slight abuse of notation, by $H^n x$ we shall mean H^n acting on the point on the pseudosphere in $\mathbb{R}^{2,2}$ that corresponds to the point x in the BTZ space-time.

[8] A finite number of images is also obtained for rational values of k.

countable but infinite number of images regardless of the distance between the plates. On the other hand, if the plates form an angle $\theta = 2\pi/k$, a finite number of images is produced, for $k \in \mathbb{Z}$, whereas a dense distribution of images are generated for a generic k. In the case of angular excesses (negative angular deficit and $M < -1$) the geometry is also described by Eq. (2.1), but the method of images is inadequate. Therefore, from now on, for NS geometries (whether rotating or not), we restrict ourselves to the case $M^2\ell^2 - J^2 < 1$ (and $M < 0$).

The identification matrix H is that in Eq. (A26) for $\beta \equiv \beta_+ = 2\sqrt{-M}$, $\beta_- = 0$, namely

$$H = \begin{pmatrix} 1 & 0 & 0 & 0 \\ 0 & \cos(\pi\beta) & -\sin(\pi\beta) & 0 \\ 0 & \sin(\pi\beta) & \cos(\pi\beta) & 0 \\ 0 & 0 & 0 & 1 \end{pmatrix}. \tag{3.10}$$

The number of terms in the sum in Eq. (3.7) is given by the number of distinct images produced by the action of the identification matrix H, which in this case is $N-1$, where N is the smallest positive integer such that $H^N = 1$. The condition that such a number N exists implies that β is a rational number. In [54] and in asymptotically flat (instead of AdS) space-time, the method of images was applied specifically to the case $\beta = 2/N$, with N a positive integer. Furthermore, in Appendix C we obtain the two-point function for this β using the method of mode sums, without relying on the method of images. Therefore, henceforth we shall consider only the case $\beta = 2/N$, $N \in \mathbb{Z}^+$, for static NSs. Both from the method of images and from the independent mode-sum calculation of Appendix C, it follows that in Eq. (3.7) the sum over the images yields

$$G^{(1)}_{NS}(x,x') = \sum_{n=0}^{N-1} G^{(1)}_A(x, H^n x') = \frac{1}{2\sqrt{2}\pi} \sum_{n=1}^{N-1} \frac{\Theta(\sigma(x,H^n x'))}{\sqrt{\sigma(x,H^n x')}}. \tag{3.11}$$

The mode expansion in [54,55] for a conical space-time without a cosmological constant can possibly be extended to the asymptotically AdS_3 case by replacing Bessel functions by Legendre functions in the homogeneous solutions—see Eq. (C3).

Let us now turn to the rotating case. In this case, the identification matrix [given in Eq. (A26)] depends on two parameters, β_+ and β_-,

$$H = \begin{pmatrix} \cos(\pi\beta_-) & 0 & 0 & -\sin(\pi\beta_-) \\ 0 & \cos(\pi\beta_+) & -\sin(\pi\beta_+) & 0 \\ 0 & \sin(\pi\beta_+) & \cos(\pi\beta_+) & 0 \\ \sin(\pi\beta_-) & 0 & 0 & \cos(\pi\beta_-) \end{pmatrix}. \tag{3.12}$$

Again, the number of terms in the sum in Eq. (3.7) is given by the number of distinct images produced by the action of the identification matrix H. We shall henceforth consider only the case $\beta_\pm = 2/N_\pm$, $N_+ \in \mathbb{N}$, $|N_-| \in \mathbb{N}$ for rotating NSs, where $|N_-| > N_+$. The smallest N for which $H^N = 1$ occurs when N is the least common multiple of N_+ and N_-. This means that the number of images in the sum in Eq. (3.7) is $N-1$ and the expression for the two-point function is formally the same as in Eq. (3.11).

B. Renormalized stress-energy tensor

Equipped with the two-point function, we now turn to the calculation of the RSET. As mentioned above, the quantum stress-energy tensor would in principle be calculated by applying a certain geometric differential operator on the two-point function $G^{(1)}(x,x')$. However, as is well known, the two-point function typically diverges at coincidence ($x = x'$)[9]—this can readily be seen in the BTZ case from Eq. (3.8) and the fact that $\sigma(x,x) = 0$. The divergence at coincidence, which can readily be seen in the BTZ case from Eq. (3.8), is an ultraviolet divergence which must be renormalized away [47]. That is, in order to obtain the RSET, one must first renormalize the two-point function by subtracting from it an appropriate bitensor $G^{(1)}_{div}(x,x')$ which is purely geometric. The RSET for the conformally coupled scalar field can thus be obtained from the Hadamard elementary function as [32,47][10]:

$$\kappa\langle T_{\mu\nu}(x)\rangle = \pi l_P \lim_{x'\to x}\Big(3\nabla^x_\mu\nabla^{x'}_\nu - g_{\mu\nu}g^{\alpha\beta}\nabla^x_\alpha\nabla^{x'}_\beta - \nabla^x_\mu\nabla^x_\nu - \frac{1}{4\ell^2}g_{\mu\nu}\Big)(G^{(1)}(x,x') - G^{(1)}_{div}(x,x')). \tag{3.13}$$

We note that the Heaviside step function in Eq. (3.8) does not actually appear in [28,32,50,51]. The reason is that these references calculate either a two-point function different from the anticommutator or else the anticommutator only in the static case. In the static case (whether BH or NS), $\sigma(x,H^n x)$ is non-negative and so the step function is redundant in this case. However, in the rotating case (whether BH or NS), $\sigma(x,H^n x)$ can be negative and so it is important to include the step function.

Let us here note some properties of the RSET. First, since we are dealing with a massless and conformally coupled scalar field, the trace of its classical stress-energy tensor

[9]Any other divergences of the two-point function are not ultraviolet divergences and so are of no relevance to the renormalization process which we are interested in here.

[10]The operator in Eq. (3.13) is 1/2 times the corresponding operator in [31,56]. The reason is that the definition of the anticommutator $G^{(1)}(x,x')$ here is 2 times the definition used in [31,56], so that all the results in here and in [31,56] agree.

must be zero. Furthermore, since we are dealing with a three-dimensional space-time, the trace of the RSET must also be zero (i.e., there is no trace anomaly) [47]. Second, the divergent term $G^{(1)}_{div}$ is constructed in a way so that the RSET is also conserved with respect to the classical background metric. In the BTZ case, the subtraction of $G^{(1)}_{div}(x,x')$ corresponds to simply removing the $n=0$ term from the n-sum in Eq. (3.7) [50,54,57]. Therefore, the n-sums for the RSET that follow from Eqs. (3.7) and (3.13) will be over the summation range $I\backslash\{0\}$, instead of the range I which we described in Sec. III A 2 for the various space-time settings.

Furthermore, as follows from Eqs. (3.7) and (3.13), the n-summands in the RSET will contain the quantity

$$d_n \equiv 2\sigma(x, H^n x) \tag{3.14}$$

as well as $\Theta(d_n)$. Therefore, in order to facilitate the notation for the n-sums we define a new summation symbol,

$$\sum_n{}' s_n \equiv \sum_n \Theta(d_n) s_n, \tag{3.15}$$

for some summand s_n and some summation range.

It follows from [32] that, by inserting the general form Eq. (3.7) for the two-point function into Eq. (3.13), and using Eq. (3.6) for σ, the RSET for a conformal scalar field satisfying transparent boundary conditions on a BTZ geometry takes the form

$$\kappa\langle T_{\mu\nu}\rangle = \frac{3l_P}{2}\sum_{n\in I\backslash\{0\}}{}'\left(S^n_{\mu\nu} - \frac{1}{3}g_{\mu\nu}g^{\lambda\rho}S^n_{\lambda\rho}\right), \tag{3.16}$$

where $S^n_{\mu\nu} \equiv \partial_\mu X^a \partial_\nu X^b S^n_{ab}$ is the pull back to AdS_3 of

$$S^n_{ab} \equiv \frac{(H^n)_{ab}}{d_n^{3/2}} + \frac{3(H^n)_{ac}X^c(H^{-n})_{bd}X^d - (H^n)_{ac}X^c(H^n)_{bd}X^d}{d_n^{5/2}}. \tag{3.17}$$

Even though this expression for the RSET was given in [32] for the BH case, it also applies to the NS with the appropriate summation range I.

We now proceed to give explicit expressions for the RSET and describe its main physical features, separately for the BH and NS cases. We will make use of the fact that the summand in Eq. (3.16) is either symmetric or antisymmetric—depending on the specific component—under $n \to -n$.

1. Black hole

Here we give the RSET in the BH geometries. Using the symmetries under $n \to -n$ mentioned above and the fact that $I = \mathbb{Z}$ is symmetric with respect to $n = 0$, the explicit expressions for the RSET that we shall give will contain n-sums involving only $n > 0$.

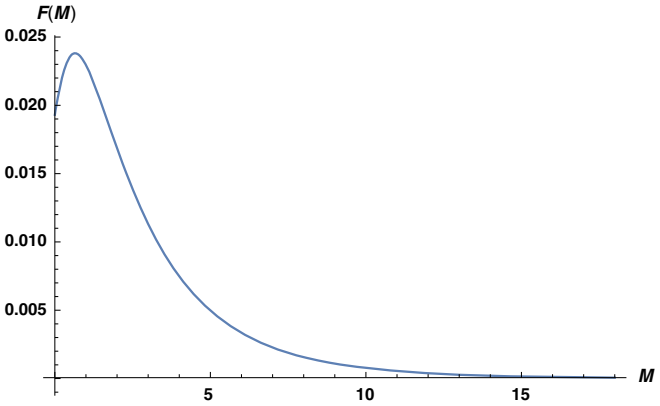

FIG. 3. The function $F(M)$ of Eq. (3.19) that defines the RSET profile for a static BH. This function has a maximum at $M \approx 0.648876$, decays exponentially for large M and $F(0^+) = \zeta(3)/(2\pi^3) \approx 0.0193841$.

We first summarize the RSET result in [29] in the static case. We then rederive (and make a slight correction to) the RSET in [32] in the nonextremal rotating case and plot its components. We finally derive the RSET in the extremal case. For the rotating BH cases, we also give the specific radii inside the Cauchy horizon at which the RSET diverges.

RSET for the static BTZ black hole.—The RSET in the static BTZ BH is obtained from Eqs. (3.16), (A3), (A4), and (A8) with ($\alpha_- = 0$), and the summation range from $-\infty < n < \infty$ in Eq. (3.8). In this setting, it is $d_n > 0$, $\forall\, n > 0$, at any space-time point, and so $\Theta(d_n) = 1$ in Eq. (3.15). The RSET in this case is

$$\kappa\langle T^\mu{}_\nu(x)\rangle = \frac{l_P}{r^3}F(M)\,\mathrm{diag}(1,1,-2), \tag{3.18}$$

in $\{t, r, \theta\}$ coordinates, where

$$F(M) \equiv \frac{M^{3/2}}{2\sqrt{2}}\sum_{n=1}^{\infty}\frac{\cosh(2n\pi\sqrt{M})+3}{(\cosh(2n\pi\sqrt{M})-1)^{3/2}}. \tag{3.19}$$

We plot the function $F(M)$ in Fig. 3. Also, we note that we obtain the same expression for the RSET regardless of which region of the space-time, $r > r_+$ [Eq. (A3)] or $0 < r < r_+$ [Eq. (A4)], we calculate it in. The result (3.19) was previously found in [28] and [32].

RSET for the rotating nonextremal BTZ black hole.—Let us now include (nonextremal) rotation to the BH. From Eqs. (3.16), (A3), (A4), (A5) and (A8) we obtain the RSET in the nonextremal BH case:

$$\kappa\langle T^{t}{}_{t}\rangle = \frac{2l_P}{(\alpha_+^2-\alpha_-^2)^2}\sum_{n=1}^{\infty}{}' \frac{2(2r^2(3a_n+(\alpha_+^2-\alpha_-^2)b_n)-\ell^2 g_n)c_n+3\alpha_+\alpha_- e_n(8r^2-\alpha_-^2\ell^2+\alpha_+^2\ell^2)}{d_n^{5/2}}, \tag{3.20}$$

$$\kappa\langle T^{r}{}_{r}\rangle = l_P\sum_{n=1}^{\infty}{}' \frac{c_n}{d_n^{3/2}}, \tag{3.21}$$

$$\kappa\langle T^{\theta}{}_{\theta}\rangle = -\frac{2l_P}{(\alpha_+^2-\alpha_-^2)^2}\sum_{n=1}^{\infty}{}' \frac{2(2r^2(3\bar{a}_n-(\alpha_+^2-\alpha_-^2)b_n)-\ell^2\bar{g}_n)c_n+3\alpha_+\alpha_- e_n(8r^2-\alpha_-^2\ell^2+\alpha_+^2\ell^2)}{d_n^{5/2}}, \tag{3.22}$$

$$\kappa\langle T^{t}{}_{\theta}\rangle = -\frac{6l_P\ell}{(\alpha_+^2-\alpha_-^2)^2}\sum_{n=1}^{\infty}{}' \frac{(4(c_n-4)r^2-a_n\ell^2)c_n\alpha_+\alpha_-+e_n(-4r^2(\alpha_-^2+\alpha_+^2)+2\alpha_-^2\alpha_+^2\ell^2)}{d_n^{5/2}}, \tag{3.23}$$

$$\kappa\langle T^{\theta}{}_{t}\rangle = \frac{6l_P}{\ell(\alpha_+^2-\alpha_-^2)^2}\sum_{n=1}^{\infty}{}' \frac{(4(c_n-4)r^2-a_n\ell^2)c_n\alpha_+\alpha_-+e_n(-4r^2(\alpha_-^2+\alpha_+^2)+\ell^2(\alpha_-^4+\alpha_+^4))}{d_n^{5/2}}, \tag{3.24}$$

with

$$a_n \equiv 2\alpha_+^2\sinh^2\left(\frac{n\pi\alpha_-}{2}\right)+2\alpha_-^2\sinh^2\left(\frac{n\pi\alpha_+}{2}\right), \tag{3.25}$$

$$\bar{a}_n \equiv 2\alpha_+^2\sinh^2\left(\frac{n\pi\alpha_+}{2}\right)+2\alpha_-^2\sinh^2\left(\frac{n\pi\alpha_-}{2}\right), \tag{3.26}$$

$$b_n \equiv \cosh(\pi n\alpha_+)-\cosh(\pi n\alpha_-) = 2\left(\sinh^2\left(\frac{\pi n\alpha_+}{2}\right)-\sinh^2\left(\frac{\pi n\alpha_-}{2}\right)\right), \tag{3.27}$$

$$c_n \equiv \cosh(\pi n\alpha_+)+\cosh(\pi n\alpha_-)+2, \tag{3.28}$$

$$e_n \equiv 2\sinh(\pi n\alpha_+)\sinh(\pi n\alpha_-), \tag{3.29}$$

$$g_n \equiv \alpha_-^2(\alpha_+^2+2\alpha_-^2)\sinh^2\left(\frac{n\pi\alpha_+}{2}\right)+\alpha_+^2(\alpha_-^2+2\alpha_+^2)\sinh^2\left(\frac{n\pi\alpha_-}{2}\right), \tag{3.30}$$

$$\bar{g}_n \equiv \alpha_-^2(\alpha_-^2+2\alpha_+^2)\sinh^2\left(\frac{n\pi\alpha_+}{2}\right)+\alpha_+^2(\alpha_+^2+2\alpha_-^2)\sinh^2\left(\frac{n\pi\alpha_-}{2}\right), \tag{3.31}$$

and, as per Eq. (3.14),

$$d_n = 2\sigma(x,H^n x) = 4\ell^2\frac{\alpha_+^2\sinh^2(\frac{\pi n\alpha_-}{2})-\alpha_-^2\sinh^2(\frac{\pi n\alpha_+}{2})+2r^2\ell^{-2}b_n}{\alpha_+^2-\alpha_-^2}. \tag{3.32}$$

In this setting, it is $d_n > 0$ for all $n > 0$ and any space-time point with $r > \ell|\alpha_-|/2$ (the Cauchy horizon of the BTZ background). Therefore, in general, the $\Theta(d_n)$ of Eq. (3.15) must be kept in the above equations. Also, we note that we obtain the same expression for the RSET regardless of which region of the space-time, $r > r_+$ [Eq. (A3)], $r_- < r < r_+$ [Eq. (A4)], or $0 < r < r_-$ [Eq. (A5)], we calculate it in.

An important issue appears in the region $r < r_-$: in this region, d_n takes negative values and it vanishes at the radii given by

$$r^2 = r_n^2 \equiv \ell^2\frac{\alpha_-^2\sinh^2(\frac{\pi n\alpha_+}{2})-\alpha_+^2\sinh^2(\frac{\pi n\alpha_-}{2})}{2b_n}, \qquad n\in\mathbb{Z}^+. \tag{3.33}$$

Consequently, all components of $\langle T^{\mu}{}_{\nu}\rangle$ diverge at these various radii $r = r_n < r_-$. Moreover, $r_n^2 \to r_-^2$ as $n\to\infty$, and therefore, r_- is an accumulation point of singularities from the left.

We note that our RSET expressions in Eqs. (3.20)–(3.24) agree with those in Eq. (19) in [32] except for a factor in one component. Equation (19) in [32] is in a different set of coordinates, which are defined in Eq. (6) in [32] and which we denote here by $\{\bar{t},\bar{r},\bar{\theta}\}$. If we transform our Eqs. (3.20)–(3.24) to $\{\bar{t},\bar{r},\bar{\theta}\}$ coordinates, our result is equal to that in Eq. (19) in [32] but with an extra factor "−2" in the $\langle T^{\bar{\theta}}{}_{\bar{t}}\rangle$ component.

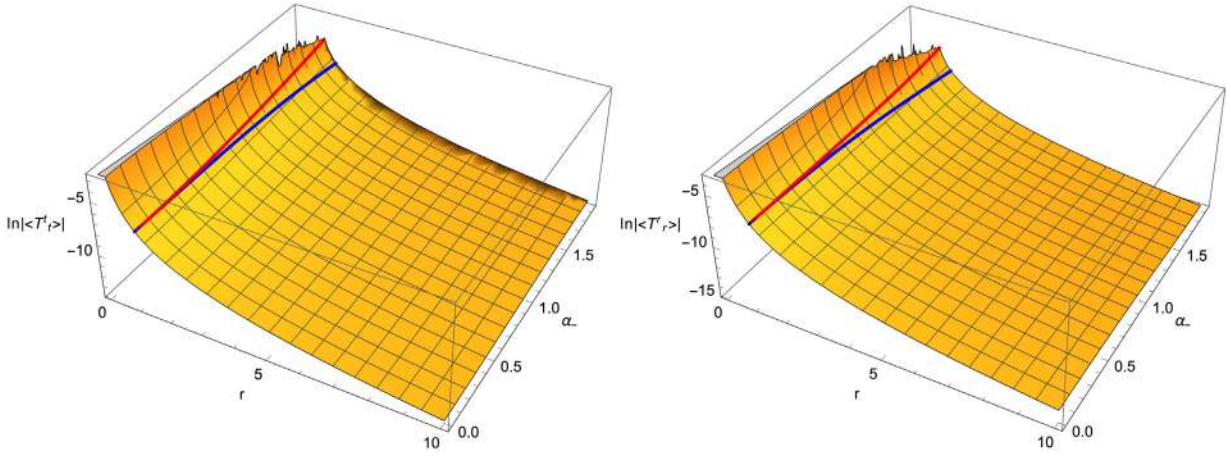

FIG. 4. Plot of the log of the absolute value of the RSET components $\langle T^{\mu}{}_{\nu}\rangle$ as functions of $r \in (r_-, 10]$ and $\alpha_- \in [0, \alpha_+]$ for the specific values of $\alpha_+ = (\sqrt{3}+1)/\sqrt{2}$, $\ell = 1$, $\kappa = 8\pi$ and $l_P = 1$. Left: $\langle T^t{}_t\rangle$; right: $\langle T^r{}_r\rangle$. The continuous red and blue lines correspond to, respectively, r_+ and r_{SL}. The vertical axis has been capped at a fixed value.

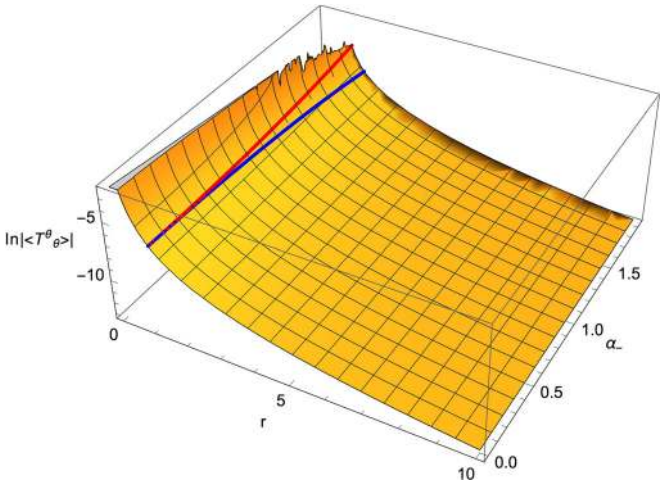

FIG. 5. Same as Fig. 4 but for the component $\langle T^{\theta}{}_{\theta}\rangle$.

In Figs. 4–6 we plot the RSET components $\langle T^{\mu}{}_{\nu}\rangle$ as functions of r and α_- for a fixed value of α_+. It can be observed that they all diverge as $r \to r_-$ as expected. For comparison with different boundary conditions, we note that Ref. [58] plotted the RSET for the case of *Dirichlet* boundary conditions—instead of transparent boundary conditions, as in our case—and explicit analytical expressions for the RSET in Dirichlet, Neumann and Robin boundary conditions are given in [59,60].

RSET for the extremal BTZ black hole.—The angular momentum in the extreme BTZ BH of mass M is $J = \gamma M\ell$ with $\gamma = \pm 1$ (i.e., $\alpha_+ = \gamma\alpha_-$). Here we define $\alpha \equiv r_+/\ell = \sqrt{M/2} > 0$. From Eqs. (3.16), (A13), (A14) and (A18) we then find the following expression for the RSET valid everywhere ($\forall\, r > 0$):

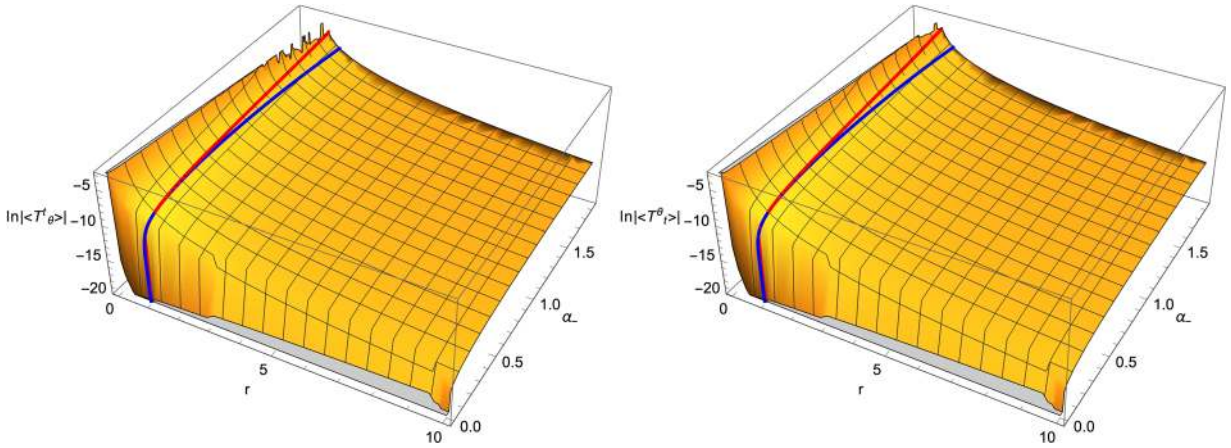

FIG. 6. Same as Fig. 4 but for the (nondiagonal) components $\langle T^{t}{}_{\theta}\rangle$ (left) and $\langle T^{\theta}{}_{t}\rangle$ (right).

$$\kappa\langle T^{t}{}_{t}\rangle = \frac{\ell^2 l_P}{2\alpha}\sum_{n=1}^{\infty}{}' \frac{1}{d_n^{5/2}}[3A(r)(6\pi^2\alpha^2n^2 + (2\pi^2\alpha^2n^2+1)\cosh(4\pi\alpha n) - 1) + 16\pi\alpha n(3\alpha - A(r))\sinh(\pi\alpha n)\cosh^3(\pi\alpha n) - 4\alpha\sinh^2(2\pi\alpha n)], \tag{3.34}$$

$$\kappa\langle T^{t}{}_{\theta}\rangle = -\frac{3\gamma\ell^3 l_P}{2\alpha}\sum_{n=1}^{\infty}{}' \frac{1}{d_n^{5/2}}[A(r)(6\pi^2\alpha^2n^2 + (2\pi^2\alpha^2n^2-1)\cosh(4\pi\alpha n) + 1) + 16\alpha\sinh(\pi\alpha n)\cosh^2(\pi\alpha n)(\pi\alpha n\cosh(\pi\alpha n) - \sinh(\pi\alpha n))], \tag{3.35}$$

$$\kappa\langle T^{r}{}_{r}\rangle = 4l_P\sum_{n=1}^{\infty}{}' \frac{\cosh^2(n\pi\alpha)}{d_n^{3/2}}, \tag{3.36}$$

$$\kappa\langle T^{\theta}{}_{t}\rangle = \frac{3\gamma\ell l_P}{2\alpha}\sum_{n=1}^{\infty}{}' \frac{1}{d_n^{5/2}}[A(r)(6\pi^2\alpha^2n^2 + (2\pi^2\alpha^2n^2-1)\cosh(4\pi\alpha n) + 1) + 16\alpha\sinh(\pi\alpha n)\cosh^2(\pi\alpha n)(\pi\alpha n\cosh(\pi\alpha n) + \sinh(\pi\alpha n))], \tag{3.37}$$

$$\kappa\langle T^{\theta}{}_{\theta}\rangle = -\frac{\ell^2 l_P}{2\alpha}\sum_{n=1}^{\infty}{}' \frac{1}{d_n^{5/2}}[3A(r)(6\pi^2\alpha^2n^2 + (2\pi^2\alpha^2n^2+1)\cosh(4\pi\alpha n) - 1) + 16\pi\alpha n(3\alpha + A(r))\sinh(\pi\alpha n)\cosh^3(\pi\alpha n) + 4\alpha\sinh^2(2\pi\alpha n)], \tag{3.38}$$

with

$$d_n = 2\sigma(x, H^n x) = 4\ell^2\sinh(\pi\alpha n)(\pi n A(r)\cosh(\pi\alpha n) + \sinh(\pi\alpha n)), \tag{3.39}$$

and

$$A(r) \equiv \frac{r^2 - \ell^2\alpha^2}{\ell^2\alpha}. \tag{3.40}$$

We note that the RSET in the extremal BH case in Eqs. (3.34)–(3.38) is actually equal to the RSET in the subextremal BH case in Eqs. (3.20)–(3.24) when taking the extremal limit $r_- \to r_+$.

Similarly to the nonextremal BH case, d_n is zero at certain values $r_n < r_+$, with

$$r_n^2 \equiv r_+^2\left(1 - \frac{\tanh(n\pi\alpha)}{n\pi\alpha}\right), \qquad n \in \mathbb{Z}^+. \tag{3.41}$$

This implies that the nth term in the series for $\langle T^{\mu}{}_{\nu}\rangle$ diverges at these radii. Moreover, since $r_n \to r_+$ as $n \to \infty$, r_+ becomes an accumulation point of singularities from the left.

2. Naked singularity

Here we give the RSET in the NS geometries. Here we shall make use of the symmetry $S^n_{\mu\nu}(x) = S^{n-N}_{\mu\nu}(x)$, a consequence of the property $H^N = 1$ that allows to symmetrize the sum over positive and negative n in Eq. (3.16) as

$$\sum_{n=1}^{N-1} f_n = \frac{1}{2}\sum_{n=1}^{N-1}(f_n + f_{n-N}) = \frac{1}{2}\sum_{n=1}^{N-1}(f_n + f_{-n}), \tag{3.42}$$

where f_n is the summand in (3.16). Depending on the specific component of the RSET, we have $f_n = f_{-n}$ or $f_n = -f_{-n}$.

We first review the RSET in the static case obtained in [31] and afterwards give our new RSET results in the rotating case (we do not consider the extremal NS because it involves an infinite sum whose convergence would need to be addressed separately).

RSET for the static NS.—We consider static NS space-times with $\beta = 2\sqrt{-M} = 2/N$ and $N \in \mathbb{Z}^+$. The RSET on this space-time can then be obtained from Eq. (3.16), the embedding Eq. (A22) and identification matrix in Eq. (A26) in the static limit ($\beta_+ = \beta$, $\beta_- = 0$), where the summation range is $1 \le n \le N-1$. As in the static BH case, it is $d_n > 0$, $\forall\, n > 0$, and for any space-point, so that $\Theta(d_n) = 1$. The result, derived in [31], is[11]

[11]The symbol N is not used for the same quantity here as in [56], but the expressions in both places are equivalent. On the other hand, there is a typographical error in Eq. (14) in [31] in that a factor of $1/2$ is missing, but the remaining formulas in [31] are correct.

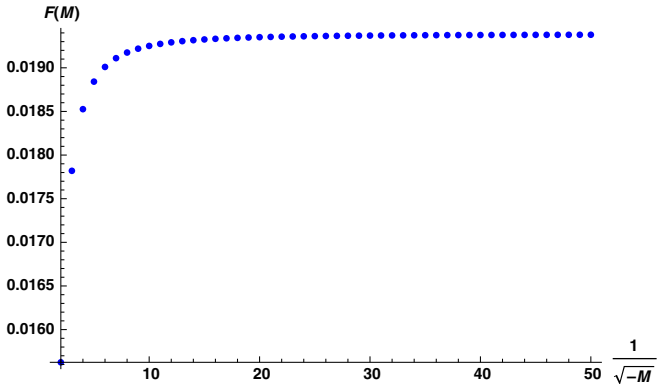

FIG. 7. The function $F(M)$ of Eq. (3.44) that defines the RSET profile as a function of $1/\sqrt{-M} = N$, where $N = 2, \ldots, 50$. The sum in Eq. (3.44) rapidly approaches the asymptotic value $F(0^-)$ in Eq. (3.45) given by the limit $N \to \infty$.

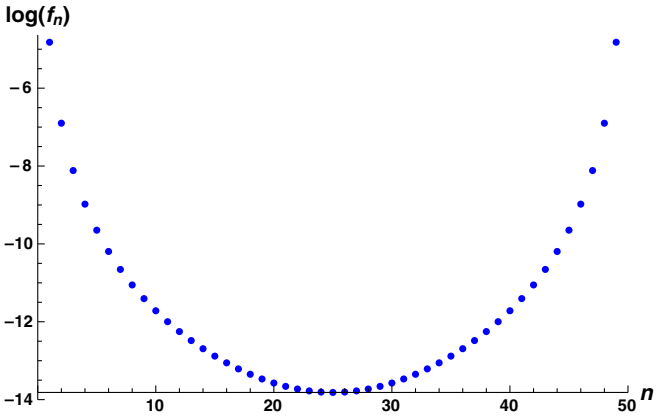

FIG. 8. Logarithm of the summand f_n in Eq. (3.44) as a function of n. The plot shows the range $n = 1, \ldots, N-1 = 49$ and exhibits the symmetry $n \to N - n$.

$$\kappa\langle T^{\mu}{}_{\nu}(x)\rangle = \frac{l_P}{r^3} F(M)\mathrm{diag}(1,1,-2), \tag{3.43}$$

in $\{t, r, \theta\}$ coordinates, where

$$F(M) \equiv \frac{(-M)^{3/2}}{4\sqrt{2}} \sum_{n=1}^{N-1} \frac{\cos(2n\pi\sqrt{-M}) + 3}{(1-\cos(2n\pi\sqrt{-M}))^{3/2}}, \tag{3.44}$$

where we have used Eq. (3.42). The function $F(M)$ is plotted in Fig. 7.

From (3.44) it is clear that the result is nontrivial for $N \geq 1$, which in turn implies $-1/4 < M < 0$. For static conical singularities with $-1 < M < -1/4$, the computation requires an integral formula instead of a sum.

The expression for the summand in $F(M)$, including the factor $(-M)^{3/2}$ in Eq. (3.44) for the NS, can be obtained from the corresponding one for the BH in Eq. (3.19) by analytic continuation, $M \to -M$. However, in the NS case, the images for n and $n - N$ are repeated, whereas in the BH case all images with different n are distinct, which accounts for the different overall factors in $F(M)$ in the two cases. Furthermore, for the NS, unlike the BH case, the sum runs over a finite range and consequently F is manifestly finite and positive.

The value of $F(0)$ may be obtained by taking the limit $M = -1/N^2 \to 0^-$ (i.e., $N \to \infty$) in Eq. (3.44), which is numerically found to be

$$F(0^-) = 0.0193841 \approx \frac{\zeta(3)}{2\pi^3}, \tag{3.45}$$

where ζ is the Riemann zeta function (see Fig. 7). This value matches the limit $M \to 0^+$ of $F(M)$ in the BH geometry, Eq. (3.19), in spite of the fact that there is apparently a mismatch by a factor of two between Eqs. (3.44) and (3.19). The apparent mismatch arises from taking the limit by applying the L'Hôpital rule to the summand and not considering the symmetry $n \to N - n$ that it has (see Fig. 8)—this symmetry adds a factor of two apparently lost in the sum in Eq. (3.44). The continuity of $F(M)$ and its derivative across $M = 0$ is manifest in Fig. 9.

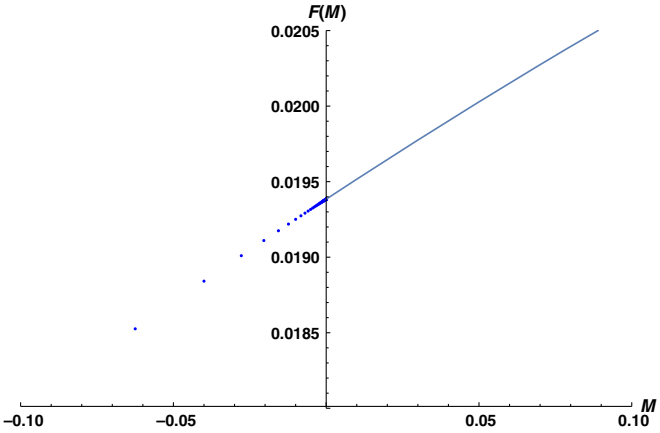

FIG. 9. The function $F(M)$ as a function of M around $M = 0$. For $M < 0$, $F(M)$ is given by the finite sum Eq. (3.44) and it is plotted using dots. For $M > 0$, $F(M)$ is given by the infinite series Eq. (3.19) and it is represented with a solid line. The figure shows that $F(M)$ and its derivative dF/dM are continuous at $M = 0$, which can be also verified analytically.

RSET for the rotating NS.—We consider the case $\beta_{\pm} = 2/N_{\pm}$, $N_{\pm} \in \mathbb{Z}^+$, where $N_- > N_+$. The number of distinct images is N, the least common multiple of N_+ and N_-. Then, using Eq. (3.16), the symmetry (3.42), as well as the embedding Eq. (A22) and identification matrix in Eq. (A26), we obtain the following components of the RSET for the rotating NS:

$$\kappa\langle T^{t}{}_{t}\rangle = \frac{l_P}{(\beta_+^2-\beta_-^2)^2}\sum_{n=1}^{N-1}{}' \frac{2(2r^2(3a_n-(\beta_+^2-\beta_-^2)b_n)+\ell^2 g_n)c_n+3\beta_+\beta_- e_n(8r^2+\beta_-^2\ell^2+\beta_+^2\ell^2)}{d_n^{5/2}}, \tag{3.46}$$

$$\kappa\langle T^{r}{}_{r}\rangle = \frac{l_P}{2}\sum_{n=1}^{N-1}{}' \frac{c_n}{d_n^{3/2}}, \tag{3.47}$$

$$\kappa\langle T^{\theta}{}_{\theta}\rangle = -\frac{l_P}{(\beta_+^2-\beta_-^2)^2}\sum_{n=1}^{N-1}{}' \frac{2(2r^2(3\bar{a}_n+(\beta_+^2-\beta_-^2)b_n)+\ell^2\bar{g}_n)c_n+3\beta_+\beta_- e_n(8r^2+\beta_-^2\ell^2+\beta_+^2\ell^2)}{d_n^{5/2}}, \tag{3.48}$$

$$\kappa\langle T^{t}{}_{\theta}\rangle = -\frac{3l_P\ell}{(\beta_+^2-\beta_-^2)^2}\sum_{n=1}^{N-1}{}' \frac{(4(c_n-4)r^2-a_n\ell^2)c_n\beta_+\beta_- + e_n(4r^2(\beta_-^2+\beta_+^2)+2\beta_-^2\beta_+^2\ell^2)}{d_n^{5/2}}, \tag{3.49}$$

$$\kappa\langle T^{\theta}{}_{t}\rangle = \frac{3l_P}{\ell(\beta_+^2-\beta_-^2)^2}\sum_{n=1}^{N-1}{}' \frac{(4(c_n-4)r^2-a_n\ell^2)c_n\beta_+\beta_- + e_n(4r^2(\beta_-^2+\beta_+^2)+\ell^2(\beta_-^4+\beta_+^4))}{d_n^{5/2}}, \tag{3.50}$$

with

$$a_n \equiv 2\beta_+^2\sin^2\left(\frac{n\pi\beta_-}{2}\right)+2\beta_-^2\sin^2\left(\frac{n\pi\beta_+}{2}\right), \tag{3.51}$$

$$\bar{a}_n \equiv 2\beta_+^2\sin^2\left(\frac{n\pi\beta_+}{2}\right)+2\beta_-^2\sin^2\left(\frac{n\pi\beta_-}{2}\right), \tag{3.52}$$

$$b_n \equiv \cos(\pi n\beta_+)-\cos(\pi n\beta_-) = 2\left(\sin^2\left(\frac{\pi n\beta_-}{2}\right)-\sin^2\left(\frac{\pi n\beta_+}{2}\right)\right), \tag{3.53}$$

$$c_n \equiv \cos(\pi n\beta_+)+\cos(\pi n\beta_-)+2, \tag{3.54}$$

$$e_n \equiv 2\sin(\pi n\beta_+)\sin(\pi n\beta_-), \tag{3.55}$$

$$g_n \equiv \beta_-^2(\beta_+^2+2\beta_-^2)\sin^2\left(\frac{n\pi\beta_+}{2}\right)+\beta_+^2(\beta_-^2+2\beta_+^2)\sin^2\left(\frac{n\pi\beta_-}{2}\right), \tag{3.56}$$

$$\bar{g}_n \equiv \beta_-^2(\beta_-^2+2\beta_+^2)\sin^2\left(\frac{n\pi\beta_+}{2}\right)+\beta_+^2(\beta_+^2+2\beta_-^2)\sin^2\left(\frac{n\pi\beta_-}{2}\right), \tag{3.57}$$

and

$$d_n = 2\sigma(x,H^n x) = 4\ell^2\frac{\beta_-^2\sin^2(\frac{\pi n\beta_+}{2})-\beta_+^2\sin^2(\frac{\pi n\beta_-}{2})-2r^2\ell^{-2}b_n}{\beta_+^2-\beta_-^2}. \tag{3.58}$$

Note that this RSET has the generic form

$$\langle T^{\mu}{}_{\nu}\rangle = \frac{1}{2}\sum_{n=1}^{N-1}{}'[\tau^{\mu}{}_{\nu}(r;n,\beta_+,\beta_-)+\tau^{\mu}{}_{\nu}(r;-n,\beta_+,\beta_-)], \tag{3.59}$$

for some tensor $\tau^{\mu}{}_{\nu}$. The components $\langle T^{t}{}_{r}\rangle$ and $\langle T^{r}{}_{\theta}\rangle$ vanish because $\tau^{r}{}_{t}$ and $\tau^{r}{}_{\theta}$ are antisymmetric under the change $n\to -n$. For instance, the component $\tau^{t}{}_{r}$ given by

$$\tau^{t}{}_{r} = -\frac{48\ell^3 r z_n\sin(\frac{1}{2}\pi\beta_+ n)}{(\beta_+^2-\beta_-^2)(\beta_-^2\ell^2+4r^2)(\beta_+^2\ell^2+4r^2)d_n^{5/2}}$$

with

$$z_n \equiv \beta_+(4r^2+\beta_-^2\ell^2)\sin(\pi\beta_- n)\sin\left(\frac{1}{2}\pi\beta_+ n\right) - 2\beta_-(4r^2+\beta_+^2\ell^2)\sin^2\left(\frac{1}{2}\pi\beta_- n\right)\cos\left(\frac{1}{2}\pi\beta_+ n\right),$$

is odd under $n \to -n$. This simplifies the backreaction problem since it is sufficient to consider a solution of the metric semiclassical equations of the stationary form in Eq. (4.17) (i.e., with no g_{tr} or $g_{r\theta}$ components).

Note that $b_n > 0$ in (3.58) implies $d_n < 0$ and therefore those terms with $b_n > 0$ do not contribute to the sum defining the RSET.[12] The special case $b_n = 0$ would make d_n to be independent of r, so that the RSET would diverge at radial infinity, thus leading to a breakdown of the perturbative approximation. It can be seen that b_n vanishes for $n = N$, which is outside the range of the sum $1 \le n \le N-1$. In addition, there is a discrete set of pairs of $\beta_\pm$ for which this also happens in the range of the sum. This set is given by

$$\mathcal{S} \equiv \{\beta_\pm | n(\beta_+ \pm \beta_-) = 2k, k \in \mathbb{Z}\} \tag{3.60}$$

and it must be removed from the analysis. For example, the case $\beta_+ = 2/3$ and $\beta_- = 1/3$, yielding $b_2 = b_4 = 0$, belongs to $\mathcal{S}$.

For $b_n < 0$, d_n grows as r^2 for sufficiently large r and the above RSET components go as r^{-3} at infinity, which is the same behavior as the RSET in the static case and as the classical stress-energy tensor.

Finally, and similarly to the BH case, d_n in Eq. (3.58) vanishes at some radii r_n given by

$$r_n^2 \equiv \frac{\ell^2}{2b_n}\left[\beta_-^2\sin^2\left(\frac{1}{2}\pi n\beta_+\right) - \beta_+^2\sin^2\left(\frac{1}{2}\pi n\beta_-\right)\right] > 0, \tag{3.61}$$

for some n. Since $b_n < 0$, the numerator of (3.61) must be negative in order for r_n to be real valued. At each of these zeroes, the RSET blows up and, therefore, the Kretschmann invariant (5.7) diverges, signaling curvature singularities.

Let us now examine under which conditions one can make sure that $b_n < 0$ for some n in order for the sum in the RSET to be nonvanishing. For $\beta_- = 0$ ($J = 0$), b_n is negative for all n, and since b_n is a continuous function of $\beta_\pm$, it should still be negative for some range $\beta_- \neq 0$ ($|J| > 0$).

Since $\beta_\pm = 2/N_\pm$, then $0 < \beta_+ \pm \beta_- \le 3$. The largest possible $\beta_+ = 2$ yields $N = |N_-|$ and $b_n \ge 0$ for all $n \in \{1, \ldots, N_- - 1\}$, hence this case is excluded. Therefore the only allowed values for $\beta_\pm$ are contained in the domain

$$0 < \beta_+ \pm \beta_- < 2. \tag{3.62}$$

The region covered by this condition corresponds to NSs in the square region $J > M > J-1$ and $-J > M > -J-1$ as shown in Fig. 10. This region includes all the static NSs with masses in the range $0 < M < -1$. One can now observe that since $\sin^2 x$ grows monotonically for small x and $\beta_+ \ge \beta_-$, at least for $n = 1$, $b_1 < 0$, and therefore the sum for the RSET always contains the first term. It is also easy to see that, in that same domain, the factor in brackets in Eq. (3.61) is negative for $n = 1$, which renders $r_1^2 > 0$.

IV. SOLUTION OF THE SEMICLASSICAL EQUATIONS

In this section we solve analytically the semiclassical Einstein equations:

$$G_{\mu\nu} - \ell^{-2}g_{\mu\nu} = \kappa\langle T_{\mu\nu}\rangle. \tag{4.1}$$

Here, the RSET is calculated on a classical BTZ background space-time (such as the one in the previous section when using transparent boundary conditions) and the solution $g_{\mu\nu}$ corresponds to the quantum-backreacted geometry (that is, $g_{\mu\nu}$ in Eq. (4.1) is *not* the classical BTZ background).

We provide details of the integration differentiating between the nonrotating and rotating cases. For the static case, this section contains a review of existing results in the literature [28,29,31] and new observations about the RSET

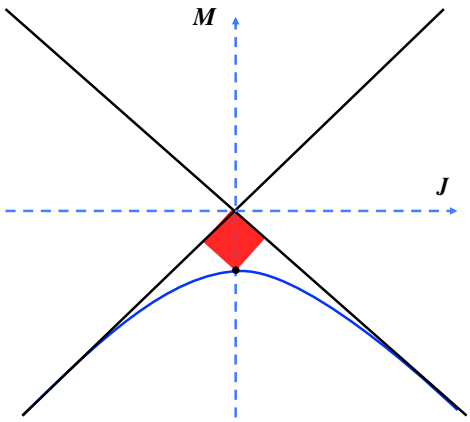

FIG. 10. Region $0 < \beta_+ + \beta_- < 2$ [see Eq. (3.62)] in the M-J plane corresponds to the central square between the zero mass state ($M = 0$, $J = 0$) and anti–de Sitter ($M = -1$, $J = 0$). In this region $b_1 < 0$, which guarantees that the RSET contains at least one nonvanishing term in the sum ($n = 1$).

[12] Writing b_n as $2(\sin^2 y - \sin^2 x)$ with $y < x$, and imposing $b_n > 0$ implies that $\sin^2 x/x^2 - \sin^2 y/y^2 < 0$, from which immediately follows that d_n would be negative.

conservation under different boundary conditions. In the rotating case we include a thorough description of the results briefly announced in [33].

A. Static geometries

Let us consider a general form for a static and circularly symmetric three-dimensional line element:

$$ds^2 = -A(r)dt^2 + \frac{dr^2}{B(r)} + r^2 d\theta^2. \tag{4.2}$$

The functions $A(r)$ and $B(r)$ are determined so that this metric is a solution of the semiclassical Eq. (4.1) with a static RSET of the form $\langle T^{\mu}{}_{\nu}\rangle = \mathrm{diag}(\langle T^{t}{}_{t}(r)\rangle, \langle T^{r}{}_{r}(r)\rangle, \langle T^{\theta}{}_{\theta}(r)\rangle)$ as a source. In particular, the RSETs of Eqs. (3.43) and (3.18) have this diagonal form; also, the static BTZ BH geometries, Eq. (2.1) or (A21) with $J = 0$, have the form in Eq. (4.2).

The semiclassical Einstein equations containing the above RSET as a source reduce to

$$\frac{B'}{2r} - \frac{1}{\ell^2} = \kappa\langle T^{t}{}_{t}\rangle, \tag{4.3}$$

$$\frac{BA'}{2rA} - \frac{1}{\ell^2} = \kappa\langle T^{r}{}_{r}\rangle, \tag{4.4}$$

$$\frac{AA'B' - B(A'^2 - 2AA'')}{4A^2} - \frac{1}{\ell^2} = \kappa\langle T^{\theta}{}_{\theta}\rangle, \tag{4.5}$$

where a prime on a function denotes derivative with respect to its argument. Using Eqs. (4.3) and (4.4), Eq. (4.5) becomes

$$\langle T^{r}{}_{r}\rangle' + \frac{A'}{2A}(\langle T^{r}{}_{r}\rangle - \langle T^{t}{}_{t}\rangle) + \frac{1}{r}(\langle T^{r}{}_{r}\rangle - \langle T^{\theta}{}_{\theta}\rangle) = 0. \tag{4.6}$$

In its turn, the only nonvanishing component of $\nabla_{\mu}\langle T^{\mu}{}_{\nu}\rangle$ is

$$\nabla_{\mu}\langle T^{\mu}{}_{r}\rangle = \langle T^{r}{}_{r}\rangle' + \frac{A'}{2A}(\langle T^{r}{}_{r}\rangle - \langle T^{t}{}_{t}\rangle) + \frac{1}{r}(\langle T^{r}{}_{r}\rangle - \langle T^{\theta}{}_{\theta}\rangle). \tag{4.7}$$

We note that Eq. (4.6) is equivalent to $\nabla_{\mu}\langle T^{\mu}{}_{r}\rangle = 0$. As expected, once the three field equations are satisfied, the conservation of $\langle T^{\mu}{}_{\nu}\rangle$ holds.

1. Dirichlet and Neumann boundary conditions

The RSET that we gave in Sec. III B was for a conformal scalar field satisfying transparent boundary conditions. From [28], one can show that the RSET components computed using Dirichlet and Neumann boundary conditions for a conformal scalar field on the BTZ BH background satisfy the following relation

$$\langle T^{r}{}_{r}\rangle' + \frac{r}{r^2 - r_+^2}(\langle T^{r}{}_{r}\rangle - \langle T^{t}{}_{t}\rangle) + \frac{1}{r}(\langle T^{r}{}_{r}\rangle - \langle T^{\theta}{}_{\theta}\rangle) = 0. \tag{4.8}$$

Comparing the above expression with Eq. (4.7), it is noted that the conservation of the RSET is guaranteed if

$$\frac{A'}{2A} = \frac{r}{r^2 - r_+^2}. \tag{4.9}$$

This condition is exactly verified by the static BTZ BH geometry, Eq. (2.1) with $J = 0$. This means that the RSET for a field satisfying Dirichlet or Neumann boundary conditions is conserved on the BTZ BH background. If, on the other hand, A were such that it did not satisfy Eq. (4.9), then the RSET would not be conserved. In that case, the integrability condition for Eqs. (4.3)–(4.5) would not be fulfilled. However, if A satisfied $A \propto (r^2 - r_+^2) + O(l_P)$, then Eq. (4.8) would be satisfied at order l_P. Then the semiclassical equations (4.3)–(4.5) for a RSET for a field satisfying Dirichlet or Neumann boundary conditions would only be compatible at linear order in l_P.

2. Transparent boundary conditions

The components of the RSET for a conformal scalar field satisfying transparent boundary conditions on the BTZ background geometries, for either BH [Eq. (3.18)] or NS [Eq. (3.43)], satisfy the algebraic relations

$$\langle T^{t}{}_{t}\rangle = \langle T^{r}{}_{r}\rangle \quad \text{and} \quad \langle T^{t}{}_{t}\rangle + \langle T^{r}{}_{r}\rangle + \langle T^{\theta}{}_{\theta}\rangle = 0, \tag{4.10}$$

which imply $\langle T^{r}{}_{r}\rangle - \langle T^{\theta}{}_{\theta}\rangle = 3\langle T^{r}{}_{r}\rangle$. In this case, Eq. (4.7) reduces to

$$\nabla_{\mu}\langle T^{\mu}{}_{r}\rangle = \langle T^{r}{}_{r}\rangle' + \frac{3}{r}\langle T^{r}{}_{r}\rangle, \tag{4.11}$$

whose right-hand side vanishes since $\langle T^{r}{}_{r}\rangle$ is proportional to r^{-3} [see Eqs. (3.18) and (3.43)]. Note that the term with A'/A in Eq. (4.7) is absent in Eq. (4.11) because $\langle T^{t}{}_{t}\rangle = \langle T^{r}{}_{r}\rangle$. This shows that a RSET calculated on a fixed background space-time and which is of the form

$$\langle T^{\mu}{}_{\nu}\rangle = \frac{\text{constant}}{r^3}\mathrm{diag}(1, 1, -2), \tag{4.12}$$

in $\{t, r, \theta\}$ coordinates is conserved on the general static metric in Eq. (4.2) and so fulfills the integrability condition for Eqs. (4.3)–(4.5). In particular, the form (4.12) is satisfied by the RSET for a field with transparent boundary conditions on a BTZ background space-time.

Because Eq. (4.5) is satisfied by virtue of (4.11), it is only necessary to solve Eqs. (4.3) and (4.4). Subtracting Eqs. (4.3) and (4.4), and using Eq. (4.10), we obtain

$$\frac{A'}{A} = \frac{B'}{B}. \tag{4.13}$$

Thus $A = B$ (up to a constant which can be taken equal to 1) and, from Eq. (4.3), we obtain

$$A = B = \frac{r^2}{\ell^2} - c_0 + 2\kappa \int r\langle T^t{}_t\rangle dr, \tag{4.14}$$

where c_0 is an integration constant.

Note that for the transparent boundary conditions and in the coordinates of Eq. (4.2), the exact solution given by Eq. (4.14) of the semiclassical equations (4.3)–(4.5) is a linear function of the source. Thus, if c_0 is chosen to be the mass M of the static BTZ geometries, then the exact (i.e., without expanding for small l_P) solution for the metric coefficients A and B coincides with the solution one would obtain if expanding A and B to linear order in l_P around a BTZ static metric.

Black hole.—Let us first briefly review the static ($J = 0$) BTZ BH case, which was analyzed in [29] considering transparent boundary conditions. Using Eq. (3.18), the integral appearing in Eq. (4.14) becomes

$$2\kappa \int r\langle T^t{}_t\rangle dr = -\frac{2l_P F(M)}{r}, \tag{4.15}$$

where $F(M)$ is given in Eq. (3.19). The backreacted metric, as given by Eqs. (4.2) and (4.14), is then

$$ds^2 = -\left(\frac{r^2}{\ell^2} - c_0 - \frac{2l_P F(M)}{r}\right)dt^2 + \frac{dr^2}{\left(\frac{r^2}{\ell^2} - c_0 - \frac{2l_P F(M)}{r}\right)} + r^2 d\theta^2. \tag{4.16}$$

This metric is that of a circularly symmetric AdS black hole (i.e., a "three-dimensional Schwarzschild-AdS" black hole), as was already noted in [29], where its thermodynamics properties for $c_0 = M$ were investigated.

Naked singularity.—In the static NS case, the RSET in Eq. (3.43) has the same structure as for the static BH case. Therefore, the quantum-backreacted metric has the same form as in Eq. (4.16), but now $F(M)$ is instead given by the finite sum (3.44).

B. Rotating geometries

In this section we set as a source of the Einstein semiclassical equations (4.1) the RSET corresponding to a conformally coupled scalar field on the rotating BTZ background geometries. In order to solve these backreaction equations we consider a general stationary and circularly symmetric three-dimensional line element:

$$ds^2 = -N(r)^2 f(r) dt^2 + \frac{dr^2}{f(r)} + r^2(d\theta + k(r)dt)^2, \tag{4.17}$$

for some functions $N(r)$, $f(r)$ and shift function $k(r)$. We are interested in finding the linear corrections in l_P to the rotating BTZ geometries. For this purpose, we write the metric functions explicitly up to order $O(l_p)$ as

$$\begin{aligned} N(r) &= N_0(r) + l_P N_1(r) + O(l_P^2), \\ f(r) &= f_0(r) + l_P f_1(r) + O(l_P^2), \\ k(r) &= k_0(r) + l_P k_1(r) + O(l_P^2), \end{aligned} \tag{4.18}$$

where the functions labeled with a subindex 0 are the background metric coefficients and those with subindex 1 correspond to their first-order backreaction corrections in l_P.

The zeroth order field equations provide the equations for the background functions:

$$N_0' = 0, \qquad k_0'' + \frac{3}{r}k_0' = 0, \qquad f_0'' + \frac{3}{r}f_0' = \frac{8}{\ell^2}$$
$$f_0' + \frac{r^3 k_0'^2}{2N_0^2} = \frac{2r}{\ell^2}, \tag{4.19}$$

where a prime means derivative with respect to their argument, r. Thus, it is $N_0(r) =$ constant, which is taken to be 1. In its turn, the first integral of the equation for k_0 gives $r^3 k_0' = J =$ constant, so that

$$k_0 = -\frac{J}{2r^2} + k_0(\infty). \tag{4.20}$$

We choose $k_0(\infty) = 0$ in order to describe the BTZ geometries in a coordinate frame such that the shift function at infinity vanishes. Thus, we have

$$N_0 = 1, \qquad k_0 = -\frac{J}{2r^2}. \tag{4.21}$$

Moreover, from Eq. (4.19) we have

$$f_0' = \frac{2r}{\ell^2} - \frac{J^2}{2r^3}, \tag{4.22}$$

and hence,

$$f_0 = \frac{r^2}{\ell^2} - M + \frac{J^2}{4r^2}, \tag{4.23}$$

where M is a constant of integration. Equation (4.23) is the usual expression for the lapse function of the BTZ geometries with mass M and angular momentum J.

The next order of the field equations provides linear differential equations for $N_1(r)$, $k_1(r)$ and $f_1(r)$. Explicitly, the $O(l_P)$ semiclassical Einstein equations (4.1) read

$$16r^6\frac{\kappa}{l_p}\langle T_{tt}\rangle = f_0(r^5(16Jk_1' - 8f_1') + 4J^2r^4N_1'' - 8J^2r^3N_1' + 8J^2r^2N_1 + 8Jr^6k_1'') + 2J^2r^4f_1'' - 3J^4rN_1' + 6J^4N_1 - 6J^3r^3k_1' + \frac{12}{\ell^2}J^2r^5N_1', \tag{4.24}$$

$$8\frac{\kappa}{l_p}\langle T_{t\theta}\rangle = -4f_0\left(J\left(N_1'' - \frac{N_1'}{r}\right) + r^2k_1'' + 3rk_1'\right) - 2Jf_1'' + 3J\left(\frac{J^2}{r^3} - \frac{4r}{\ell^2}\right)N_1' - \frac{6J^3N_1}{r^4} + \frac{6J^2k_1'}{r}, \tag{4.25}$$

$$\frac{\kappa}{l_p}\langle T_{rr}\rangle = \frac{r^3(f_1' + Jk_1') - J^2N_1}{2r^4f_0} + \frac{N_1'}{r}, \tag{4.26}$$

$$4\frac{\kappa}{l_p}\langle T_{\theta\theta}\rangle = 4r^2f_0N_1'' + 2r^2f_1'' + \left(\frac{12r^3}{\ell^2} - \frac{3J^2}{r}\right)N_1' + \frac{6J^2N_1}{r^2} - 6Jrk_1'. \tag{4.27}$$

We first isolate the relevant second derivatives appearing in these equations:

$$r^4Jk_1'' = (-r^3Jk_1' + 2r^3f_1' + J^2rN_1' - 2J^2N_1) + \frac{1}{f_0}\left(2Jr^2\frac{\kappa}{l_p}\langle T_{t\theta}\rangle + 4r^4\frac{\kappa}{l_p}\langle T_{tt}\rangle\right), \tag{4.28}$$

$$4r^2f_0N_1'' + 2r^2f_1'' = 4\frac{\kappa}{l_p}\langle T_{\theta\theta}\rangle - \left(\frac{12r^3}{\ell^2} + \frac{3J^2}{r}\right)N_1' - \frac{6J^2N_1}{r^2} + 6Jrk_1'. \tag{4.29}$$

Substituting these equations into Eq. (4.24) we obtain

$$\mathcal{A} \equiv 4J^2r^2\frac{\kappa}{l_p}\langle T_{\theta\theta}\rangle + 16Jr^4\frac{\kappa}{l_p}\langle T_{t\theta}\rangle + 16r^6\frac{\kappa}{l_p}\langle T_{tt}\rangle = -8r^2f_0(r^3(Jk_1' + f_1') - J^2N_1), \tag{4.30}$$

which combined with Eq. (4.26) gives

$$N_1' = r\frac{\kappa}{l_p}\langle T_{rr}\rangle + \frac{\mathcal{A}}{16r^5f_0^2}. \tag{4.31}$$

This last equation determines N_1. Since the RSET is traceless, we obtain

$$\langle T_{tt}\rangle = f_0^2\langle T_{rr}\rangle + \left(\frac{1}{\ell^2} - \frac{M}{r^2}\right)\langle T_{\theta\theta}\rangle - \frac{J}{r^2}\langle T_{t\theta}\rangle, \tag{4.32}$$

so that $\mathcal{A}$ becomes

$$\mathcal{A} = 16r^6\frac{\kappa}{l_p}f_0\left(f_0\langle T_{rr}\rangle + \frac{1}{r^2}\langle T_{\theta\theta}\rangle\right). \tag{4.33}$$

We now use the combination of Eqs. (4.26) and (4.27) that eliminates k_1', together with Eqs. (4.32) and (4.31), and obtain

$$(r^3f_1')' = -\frac{\mathcal{A}}{8r^3f_0} - 2r^2N_1'\left(\frac{4r^2}{\ell^2} - M - \frac{J^2}{2r^2}\right) - 2r^3f_0N_1''. \tag{4.34}$$

This equation allows to solve for f_1. Finally, the equation determining k_1 comes from Eq. (4.30):

$$Jk_1' = -f_1' + \frac{J^2N_1}{r^3} - \frac{\mathcal{A}}{8r^5f_0}. \tag{4.35}$$

In this way, we have decoupled the semiclassical Einstein equations at the linear approximation in l_P. We note that the components of the RSET satisfy the integrability condition of these equations,

$$\frac{d\langle T_{rr}\rangle}{dr}=\left(\frac{J^2\ell^2-2\ell^2r^2f_0-4r^4}{\ell^2r^3f_0}\right)\langle T_{rr}\rangle+\frac{\ell^2\langle T_{tt}\rangle-\langle T_{\theta\theta}\rangle}{\ell^2rf_0^2}, \tag{4.36}$$

which corresponds to the covariant conservation (at first order in l_P) of the RSET.

The integration of Eqs. (4.31), (4.34) and (4.35) give

$$N_1(r)=\frac{\kappa}{l_P}\int dr\left(2r\langle T_{rr}\rangle+\frac{\langle T_{\theta\theta}\rangle}{rf_0(r)}\right)+c_1, \tag{4.37}$$

$$f_1(r)=\int dr\left[-2f_0(r)N_1'(r)+N_1(r)\left(-\frac{2M}{r}+\frac{J^2}{r^3}\right)+\frac{2}{r^3}\int dr\left(2MrN_1(r)+\frac{\kappa}{l_P}r^3f_0(r)\langle T_{rr}\rangle\right)\right]+\frac{c_2}{r^2}+c_3, \tag{4.38}$$

$$Jk_1(r)=-f_1(r)-2f_0(r)N_1(r)+2\int rdr\left(\frac{2N_1(r)}{\ell^2}+f_0(r)l_P^{-1}\kappa\langle T_{rr}\rangle\right)+c_4. \tag{4.39}$$

The integration constants c_1, c_2, c_3 and c_4 are set to zero so that N_1, f_1 and k_1 vanish for vanishing RSET. Note that f_1 and k_1 are determined by N_1 and $\langle T^r_r\rangle=f_0(r)\langle T_{rr}\rangle$.

We next give the explicit form of the semiclassical corrections for the different BTZ backgrounds.

1. Semiclassical corrections to the nonextremal black hole

The backreaction corrections to the nonextremal rotating BTZ BH are determined using Eqs. (3.20)–(3.24) together with Eqs. (4.37)–(4.39), yielding

$$N_1(r)=\frac{\ell^2}{(\alpha_+^2-\alpha_-^2)}\sum_{n=1}^{\infty}{}'\frac{a_nc_n-2\alpha_-\alpha_+e_n}{b_nd_n^{3/2}}, \tag{4.40}$$

$$f_1(r)=-\frac{1}{32r^2(\alpha_+^2-\alpha_-^2)}\times\sum_{n=1}^{\infty}{}'\frac{4h_n(a_nc_n-2\alpha_-\alpha_+e_n)+c_nd_n^2(\alpha_+^2-\alpha_-^2)^3}{b_n^2d_n^{3/2}}, \tag{4.41}$$

$$k_1(r)=\frac{\ell}{4r^2}\sum_{n=1}^{\infty}{}'\frac{(\alpha_-^2+\alpha_+^2)e_n-\alpha_-\alpha_+(c_n-4)c_n}{b_n^2d_n^{1/2}}, \tag{4.42}$$

where a_n, b_n, c_n, e_n and d_n are given in Eqs. (3.25), (3.27), (3.28), (3.29) and (3.32), respectively, with

$$h_n\equiv(4r^2-\ell^2\alpha_+^2)(4r^2-\ell^2\alpha_-^2)b_n+(\alpha_+^2-\alpha_-^2)\left(4r^2-\frac{(\alpha_+^2+\alpha_-^2)\ell^2}{2}\right)d_n. \tag{4.43}$$

For plots of the (equivalent of the) functions $N_1(r)$, $f_1(r)$ and $k_1(r)$ in the backreacted metric, we refer the reader to [56].

2. Semiclassical corrections to the extremal black hole

Using Eqs. (3.34)–(3.38) together with Eqs. (4.37)–(4.39) we obtain the semiclassical corrections to the extremal BTZ BH case:

$$N_1(r)=\sum_{n=1}^{\infty}{}'\frac{A_n}{2\pi n\alpha\sinh(2\pi n\alpha)d_n^{3/2}}, \tag{4.44}$$

$$f_1(r)=-\ell^4\sum_{n=1}^{\infty}{}'\frac{(\frac{r^2}{\ell^2}-\alpha^2)^2B_n+2\alpha(\frac{r^2}{\ell^2}-\alpha^2)\sinh(2\pi\alpha n)C_n+D_n}{r^2\pi^2n^2\alpha\sinh(2\pi\alpha n)d_n^{3/2}}, \tag{4.45}$$

$$k_1(r)=-\gamma\ell\sum_{n=1}^{\infty}{}'\frac{2\pi^2\alpha^2n^2(\cosh^2(2\pi n\alpha)+1)-\sinh^2(2\pi n\alpha)}{2r^2\pi^2n^2\sinh^2(2\pi n\alpha)d_n^{1/2}}, \tag{4.46}$$

where

$$A_n\equiv\ell^2(\sinh^2(2\pi n\alpha)+2\pi^2n^2\alpha^2(\cosh^2(2\pi n\alpha)+1)-2\pi n\alpha(\cosh(2\pi n\alpha)+1)\sinh(2\pi n\alpha)), \tag{4.47}$$

$$B_n\equiv 6n^3\pi^3\alpha^2(\cosh^2(2\pi\alpha n)+1)-4n^2\pi^2\alpha\sinh(2\pi\alpha n)\cosh^2(\pi\alpha n)+3n\pi\sinh^2(2\pi\alpha n), \tag{4.48}$$

$$C_n\equiv n^2\pi^2\alpha^2(\cosh^2(2\pi\alpha n)+1)\mathrm{sech}^2(\pi\alpha n)+2n\pi\alpha\sinh(2\pi\alpha n)+2\sinh^2(\pi\alpha n), \tag{4.49}$$

$$D_n\equiv 8\alpha^3\sinh^2(\pi\alpha n)\sinh(2\pi\alpha n), \tag{4.50}$$

with d_n given in Eq. (3.39). We remind the reader that $\alpha=r_+/\ell=\sqrt{M/2}>0$ and the angular momentum $J=\gamma M\ell$ with $\gamma=\pm1$.

3. Semiclassical corrections to the nonextremal naked singularity

In the case of the nonextremal NS, using Eqs. (3.46)–(3.50) together with Eqs. (4.37)–(4.39), the following backreaction corrections are found:

$$N_1(r) = -\frac{\ell^2}{2(\beta_+^2-\beta_-^2)}\sum_{n=1}^{N-1}{}' \frac{a_n c_n - 2\beta_+\beta_- e_n}{b_n d_n^{3/2}}, \tag{4.51}$$

$$f_1(r) = \sum_{n=1}^{N-1}{}' \frac{4h_n(a_n c_n - 2\beta_+\beta_- e_n) - c_n d_n^2(\beta_+^2-\beta_-^2)^3}{64r^2(\beta_+^2-\beta_-^2)b_n^2 d_n^{3/2}}, \tag{4.52}$$

$$k_1(r) = -\frac{\ell}{8r^2}\sum_{n=1}^{N-1}{}' \frac{(\beta_-^2+\beta_+^2)e_n + \beta_+\beta_-(c_n-4)c_n}{b_n^2 d_n^{1/2}}, \tag{4.53}$$

where a_n, b_n, c_n, e_n and d_n are given in Eqs. (3.51), (3.53), (3.54), (3.55) and (3.58), respectively, with

$$h_n = (4r^2+\ell^2\beta_+^2)(4r^2+\ell^2\beta_-^2)b_n - (\beta_+^2-\beta_-^2)\left(4r^2+\frac{(\beta_+^2+\beta_-^2)\ell^2}{2}\right)d_n. \tag{4.54}$$

The integrals involving the RSET components were computed assuming $b_n \neq 0$, which is indeed the case.

Aside from the limits in the sums, the above expressions (4.51)–(4.53) are equal to the nonextremal rotating BH corrections (4.40)–(4.42) by means of the replacements $\alpha_\pm^2 \to -\beta_\pm^2$, $\cosh(\pi n\alpha_\pm) \to \cos(\pi n\beta_\pm)$, and $\alpha_+\alpha_- \sinh(\pi n\alpha_+)\times\sinh(\pi n\alpha_-) \to \beta_+\beta_- \sin(\pi n\beta_+)\sin(\pi n\beta_-)$.

V. ANALYSIS OF THE SEMICLASSICAL-BACKREACTED GEOMETRIES

In this section we shall investigate the physical properties of the geometries given by the semiclassical-backreacted metrics which we have obtained in the previous section. As usual, we shall split this investigation between the different background space-times.

A. Static black hole

As shown in [29] for the static BH case, by setting c_0 in Eq. (4.16) to be equal to the mass $M > 0$ of the background BH, the quantum corrections lead to a growth of order l_P of the event horizon and to the formation of a curvature singularity at $r = 0$.

B. Static naked singularity

The static solution of semiclassical Einstein equation given in (4.14) has an arbitrary integration constant c_0 whose choice corresponds to the freedom of describing different physical setups. The analysis of the space-time structure, performed in [31] considering $c_0 = M \leq 0$ in Eq. (4.14) corresponds to the study of quantum corrections on the classical conical singularities of mass M. For finite M a horizon forms at the radius

$$r_+^{(q)}(l_P \to 0) = \frac{2F(M)}{-M} l_P + O(l_P^2), \tag{5.1}$$

while for $M \to 0^-$, the horizon is at

$$r_+^{(q)}(M \to 0^-) = \left[2\frac{l_p}{\ell}F(0)\right]^{1/3}\ell + O(M). \tag{5.2}$$

This horizon hides a curvature singularity inside (at $r = 0$). In the background space-time, the (naked) singularity was a causal singularity and of timelike character. On the other hand, in the backreacted space-time, the (horizon-hidden) singularity is a curvature singularity and of spacelike character (as in Schwarzschild space-time).

The fact that the backreacted metric corresponds to a BH prompts the question of whether there is a classical solution of Einstein equations that corresponds to this metric. We examine this possibility by choosing $c_0 = 3(F(M)l_P/\ell)^{2/3}$ in Eq. (4.14), so as to match the BH classical solution (2.13), which exhibits an event horizon with radius

$$r_+ = 2\ell\left(\frac{c_0}{3}\right)^{1/2} = 2\ell\left(\frac{l_p}{\ell}F(M)\right)^{1/3}. \tag{5.3}$$

This horizon is of the same order in l_P as the result in Eq. (5.2). This classical solution for the metric extremizes the one-loop effective action where the role of the classical scalar field is played by $\sqrt{\frac{8C}{\kappa(r+C)}}$ [see Eq. (2.15)], with $C = \ell(F(M)l_p/\ell)^{1/3}$. This dressed BH has a mass—the conserved charge associated with the time translation symmetry at infinity—given by [46]

$$\mathcal{M} = 3\left(\frac{l_P F(M)}{\ell}\right)^{2/3}. \tag{5.4}$$

The corresponding temperature and entropy of this black hole are [46]

$$T = \frac{3\sqrt{3}}{\pi}\left(\frac{l_P}{\ell}\right)\mathcal{M}^{1/2}, \qquad S = \frac{2\pi}{3\sqrt{3}}\left(\frac{\ell}{l_P}\right)\mathcal{M}^{1/2}, \tag{5.5}$$

respectively.[13] The first law of thermodynamics $d\mathcal{M} = TdS$ is directly verified from Eqs. (5.4) and (5.5). As noted in [46], due to the conformal coupling, the area law for entropy is corrected as

$$S = \left(1-\frac{\kappa}{8}\phi^2(r_+)\right)\frac{\pi r_+}{2l_p} = \frac{\pi r_+}{3l_p}. \tag{5.6}$$

[13] In Eqs. (5.4) and (5.5) we have set $\kappa = \pi$.

C. Rotating black hole

From the analytical solution of the backreaction equations given in the previous section, we shall now investigate how the quantum corrections modify the background BH geometry. It is important to stress that our results are valid for nonextremal BHs as well as for extremal ones.

1. Asymptotic structure

At infinity the corrections are negligible, since $N_1 \to \frac{1}{r^3}$, $f_1 \sim \frac{1}{r}$ and $k_1 \sim \frac{1}{r^3}$ as $r \to \infty$ (we remind the reader that $N_0(r) = 1$, $k_0(r) = O(\frac{1}{r^2})$ and $f_0(r) \to r^2$). Therefore, the quantum corrections do not modify the asymptotic structure of the BTZ background space-time.

2. Horizons

Let us now study the quantum backreaction on the Cauchy and event horizons. In order to study their stability properties it is useful to compute the curvature invariants of the quantum-backreacted space-time. The correction "$-2\kappa\langle T^{\mu}{}_{\mu}\rangle$" [which is $O(l_P)$] to the background Ricci scalar $R = 6\Lambda$ is zero because the RSET, which is the source of the semiclassical Einstein equations, is traceless. In its turn, the Kretschmann of the backreacted metric is

$$R_{\mu\nu\rho\sigma}R^{\mu\nu\rho\sigma} = 4R_{\mu\nu}R^{\mu\nu} - R^2 = 12\Lambda^2 + 4\kappa^2\langle T^{\mu}{}_{\nu}\rangle\langle T^{\nu}{}_{\mu}\rangle, \tag{5.7}$$

where the semiclassical Einstein equations and the tracelessness of the RSET have been used.

With regards to the event horizon, we first note that the RSET is regular at the classical event horizon. At $r = r_+ = \ell\alpha_+/2$, we have from Eqs. (3.20)–(3.24) that

$$\kappa^2\langle T^{\mu}{}_{\nu}\rangle\langle T^{\nu}{}_{\mu}\rangle|_{r=r_+} = \frac{3l_P^2}{4\ell^6}\sum_{n,m=1}^{\infty}\frac{c_n c_m}{(\cosh(n\pi\alpha_+)-1)^{3/2}(\cosh(m\pi\alpha_+)-1)^{3/2}}, \tag{5.8}$$

with $c_n = \cosh(n\pi\alpha_+) + \cosh(n\pi\alpha_-) + 2$, already defined in (3.28). The invariant (5.8) is regular and so, from Eq. (5.7), it follows that the Kretschmann scalar at the event horizon (of the background space-time) is also regular.

In order to find the event horizon of the quantum-corrected solution, we look for the largest root of

$$g^{rr} = f(r) = \frac{r^2}{\ell^2} - M + \frac{J^2}{4r^2} + l_P f_1(r) = 0 \tag{5.9}$$

where we have used Eqs. (4.18), (4.21) and (4.23). Working at $O(l_P)$, it is enough to replace $f_1(r)$ with $f_1(r_+)$, provided $r_+ \gg l_P$, and consider the largest solution of the resulting quartic equation.[14] The radius $r_+^{(q)}$ of the event horizon of the backreacted metric is then given by

$$\left(\frac{r_+^{(q)}}{\ell}\right)^2 = \frac{M - l_P f_1(r_+)}{2} + \frac{1}{2}\sqrt{(M - l_P f_1(r_+))^2 - \frac{J^2}{\ell^2}}. \tag{5.10}$$

It is understood that the above expression must be expanded at leading order in l_P, which in the nonextremal case yields

$$r_+^{(q)} = r_+\left(1 - \frac{2l_P f_1(r_+)}{\alpha_+^2 - \alpha_-^2}\right), \tag{5.11}$$

with $\alpha_+^2 - \alpha_-^2 = 4\sqrt{M^2 - J^2\ell^{-2}}$.

From Eq. (4.41) we arrive at

$$f_1(r_+) = -\frac{\sqrt{2}(\alpha_+^2 - \alpha_-^2)}{8\ell\alpha_+^2}\sum_{n=1}^{\infty}\frac{\alpha_+^2 c_n(c_n - 4) - 2\alpha_+\alpha_- e_n}{b_n^2\sqrt{\cosh(n\pi\alpha_+) - 1}}. \tag{5.12}$$

One can proof that $f_1(r_+) < 0$. In fact, by writing $\alpha_\pm \equiv s \pm \Delta$, where $s > 0$ and $\Delta > 0$, we have that the numerator of the summand in Eq. (5.12) is

$$\begin{aligned}&\alpha_+^2((\cosh(n\pi\alpha_+) + \cosh(n\pi\alpha_-))^2 - 4) - 4\alpha_+\alpha_-\sinh(n\pi\alpha_+)\sinh(n\pi\alpha_-)\\ &\quad = 4(s+\Delta)[s\sinh^2(n\pi\Delta)(1 + \cosh^2(n\pi s)) + \Delta\sinh^2(n\pi s)(1 + \cosh^2(n\pi\Delta))] > 0.\end{aligned} \tag{5.13}$$

Thus, Eq. (5.11) implies $r_+^{(q)} > r_+$. That is, the radius of the quantum-corrected event horizon is larger than the classical one.

The event horizon of the extreme BTZ black hole is located at $r_+^{\text{ext}} = \ell\sqrt{M/2} \equiv \ell\alpha$. From Eq. (4.45) we obtain

$$f_1^{\text{ext}}(\ell\alpha) \equiv f_1(r_+^{\text{ext}}) = -\frac{1}{\ell\pi^2}\sum_{n=1}^{\infty}\frac{1}{n^2\sinh(n\pi\alpha)} < 0. \tag{5.14}$$

Following the same procedure for obtaining the radius of the event horizon in the nonextremal case, we obtain the corrected horizon radius

[14] Clearly, this procedure would not work if we wanted to analytically extend our solution to the NS regime, where there is no horizon at the classical level.

$$r_+^{\mathrm{ext}(q)} = r_+^{\mathrm{ext}} + \frac{\ell}{2}\sqrt{-l_P f_1^{\mathrm{ext}}(\ell\alpha)}, \tag{5.15}$$

where the leading order correction term is now $O(\sqrt{l_P})$, instead of $O(l_P)$ as in the nonextremal case shown in Eq. (5.11). Note that the corrected horizon $r_+^{\mathrm{ext}(q)}$ is greater than the classical one r_+^{ext}. Moreover, from Eqs. (5.12) and (5.14), it is easy to see that $f_1^{\mathrm{ext}}(\ell\alpha) = \lim_{J\to M\ell} f_1(r_+)$.

Let us now consider the quantum corrections at the inner (Cauchy) horizon r_-. As already remarked in [32] and as we mentioned in Sec. III B, the RSET in Eqs. (3.20)–(3.24) is divergent at a series of circles $r = r_n$ for which d_n vanishes, i.e., at

$$\frac{r_n^2}{\ell^2} = \frac{\alpha_-^2(\cosh(n\pi\alpha_+) - 1) - \alpha_+^2(\cosh(n\pi\alpha_-) - 1)}{4(\cosh(n\pi\alpha_+) - \cosh(n\pi\alpha_-))}. \tag{5.16}$$

As $n \to \infty$, r_n approaches r_- from the inside, i.e., $\frac{r_n^2}{\ell^2} \to \frac{\alpha_-^2}{4}$. This accumulation produces an essential singularity at r_-. We see via Eq. (5.7) that the divergence of $\langle T^{\mu}{}_{\nu}\rangle\langle T^{\nu}{}_{\mu}\rangle$ at r_- produces a curvature singularity (in the Kretschmann scalar) there. As mentioned, the singularity at the Cauchy horizon arises when approaching it from its inside, i.e., as $r \to r_-^-$. In Kerr, it has been shown that classical field perturbations in the region inside the Cauchy horizon possess unstable modes [61]. However, near the singularity in Kerr there exist closed timelike curves and so the initial value problem is in principle not well posed there (even after requiring specific boundary conditions on the singularity). The rotating BTZ BH case here, on the other hand, possesses no closed timelike curves anywhere and so we are free from their troubles.

A singularity at the Cauchy horizon is not unexpected. In (3 + 1)-D, classical perturbations of the external region of Reissner-Nordström and Kerr space-times grow without bound at the inner (Cauchy) horizon, thus producing a "mass inflation" curvature singularity there [8,11–13]. It was shown in [35] that a similar unbounded growth of the perturbations (and of the local mass function) happens in (2 + 1)-D for the rotating BTZ BH at r_-. Furthermore, at a quantum level, there are indications that the RSET diverges in at least a part of the CH in Reissner-Nordström and Kerr(-Newman) background space-times [19–22].

Within our linear perturbative analysis, and following the same reasoning adopted in [62], we can study the quantum corrections to the inner horizon. As we did for the event horizon, provided $r_- \gg l_P$, we can replace $f_1(r)$ with $f_1(r_-)$ in Eq. (5.9) and consider its smallest positive root. The radius $r_-^{(q)}$ of the Cauchy horizon of the backreacted metric is then given via

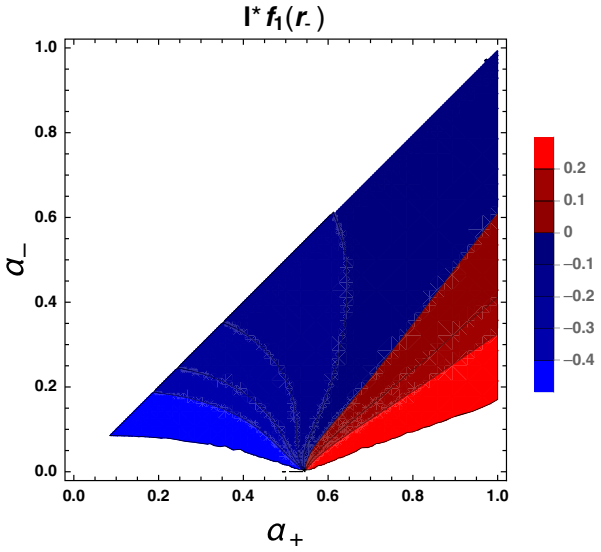

FIG. 11. This is $f_1(r_-)$ in Eq. (5.19) as a function of α_- and $\alpha_+(>\alpha_-)$. The red and blue shades correspond to, respectively, positive and negative values of $f_1(r_-)$. Equation (5.19) shows that $f_1(r_-)$ diverges in the static limit $\alpha_- \to 0$, as the plot indicates (N.B.: the numerical calculation was not accurate enough for α_- very close to zero).

$$\left(\frac{r_-^{(q)}}{\ell}\right)^2 = \frac{M - l_P f_1(r_-)}{2} - \frac{1}{2}\sqrt{(M - l_P f_1(r_-))^2 - \frac{J^2}{\ell^2}}, \tag{5.17}$$

which at $O(l_P)$ reduces to

$$r_-^{(q)} = r_-\left(1 + \frac{2l_P f_1(r_-)}{\alpha_+^2 - \alpha_-^2}\right). \tag{5.18}$$

It turns out that the sign of the quantum correction to the radius of the inner horizon is given by the sign of $f_1(r_-)$, where

$$f_1(r_-) = \frac{\sqrt{2}(\alpha_+^2 - \alpha_-^2)}{8\ell\alpha_-^2}\sum_{n=1}^{\infty}\frac{\alpha_-^2 c_n(c_n - 4) - 2\alpha_+\alpha_- e_n}{b_n^2\sqrt{\cosh(n\pi\alpha_-) - 1}}. \tag{5.19}$$

One can show that, close to extremality, $f_1(r_-)$ is finite and negative. This means that the inner horizon is pushed inwards (i.e., $r_-^{(q)} < r_-$) and "disappears from the space-time", which ends up in the future at a spacelike curvature singularity at r_-. Thus, the causal structure of the back-reacted rotating black hole is essentially that of the static black hole in Fig. 1(a). This means that, in this case, quantum effects act to preserve strong CCH. The same considerations apply to the extremal case, where $f_1(r_-)$ is given by (5.14) and the corrected inner horizon radius takes the form (5.15) but with r_+ replaced by r_- and a minus sign in front of the correction term.

We cannot check, with our method, what happens in the opposite regime (i.e., in the weak rotating limit) since, in this regime, the inner horizon is close to $r = 0$ and so $f_1(r)$ cannot be replaced with $f_1(r_-)$ in Eq. (5.9). We plot $f_1(r_-)$ in Fig. 11. This plot shows that the sign of $f_1(r_-)$ changes when varying M and J. When it is negative, the radius of the Cauchy horizon diminishes and is smaller than the radius where the curvature singularity is. Therefore, in this case, the singularity is also spacelike and strong CCH is preserved. On the other hand, when $f_1(r_-)$ is positive, the radius of the Cauchy horizon increases and is larger than the radius where the singularity is. Therefore, in this case, the singularity is timelike and strong CCH continues to be violated even in the backreacted space-time. Figure 11 also indicates a divergence in $f_1(r_-)$ in the static limit. This divergence seems to come from the fact that the image of the point $r = 0$ in the static case is itself, and so the chordal distance in Eq. (3.32) is equal to zero in the static case for the point $r = 0$.

3. Hypersurfaces outside rotating black holes: Ergosphere and absence of superradiant instability

Another surface of interest in the rotating BTZ space-time is the static limit surface, defined by $g_{tt} = 0$. In order to find the radius of the static limit surface of the quantum-corrected space-time, we solve

$$g_{tt} = -N^2(r)f(r) + r^2k^2(r) = 0. \tag{5.20}$$

Working at $O(l_P)$, the equation to solve is

$$-\left(\frac{r^2}{\ell^2} - M\right) - l_P(2f_0N_1 + f_1 + Jk_1) = 0. \tag{5.21}$$

Using the results in Eqs. (4.40)–(4.42), we see that the three last terms take a rather simple form:

$$2f_0N_1 + f_1 + Jk_1 = -\sum_{n=1}^{\infty}{}' \frac{(\alpha_+^2 + \alpha_-^2)c_n(c_n - 4) - 4\alpha_+\alpha_-e_n}{4b_n^2 d_n^{1/2}}, \tag{5.22}$$

which is shown to be negative[15] for all r such that $d_n > 0$.

In order to solve Eq. (5.21), for large enough radius in comparison with l_P, we evaluate the terms in Eq. (5.22) [which are multiplied by l_P when appearing in Eq. (5.21)] on the classical static limit surface $r_{\rm SL}^2 = \ell^2 M = \ell^2(\alpha_+^2 + \alpha_-^2)/4$. Let us denote by $r_{\rm SL}^{(q)}$ and $r_{\rm SL}^{{\rm ext}(q)}$ the radii of the static limit surface of the quantum-backreacted nonextremal and extremal BH geometries, respectively. For the nonextremal geometry, we obtain

$$\frac{r_{\rm SL}^{(q)2}}{\ell^2} - \frac{r_{\rm SL}^2}{\ell^2} = -l_P(2f_0N_1 + f_1 + Jk_1)|_{r=r_{\rm SL}} > 0. \tag{5.23}$$

Therefore, like for the event horizon, the quantum corrections increase the radius of the static limit surface. In the extremal case we obtain, from Eq. (5.21) and using Eqs. (4.44)–(4.46),

$$(r_{\rm SL}^{{\rm ext}(q)})^2 - (r_{\rm SL}^{\rm ext})^2 = l_P\ell \sum_{n=1}^{\infty} \frac{\sinh^2(2n\pi\alpha) + n^2\pi^2\alpha^2(\cosh(4n\pi\alpha) + 3)}{2\pi^2 n^2 \sinh^2(2n\pi\alpha)\sqrt{\sinh(n\pi\alpha)(\sinh(n\pi\alpha) + n\pi\alpha\cosh(n\pi\alpha))}}, \tag{5.24}$$

which is also positive. At this point, it is interesting to evaluate the quantum correction to the "size" $r_{\rm SL} - r_+$ of the ergoregion by computing, from Eqs. (5.11) and (5.23),

$$[(r_{\rm SL}^{(q)})^2 - (r_+^{(q)})^2] - [r_{\rm SL}^2 - r_+^2] = \frac{\sqrt{2}l_P\ell}{8}\sum_{n=1}^{\infty}\left[\frac{\sqrt{\alpha_+^2 - \alpha_-^2}((\alpha_+^2 + \alpha_-^2)c_n(c_n - 4) - 4\alpha_+\alpha_-e_n)}{b_n^2\sqrt{\alpha_+^2(\cosh(n\pi\alpha_+) - 1) - \alpha_-^2(\cosh(n\pi\alpha_-) - 1)}} - \frac{\alpha_+^2 c_n(c_n - 4) - 2\alpha_+\alpha_-e_n}{b_n^2\sqrt{\cosh(n\pi\alpha_+) - 1}}\right]. \tag{5.25}$$

We could not determine the sign of the right-hand side of Eq. (5.25) analytically. However, we carried out a numerical evaluation and this sign seems to be always negative (although for α_- very close to zero the numerics were not reliable).

In the extremal case, where the $O(\sqrt{l_P})$ correction to r_+ is larger than the $O(l_P)$ correction to $r_{\rm SL}$, we have

$$[(r_{\rm SL}^{{\rm ext}(q)})^2 - (r_+^{{\rm ext}(q)})^2] - [(r_{\rm SL}^{\rm ext})^2 - (r_+^{\rm ext})^2] = -\ell r_+^{\rm ext}\sqrt{-l_P f_1^{\rm ext}(\ell\alpha)} < 0, \tag{5.26}$$

where $r_+^{{\rm ext}(q)}$ denotes the radius of the event horizon of the backreacted extremal BH geometry.

We shall now turn to the evaluation of the quantum corrections to the angular velocity of the BH using

[15]This statement can be checked by writing $\alpha_\pm = s \pm \Delta$, and so we have that the numerator of the summand in Eq. (5.22) is $(\alpha_+^2 + \alpha_-^2)((\cosh(n\pi\alpha_+) + \cosh(n\pi\alpha_-))^2 - 4) - 8\alpha_+\alpha_-\sinh(n\pi\alpha_+)\sinh(n\pi\alpha_-) = 8[s^2\sinh^2(n\pi\Delta)(1 + \cosh^2(n\pi s)) + \Delta^2\sinh^2(n\pi s)(1 + \cosh^2(n\pi\Delta))] > 0$.

Eq. (4.21). We find that the angular velocity of the quantum-corrected BH is

$$\Omega_H^{(q)} = \left.\frac{g^{t\theta}}{g^{tt}}\right|_{r=r_+^{(q)}} = -k|_{r=r_+^{(q)}} = \frac{J}{2(r_+^{(q)})^2} - l_P k_1(r_+). \tag{5.27}$$

In the nonextremal case, combining the two contributions to $\Omega_H^{(q)}$, we find at $O(l_P)$,

$$\Omega_H^{(q)} - \Omega_H = -\frac{\sqrt{2} l_P(\alpha_+^2 - \alpha_-^2)}{\ell^2 \alpha_+^2} \sum_{n=1}^{\infty} \frac{\sinh(n\pi\alpha_+)\sinh(n\pi\alpha_-)}{b_n^2(\cosh(n\pi\alpha_+)-1)^{1/2}}, \tag{5.28}$$

where $\Omega_H = J/(2r_+^2)$. Note that the right-hand side of (5.28) has a sign opposite to that of Ω_H because $J\sinh(n\pi\alpha_-) > 0$. Therefore, the quantum corrections to the angular velocity reduce its absolute value. The same effect occurs in the extremal case. We denote by $\Omega_H^{\mathrm{ext}(q)}$ and Ω_H^{ext} the angular velocity of the black hole in, respectively, the backreacted and background geometries. From Eq. (5.27) and Eqs. (4.44)–(4.46), we obtain

$$\Omega_H^{\mathrm{ext}(q)} - \Omega_H^{\mathrm{ext}} = -\frac{\gamma\sqrt{-f_1^{\mathrm{ext}}(\ell\alpha)}}{2\sqrt{2}\alpha\ell}\sqrt{l_P}, \tag{5.29}$$

with $\Omega_H^{\mathrm{ext}} = \gamma/(2\ell)$. Since the quantum correction to r_+^{ext} is of the order $O(l_P^{1/2})$ [see Eq. (5.15)], we obtain the same leading order for the correction to the angular velocity.

Finally, we inspect the possible appearance of a speed of light surface, which would—likely—make the space-time superradiantly unstable [63].[16] For this purpose, we consider the quantum-corrected Killing vector $\chi^{(q)} = \partial/\partial t + \Omega_H^{(q)}\partial/\partial\theta$. This vector has squared norm

$$\begin{aligned}\chi^{(q)2} = g_{\mu\nu}\chi^{(q)\mu}\chi^{(q)\nu} &= -N^2 f + r^2 k^2 + 2r^2 k\Omega_H^{(q)} + r^2\Omega_H^{2(q)} \\ &= -(f_0(r) + l_P f_1(r)) - 2l_P f_0(r)N_1 \\ &\quad + \frac{J^2}{4r^2}\left(\frac{r^2}{r_+^{2(q)}} - 1\right)^2 - Jl_P\left(\frac{r^2}{r_+^2} - 1\right) \\ &\quad \times (k_1(r_+) - k_1(r)) + O(l_P^2).\end{aligned} \tag{5.30}$$

Classically,

[16]Although the BTZ BH is unstable under *massive* scalar field perturbations due to modes whose frequency has a real part that lies within the superradiant regime [64], this is not considered the "standard" superradiant instability, which refers to a massless scalar field.

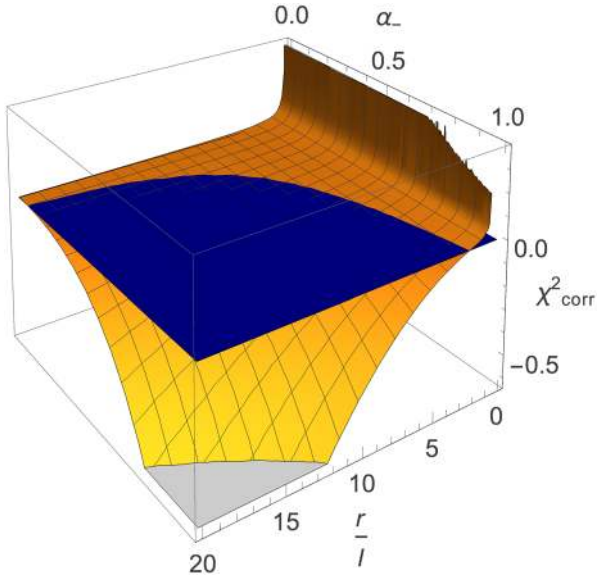

FIG. 12. Plot of the $O(l_P)$ correction (χ^2_{corr}) to χ^2 in Eq. (5.34) as a function of r and α_- for the fixed value of $\alpha_+ = (\sqrt{3}+1)/\sqrt{2} \approx 1.93$. The blue horizontal plane corresponds to zero.

$$\chi^2 = -\frac{(r_+^2 - r_-^2)(r^2 - r_+^2)}{l^2 r_+^2}. \tag{5.31}$$

The vector $\chi^{(q)}$ is timelike in the near-horizon region [where the terms in the second line of (5.30) go like "$-A(r^2 - r_+^{(q)^2})$", with A a positive constant, and the terms in the third line go like $\sim(r^2 - r_+^{(q)^2})^2$] and becomes null on the horizon. At radial infinity, where N_1, f_1, $k_1 \to 0$, we have that

$$\chi^{(q)^2} \sim -\frac{r^2}{\ell^2}(1 - \ell^2\Omega_H^{(q)2}), \qquad r \to \infty. \tag{5.32}$$

The condition for it to be spacelike, and (likely) for the space-time to develop a superradiant instability is

$$\ell\Omega_H^{(q)} > 1. \tag{5.33}$$

Classically, this condition is not met, i.e., $\ell\Omega_H \leq 1$ (the equality being realized in the extremal case). Equation (5.28) implies that, in the nonextremal case, it is $\ell\Omega_H^{(q)} < \ell\Omega_H < 1$, and, in the extremal case, $\ell\Omega_H^{ext(q)} < \ell\Omega_H^{\mathrm{ext}} = 1$. This suggests that the quantum effects do not change the superradiant stability property of the BTZ BH.

In order to investigate the norm of χ^2 more widely, we first obtain explicitly the $O(l_P)$ correction to χ^2 in the subextremal case from Eqs. (5.30) and (5.11):

$$\chi^{(q)^2} = \chi^2 + l_P\Bigg(-f_1(r) - 2f_0(r)N_1 + \frac{J^2\ell^2 f_1(r_+)}{2r_+^4}\frac{(r^2-r_+^2)}{(r_+^2-r_-^2)} - J\left(\frac{r^2}{r_+^2}-1\right) \times (k_1(r_+)-k_1(r))\Bigg) + O(l_P^2). \tag{5.34}$$

We plot this $O(l_P)$ correction to χ^2 in Fig. 12. [N.B.: for the large-r behavior in Eq. (5.32) to be seen in Fig. 12 for small α_-, the plot should be performed to larger values of r].

In the extremal case, where $\chi^2 = 0$ identically [see (5.31)], the quantum-corrected $\chi^{ext(q)^2}$ is entirely given by the quantum corrections, whose leading term, $O(\sqrt{l_p})$, comes from the first term in the last line of Eq. (5.30) and from $r_+^{(q)}$ [see Eq. (5.15)]. We then obtain

$$\chi^{ext(q)^2} = -\frac{J^2\ell}{2(r_+^{\rm ext})^3}\left(\frac{r^2}{r_+^2}-1\right)\sqrt{-l_p f_1(l\alpha)} < 0. \tag{5.35}$$

Thus the quantum corrections turn the classically identically null $\chi^{\rm ext}$ timelike.

D. Rotating naked singularity

1. Emergence of an event horizon

The first-order quantum correction to the metric component g^{rr} of the NS geometry, $f_1(r)$ in Eq. (4.18), is responsible for the formation of a horizon. In order to see this, we note that $f_1(r)$ has a finite number of poles at radii r_n where d_n vanishes [see Eq. (3.61)]. As we will shown below at these poles $f_1 \to -\infty$, turning the otherwise positive definite $g^{rr}_{\rm classical} = f_0(r)$, into a function that vanishes at some finite radii. The largest radius at which g^{rr} vanishes is the event horizon of the quantum-backreacted metric, $r_+^{(q)}$.

The zeroes of d_n form a finite set, the largest of them, which we denote by r_*, occurs at a certain value $n = n_*$,

$$r_*^2 = \frac{\ell^2}{2b_{n_*}}\left(\beta_-^2\sin^2\left(\frac{1}{2}\pi n_*\beta_+\right) - \beta_+^2\sin^2\left(\frac{1}{2}\pi n_*\beta_-\right)\right). \tag{5.36}$$

This zero appears twice in the sum that defines $f_1(r)$ due the symmetry of the summand in Eq. (4.52) under $n \to N-n$. At $r = r_*$ the geometry has a curvature singularity (since the Kretschmann invariant (5.7) diverges) and therefore the spacetime cannot be extended to $r < r_*$.

From (4.52) the correction $f_1(r)$ can be seen to diverge as $(r-r_*)^{3/2}$ near r_*,

$$f_1(r) = \frac{\Xi f_0(r_*)}{(r-r_*)^{3/2}} + C, \qquad r \to r_*, \tag{5.37}$$

where C is a finite constant and

$$\Xi \equiv \frac{\sqrt{\beta_+^2-\beta_-^2}\,\ell^2(a_{n^*}c_{n^*} - 2\beta_-\beta_+ e_{n^*})}{32 b_{n^*}(-b_{n^*}r^*)^{3/2}}. \tag{5.38}$$

First, we note that the combination $a_{n_*}c_{n_*} - 2\beta_-\beta_+ e_{n_*}$ in the numerator of the above equation is positive definite. Moreover, since $b_{n_*} < 0$, $\Xi < 0$. Then, using Eq. (5.37), the condition $g^{rr}|_{r_+^{(q)}} = 0$ that defines the quantum-corrected horizon can be written as

$$(f_0(r_+^{(q)}) + l_P C)(r_+^{(q)} - r_*)^{3/2} + l_P \Xi f_0(r_*) = 0. \tag{5.39}$$

Since $f_0(r)$ is an analytic function for $r \neq 0$, one can write $f_0(r_+^{(q)}) = f_0(r_*) + f_0'(r_*)(r_+^{(q)} - r_*) + O(r_+^{(q)} - r_*)^2$ near r_*. Replacing this Taylor expansion in Eq. (5.39), one finds that: (i) $r_+^{(q)} - r_*$ must be of the order $l_P^{2/3}$, (ii) C can be ignored and consequently,

$$r_+^{(q)} = r_* + (-\Xi l_P)^{2/3} + O(l_P^{7/3}). \tag{5.40}$$

Thus, the existence of a horizon and its radius have been established for the backreacted spacetime. The classical NS has been replaced by a rotating black hole whose horizon encloses a curvature singularity. This singularity at $r = r_*$ is spacelike since g^{rr} has no zero within $[r_*, r_+^{(q)})$.

Thus, in the cases that satisfy Eq. (3.62), except for the set $\mathcal{S}$ defined in Eq. (3.60), an event horizon forms; the other cases would have to be investigated separately.

2. Ergosphere

The radius of the static limit surface, which is the boundary of the ergosphere, is determined by Eq. (5.21). This equation can be solved near the singularity $r = r_*$, yielding

$$r_{\rm SL}^{(q)} = r_* + \mu l_P^2, \tag{5.41}$$

with

$$\mu \equiv \frac{(\beta_+^2-\beta_-^2)((\beta_-^2+\beta_+^2)(4-c_{n_*})c_{n_*} - 4\beta_-\beta_+ e_{n_*})^2}{16(-b_{n_*})^5 r_*((\beta_-^2+\beta_+^2) + (\frac{2r_*}{\ell})^2)^2}. \tag{5.42}$$

It follows that the right-hand side of the above equation is positive because $b_{n_*} < 0$. Since the distance $r_{\rm SL}^{(q)} - r_*$ is of order $O(l_P^2)$ and $r_+^{(q)} - r_*$ is of order $O(l_P^{2/3})$, as shown in Eq. (5.40), the static limit surface is located behind the event horizon.

VI. SUMMARY AND DISCUSSION

In this paper we have considered the $O(l_P)$ RSET for a conformally coupled massless scalar field in a background

$(2+1)$-dimensional BTZ geometry. This background corresponds to a black hole ($M > 0$) or to a naked conical singularity ($M < 0$). Using this RSET as an effective source for the Einstein equations, we have computed the quantum corrections to the original background metric (backreaction) both in the static and rotating cases. Our findings can be summarized as follows:

A. Static black hole

(i) The RSET given in Eqs. (3.18) is diagonal, traceless and conserved with respect to the background black hole geometry. For a fixed M, the backreacted metric has a quantum-corrected horizon with a radius larger than the classical one,

$$r_+^{(q)} = r_+ + \frac{F(M)}{M} l_P + O(l_P^2) > r_+, \quad (6.1)$$

where $F(M)$ is given in Eq. (3.19) and $r_+ = \sqrt{M}\ell$. For very small mass,

$$r_+^{(q)} = \left(2\frac{l_p}{\ell} F(0^+)\right)^{1/3} \ell + O(M), \quad (6.2)$$

where $F(0^+) = \zeta(3)/(2\pi^3) \approx 0.0193841$.

(ii) A *curvature* spacelike singularity is formed at $r = 0$.

B. Rotating black hole

(i) The RSET given in Eqs. (3.20)–(3.24) is traceless and conserved with respect to background black hole geometry (4.17). Its only off-diagonal $t-\theta$ components are compatible with the stationary rotating black hole solution. Again, the nonextremal backreacted metric has a quantum-corrected event horizon with a radius larger than the classical one,

$$r_+^{(q)} = r_+ - \frac{2f_1(r_+)r_+}{\alpha_+^2 - \alpha_-^2} l_P + O(l_P)^2 > r_+, \quad (6.3)$$

where $f_1(r_+) < 0$.

(ii) The radius r_- (which is the inner—Cauchy—horizon of the classical background space-time) becomes an accumulation surface for divergent contributions to the RSET at which the Kretschmann invariant blows up. In the quantum-corrected space-time, the curvature singularity at r_- can be either spacelike ($r_-^{(q)} < r_-$; this is the case close to, and at, extremality) or, depending on the values of M and J, timelike ($r_-^{(q)} > r_-$). In the former case, quantum mechanics provides a mechanism for strong cosmic censorship.

(iii) Similarly to the event horizon, the ergosphere is also pushed outwards (the quantum correction to its radius is always positive), while the black hole angular velocity generically diminishes.

(iv) In the extremal limit, our results could be interpreted by saying that the quantum corrections take the solution away from extremality.

C. Static naked singularity

(i) The RSET given in Eq. (3.43) is diagonal, traceless and conserved with respect to the background static conical geometry. The backreacted metric presents a horizon of nonvanishing radius,

$$r_+^{(q)} = \frac{2F(M)}{-M} l_P + O(l_P^2), \quad (6.4)$$

where $F(M)$ is given in Eq. (3.44). This result is valid for a finite mass M. In the limit $M \to 0^-$, the horizon radius is given by

$$r_+^{(q)} = \left[2\frac{l_p}{\ell} F(0)\right]^{1/3} \ell + O(M). \quad (6.5)$$

Figure 9 shows the continuity at $M = 0$ between the radius of the event horizon of the quantum-backreacted black hole and the radius of the newly formed event horizon of the quantum-backreacted naked singularity.

(ii) A *spacelike curvature* singularity is formed at $r = 0$. The appearance of a horizon around the classical naked singularity, and the fact that the timelike singularity of the background spacetime has become spacelike in the backreacted spacetime, means that, at least in this simplified setting, quantum mechanics provides a mechanism for strong cosmic censorship.

(iii) The backreacted geometry is obtained as a classical solution of the Einstein equations in the presence of the RSET given in Eq. (3.43). This stress-energy tensor happens to be the same as that for the Einstein-Hilbert action conformally coupled to a scalar field, Eq. (2.17) with $C = \ell[F(M)l_P/\ell]^{1/3}$. Hence, the backreacted metric can be interpreted as a classical solution of the form

$$ds^2 = -f(r)dt^2 + f^{-1}(r)dr^2 + r^2 d\theta^2, \quad (6.6)$$

with $f(r) \equiv \frac{1}{\ell^2}(r^2 - 3C^2 - \frac{2C^3}{r})$. In this interpretation, the geometry is that of a black hole with a tiny positive mass, $\mathcal{M} = 3[F(M)l_P/\ell]^{2/3}$, and a horizon radius $\tilde{r}_+$ of order $l_P^{1/3}$, $\tilde{r}_+^2 = (4/3)\mathcal{M}\ell^2$.

(iv) In [65], black holes localized on the brane in $3+1$-dimensional Randall-Sundrum braneworlds [66,67] were interpreted, via the AdS/conformal field theory (CFT) correspondence, as static quantum-corrected BTZ black holes and naked singularities. In particular, and despite the fact that the dual quantum

theory (CFT) living on the brane is poorly known, use of the AdS/CFT dictionary gives a brane black hole metric that has the same form as ours:

$$ds^2 = -\left(\frac{r^2}{\ell^2} - M - \frac{r_1(M)}{r}\right)dt^2 + \frac{dr^2}{\left(\frac{r^2}{\ell^2} - M - \frac{r_1(M)}{r}\right)} + r^2 d\theta^2, \tag{6.7}$$

for some function $r_1(M)$. For a slightly curved brane, it is $r_1(M) \sim N l_p f(M)$ (N being the (large) number of d.o.f. of the CFT on the brane) and f is a function that depends on the mass M. For zero-mass black holes, where $f(0) \sim O(1)$, as well as for naked singularities ($M < 0$), the correction term $\frac{r_1(M)}{r}$ leads to the formation of a horizon, in agreement with our results.

D. Rotating naked singularity

(i) The RSET given in Eqs. (3.46)–(3.50) is traceless and conserved with respect to the background rotating conical geometry. Similarly to the rotating black hole background above, its only off-diagonal $t-\theta$ components are compatible with the stationary rotating solution (4.17). Again, the backreacted metric also has an event horizon of radius

$$r_+^{(q)} = r_* + (-\Xi l_P)^{2/3}, \tag{6.8}$$

where r_* is the largest zero of d_n, and Ξ is the finite expression given in Eq. (5.38).

(ii) A *spacelike curvature* singularity is formed at the radius r_* given by Eq. (5.36). As in the static case, the appearance of a horizon and the spacelike character of the singularity in the backreacted spacetime mean that quantum mechanics acts as a strong cosmic censor.

(iii) A legitimate concern is about the validity of the perturbative approximation in powers of l_P for the geometry in view of the fact that $l_P f_1$ diverges at some finite r. This divergence is responsible for the formation of a horizon, which implies a change of topology and of the causal structure of the spacetime. The point is that for $r \gg l_P$ the geometry receives a very small correction of order $\hbar$ (as clearly seen in the static case, with a small horizon of the same order, $r_+ \sim l_P$). This is not too different from a perturbation of the Schwarzschild geometry by the addition of a small electric charge or angular momentum: the appearance of a (small) second horizon produces a small correction to the exterior metric. Depending on the experimental resolution, it might be irrelevant for an external observer whether the geometry has a second horizon or not, even if the topology and the causal structure both suffer major changes. For a small $M < 0$, the perturbative approximation is certainly more reliable and $r_+^{(q)} \sim (l_P)^{1/3}$ for $J = 0$, and $r_+^{(q)} \sim (l_P)^{2/3}$ for $J \neq 0$.

E. Extensions and open questions

(i) For rotating naked singularities we have assumed $\beta_\pm = 2/N_\pm$, with integer $N_\pm$. The method of images can also be extended to arbitrary rational values of $\beta_\pm$, but we did not consider this case in order to keep the discussion as simple as possible and to be able to make definite claims. Despite of the restriction on the values of $\beta_\pm$, our results are sufficient to explore rotating geometries for small angular momentum to claim that the conclusions drawn for the static case are generic and not an accidental consequence of the static symmetry. In the case of static flat space, the authors of [54] have shown that for continuous values of the angular deficit the resulting RSET interpolates between the discrete values obtained for $\beta = 2/N$. This suggests that a similar extension to arbitrary real values of $\beta_\pm$ is possibly doable in the spirit of [55].

(ii) An obvious direction for extension is imposing boundary conditions on the field different from the transparent conditions that we have considered here. In the static black hole case, Lifschytz and Ortiz [28] derive the RSET and investigate backreaction effects using Dirichlet and Neumann boundary conditions. From the expression for the RSET in Eq. (5.1) of [28] they show that the horizon grows for these two types of boundary conditions. Furthermore, letting $M \to -M$ in Eq. (5.1) of [28] so as to naively analytically continue from the black hole to the naked singularity case (ignoring differences in the summation limits), the backreaction on the naked singularity with Dirichlet and Neumann conditions can also be seen to be qualitatively the same as with transparent conditions. We expect that these qualitative backreaction behaviors are perturbatively reproduced in the rotating black hole and naked singularity cases.

(iii) Another direction in which this work can be extended is the inclusion of quantum matter to examine backreaction on other spacetimes. For example, other $(2+1)$-D geometries with naked singularities like BTZ spacetimes with $M < -1$ (angular excesses), or with $M\ell < |J|$; spacetimes with closed timelike curves [68], etc.

(iv) Quantum matter was also shown to form a horizon around conical singularities in asymptotically *flat* three-dimensional spacetimes in [54,69]. Although those papers did not identify the backreacted geometry as a black hole—perhaps because the existence

of black holes in $2+1$ dimensions was not widespread at the time—they suggest that results similar to ours could be found for naked singularities in flat and de Sitter three-dimensional spacetimes.

(v) The existence of locally propagating d.o.f. in higher dimensions means that, without a quantum theory of gravity, the cosmic censorship hypothesis for $D \geq 4$ could only be tested semiclassically: quantum effects on cosmic strings, the big bang or big crunch singularities in $3+1$ dimensions could only be examined with quantum matter on a classical background.

ACKNOWLEDGMENTS

We are thankful to Adrian C. Ottewill and Elizabeth Winstanley for useful discussions. M. C. acknowledges partial financial support by CNPq (Brazil), process number 310200/2017-2. This work has been partially funded by the Fondecyt Grants No. 1161311 and No. 1180368. The Centro de Estudios Científicos (CECs) is funded by the Chilean Government through the Centers of Excellence Base Financing Program of Conicyt. A. F. acknowledges partial financial support by the Spanish Ministerio de Economía, Industria y Competitividad Grants No. FIS2014-57387-C3-1-P and No. FIS2017-84440-C2-1-P, the Generalitat Valenciana Project No. SEJI/2017/042 and the Severo Ochoa Excellence Center Project No. SEV-2014-0398.

APPENDIX A: BLACK HOLES AND NAKED SINGULARITIES AS IDENTIFICATIONS IN $\mathbb{R}^{2,2}$

A general Killing vector $\mathbf{k}$ for the pseudosphere Eq. (2.8) embedded in $\mathbb{R}^{2,2}$ can be written in terms of the $so(2,2)$ generators $J_{ab} \coloneqq X_b\partial_a - X_a\partial_b$. Let us parametrize the pseudosphere with coordinates (t, r, θ). The BTZ geometries are then obtained by identifying points in the pseudosphere via the Killing vector

$$\mathbf{k} = \partial_\theta = \frac{\partial X^a}{\partial\theta}\partial_a = \frac{1}{2}\omega^{ab}J_{ab}, \tag{A1}$$

where the antisymmetric matrix ω^{ab} characterizes the identification.

Since $\mathbf{k} = \partial_\theta$, the identification corresponding to the action of the vector $2\pi\mathbf{k}$ means that the geometry is periodic in θ with period 2π. Identifying a point in the manifold with itself rotated by 2π can also be represented by the action of the matrix $H \coloneqq e^{2\pi\mathbf{k}}$ in the embedding space, such that $H^a{}_b X^b(\theta) = X^a(\theta + 2\pi)$.

1. Rotating nonextremal BTZ black hole

The rotating BTZ BH with mass M and angular momentum J is described by the line element in Eq. (2.1). It may be expressed in terms of $\alpha_\pm$ in Eq. (2.2) as

$$ds^2 = -\left(\frac{r^2}{\ell^2} - \frac{\alpha_+^2+\alpha_-^2}{4}\right)dt^2 + \frac{dr^2\ell^2r^2}{(r^2-\frac{\ell^2\alpha_+^2}{4})(r^2-\frac{\ell^2\alpha_-^2}{4})} - \frac{\ell\alpha_+\alpha_-}{2}dtd\theta + r^2d\theta^2. \tag{A2}$$

The various BTZ BH regions can be parametrized in terms of (t, r, θ) coordinates in the following way:
Region I: $r > r_+$.

$$X^0 = \sqrt{A_-}\cosh\left(\frac{\alpha_+\ell\theta - \alpha_- t}{2\ell}\right), \qquad X^1 = \sqrt{A_-}\sinh\left(\frac{\alpha_+\ell\theta - \alpha_- t}{2\ell}\right),$$
$$X^2 = \sqrt{A_+}\cosh\left(\frac{\alpha_+ t - \alpha_-\ell\theta}{2\ell}\right), \qquad X^3 = \sqrt{A_+}\sinh\left(\frac{\alpha_+ t - \alpha_-\ell\theta}{2\ell}\right). \tag{A3}$$

Region II: $r_- < r < r_+$.

$$X^0 = \sqrt{A_-}\cosh\left(\frac{\alpha_+\ell\theta - \alpha_- t}{2\ell}\right), \qquad X^1 = \sqrt{A_-}\sinh\left(\frac{\alpha_+\ell\theta - \alpha_- t}{2\ell}\right),$$
$$X^2 = -\sqrt{A_+}\sinh\left(\frac{\alpha_+ t - \alpha_-\ell\theta}{2\ell}\right), \qquad X^3 = -\sqrt{A_+}\cosh\left(\frac{\alpha_+ t - \alpha_-\ell\theta}{2\ell}\right). \tag{A4}$$

Region III: $0 < r < r_-$.

$$X^0 = \sqrt{-A_-}\sinh\left(\frac{\alpha_+\ell\theta - \alpha_- t}{2\ell}\right), \qquad X^1 = \sqrt{-A_-}\cosh\left(\frac{\alpha_+\ell\theta - \alpha_- t}{2\ell}\right),$$
$$X^2 = -\sqrt{-A_+}\sinh\left(\frac{\alpha_+ t - \alpha_-\ell\theta}{2\ell}\right), \qquad X^3 = -\sqrt{-A_+}\cosh\left(\frac{\alpha_+ t - \alpha_-\ell\theta}{2\ell}\right), \tag{A5}$$

where

$$A_\pm \equiv \frac{4r^2 - \alpha_\pm^2\ell^2}{\alpha_+^2 - \alpha_-^2}. \tag{A6}$$

The rotating BTZ space-time is obtained through identifications generated by the Killing vector

$$\mathbf{k} = \frac{\alpha_+}{2}J_{01} + \frac{\alpha_-}{2}J_{23}. \tag{A7}$$

The identification matrix $H = e^{2\pi\mathbf{k}}$ then takes the form

$$H = \begin{pmatrix} \cosh(\pi\alpha_+) & \sinh(\pi\alpha_+) & 0 & 0 \\ \sinh(\pi\alpha_+) & \cosh(\pi\alpha_+) & 0 & 0 \\ 0 & 0 & \cosh(\pi\alpha_-) & -\sinh(\pi\alpha_-) \\ 0 & 0 & -\sinh(\pi\alpha_-) & \cosh(\pi\alpha_-) \end{pmatrix}. \tag{A8}$$

Using coordinates (t, r, θ), the chordal distance $\sigma(x, x')$ [Eq. (3.6)] for each region of the BTZ BH spacetime is given by:
Region I: $r > r_+$,

$$\sigma(x,x') = \sqrt{\frac{4r^2 - \alpha_-^2\ell^2}{\alpha_+^2 - \alpha_-^2}}\sqrt{\frac{4r'^2 - \alpha_-^2\ell^2}{\alpha_+^2 - \alpha_-^2}}\cosh\left(\frac{\alpha_+\ell(\theta'-\theta) + \alpha_-(t-t')}{2\ell}\right)$$
$$- \sqrt{\frac{4r^2 - \alpha_+^2\ell^2}{\alpha_+^2 - \alpha_-^2}}\sqrt{\frac{4r'^2 - \alpha_+^2\ell^2}{\alpha_+^2 - \alpha_-^2}}\cosh\left(\frac{\alpha_-\ell(\theta-\theta') + \alpha_+(t'-t)}{2\ell}\right) - \ell^2. \tag{A9}$$

Region II: $r_- < r < r_+$,

$$\sigma(x,x') = \sqrt{\frac{4r^2 - \alpha_-^2\ell^2}{\alpha_+^2 - \alpha_-^2}}\sqrt{\frac{4r'^2 - \alpha_-^2\ell^2}{\alpha_+^2 - \alpha_-^2}}\cosh\left(\frac{\alpha_+\ell(\theta'-\theta) + \alpha_-(t-t')}{2\ell}\right)$$
$$+ \sqrt{\frac{\alpha_+^2\ell^2 - 4r^2}{\alpha_+^2 - \alpha_-^2}}\sqrt{\frac{\alpha_+^2\ell^2 - 4r'^2}{\alpha_+^2 - \alpha_-^2}}\cosh\left(\frac{\alpha_-\ell(\theta-\theta') + \alpha_+(t'-t)}{2\ell}\right) - \ell^2. \tag{A10}$$

Region III: $0 < r < r_-$,

$$\sigma(x,x') = -\sqrt{\frac{\alpha_-^2\ell^2 - 4r^2}{\alpha_+^2 - \alpha_-^2}}\sqrt{\frac{\alpha_-^2\ell^2 - 4r'^2}{\alpha_+^2 - \alpha_-^2}}\cosh\left(\frac{\alpha_+\ell(\theta'-\theta) + \alpha_-(t-t')}{2\ell}\right)$$
$$+ \sqrt{\frac{\alpha_+^2\ell^2 - 4r^2}{\alpha_+^2 - \alpha_-^2}}\sqrt{\frac{\alpha_+^2\ell^2 - 4r'^2}{\alpha_+^2 - \alpha_-^2}}\cosh\left(\frac{\alpha_-\ell(\theta-\theta') + \alpha_+(t'-t)}{2\ell}\right) - \ell^2. \tag{A11}$$

2. Extremal BTZ black hole

The extremal BTZ BH of mass M is described by the line element

$$ds^2 = -dt^2\left(\frac{r^2}{\ell^2} - 2\alpha^2\right) + \frac{dr^2\ell^2r^2}{(r^2 - \ell^2\alpha^2)^2} - 2\gamma\ell\alpha^2 dt d\theta + r^2 d\theta^2, \tag{A12}$$

where $\alpha \equiv r_+/\ell = \sqrt{M/2} > 0$ and the angular momentum is $J = \gamma M \ell$ with $\gamma = \pm 1$. The coordinate ranges are $-\infty < t < \infty, 0 < r < \infty, 0 \le \theta < 2\pi$ (periodic). We note that line element for the extremal black hole is equal to the extremal limit of the line element for the nonextremal rotating black hole, Eq. (A2).

The extremal BTZ BH can be embedded in $\mathbb{R}^{2,2}$ in the following way. For the region $r > r_+$,

$$
\begin{aligned}
X^0 &= \frac{\ell\left(\left(\sqrt{A(r)}(u-1)+\frac{1}{\sqrt{A(r)}}\right)\sinh\alpha v+\left(\sqrt{A(r)}(u+1)+\frac{1}{\sqrt{A(r)}}\right)\cosh\alpha v\right)}{2\sqrt{2}},\\
X^1 &= \frac{\ell\left(\left(\sqrt{A(r)}(u+1)+\frac{1}{\sqrt{A(r)}}\right)\sinh\alpha v+\left(\sqrt{A(r)}(u-1)+\frac{1}{\sqrt{A(r)}}\right)\cosh\alpha v\right)}{2\sqrt{2}},\\
X^2 &= \frac{\ell\left(\left(\frac{1}{\sqrt{A(r)}}-\sqrt{A(r)}(u-1)\right)\sinh\alpha v+\left(\sqrt{A(r)}(u+1)-\frac{1}{\sqrt{A(r)}}\right)\cosh\alpha v\right)}{2\sqrt{2}},\\
X^3 &= \frac{\ell\left(\left(\frac{1}{\sqrt{A(r)}}-\sqrt{A(r)}(u+1)\right)\sinh\alpha v+\left(\sqrt{A(r)}(u-1)-\frac{1}{\sqrt{A(r)}}\right)\cosh\alpha v\right)}{2\sqrt{2}},
\end{aligned}
\tag{A13}
$$

and for the region $r < r_+$ we have

$$
\begin{aligned}
X^0 &= -\frac{\ell\left(\left(\frac{1}{\sqrt{-A(r)}}-(u+1)\sqrt{-A(r)}\right)\sinh(\alpha v)+\left((1-u)\sqrt{-A(r)}+\frac{1}{\sqrt{-A(r)}}\right)\cosh(\alpha v)\right)}{2\sqrt{2}},\\
X^1 &= -\frac{\ell\left(\left((1-u)\sqrt{-A(r)}+\frac{1}{\sqrt{-A(r)}}\right)\sinh(\alpha v)+\left(\frac{1}{\sqrt{-A(r)}}-(u+1)\sqrt{-A(r)}\right)\cosh(\alpha v)\right)}{2\sqrt{2}},\\
X^2 &= \frac{\ell\left(\left((u+1)\sqrt{-A(r)}+\frac{1}{\sqrt{-A(r)}}\right)\sinh(\alpha v)+\left((1-u)\sqrt{-A(r)}-\frac{1}{\sqrt{-A(r)}}\right)\cosh(\alpha v)\right)}{2\sqrt{2}},\\
X^3 &= \frac{\ell\left(\left(\frac{1}{\sqrt{-A(r)}}-(1-u)\sqrt{-A(r)}\right)\sinh(\alpha v)+\left(-(u+1)\sqrt{-A(r)}-\frac{1}{\sqrt{-A(r)}}\right)\cosh(\alpha v)\right)}{2\sqrt{2}}.
\end{aligned}
\tag{A14}
$$

Here,

$$
A(r) \equiv \frac{r^2-\ell^2\alpha^2}{\ell^2\alpha}, \qquad u \equiv \theta+\frac{\gamma t}{\ell}, \qquad v \equiv \theta-\frac{\gamma t}{\ell}. \tag{A15}
$$

The extremal BH is obtained through identifications generated by the Killing vector

$$
\mathbf{k} = \alpha(J_{01}+J_{23})+\frac{1}{2}(J_{02}+J_{03}+J_{12}+J_{13}), \tag{A16}
$$

so that the identification matrix $H = e^{2\pi\mathbf{k}}$ takes the form

$$
H = \begin{pmatrix}
\cosh(2\pi\alpha) & \sinh(2\pi\alpha) & e^{2\pi\alpha}\pi & -e^{2\pi\alpha}\pi \\
\sinh(2\pi\alpha) & \cosh(2\pi\alpha) & e^{2\pi\alpha}\pi & -e^{2\pi\alpha}\pi \\
e^{-2\pi\alpha}\pi & -e^{-2\pi\alpha}\pi & \cosh(2\pi\alpha) & -\sinh(2\pi\alpha) \\
e^{-2\pi\alpha}\pi & -e^{-2\pi\alpha}\pi & -\sinh(2\pi\alpha) & \cosh(2\pi\alpha)
\end{pmatrix}. \tag{A17}
$$

The nth power of H is

$$H^n = \begin{pmatrix} \cosh(2n\pi\alpha) & \sinh(2n\pi\alpha) & ne^{2n\pi\alpha}\pi & -ne^{2n\pi\alpha}\pi \\ \sinh(2n\pi\alpha) & \cosh(2n\pi\alpha) & ne^{2n\pi\alpha}\pi & -ne^{2n\pi\alpha}\pi \\ ne^{-2n\pi\alpha}\pi & -ne^{-2n\pi\alpha}\pi & \cosh(2n\pi\alpha) & -\sinh(2n\pi\alpha) \\ ne^{-2n\pi\alpha}\pi & -ne^{-2n\pi\alpha}\pi & -\sinh(2n\pi\alpha) & \cosh(2n\pi\alpha) \end{pmatrix}. \tag{A18}$$

In terms of the coordinates (t, r, θ), the chordal distance $\sigma(x, x')$ [Eq. (3.6)] for the extremal BTZ BH is

$$\sigma(x,x') = \frac{\ell\sqrt{A(r)A(r')}}{2}(\ell(\theta-\theta')+\gamma(t-t'))\sinh\left(\frac{\alpha(\ell(\theta-\theta')+\gamma(t'-t))}{\ell}\right) + \frac{\ell^2(A(r)+A(r'))}{2\sqrt{A(r)A(r')}}\cosh\left(\frac{\alpha(\ell(\theta-\theta')+\gamma(t'-t))}{\ell}\right)-1, \tag{A19}$$

in the region $r > r_+$, and

$$\sigma(x,x') = \frac{\ell\sqrt{A(r)A(r')}}{2}(\ell(\theta'-\theta)+\gamma(t'-t))\sinh\left(\frac{\alpha(\ell(\theta-\theta')+\gamma(t'-t))}{\ell}\right) - \frac{\ell^2(A(r)+A(r'))}{2\sqrt{A(r)A(r')}}\cosh\left(\frac{\alpha(\ell(\theta-\theta')+\gamma(t'-t))}{\ell}\right)-1, \tag{A20}$$

in the region $r < r_+$.

3. Rotating nonextremal naked singularity

The spinning NS with mass $M < 0$ and angular momentum J ($M \neq -1$ if $J = 0$) is described by the line element

$$ds^2 = -\left(\frac{r^2}{\ell^2}+\frac{\beta_+^2+\beta_-^2}{4}\right)dt^2 + \frac{dr^2\ell^2r^2}{\left(r^2+\frac{\ell^2\beta_+^2}{4}\right)\left(r^2+\frac{\ell^2\beta_-^2}{4}\right)} - \frac{\ell\beta_+\beta_-}{2}dtd\theta + r^2d\theta^2, \tag{A21}$$

with $-\infty < t < \infty, 0 < r < \infty, 0 \le \theta < 2\pi$ (periodic). In this case, the embedding is given by

$$X^0 = A_+(r)\cos\left(\frac{\ell\theta\beta_- + t\beta_+}{2\ell}\right), \qquad X^1 = A_-(r)\cos\left(\frac{t\beta_- + \ell\theta\beta_+}{2\ell}\right),$$
$$X^2 = A_-(r)\sin\left(\frac{t\beta_- + \ell\theta\beta_+}{2\ell}\right), \qquad X^3 = A_+(r)\sin\left(\frac{\ell\theta\beta_- + t\beta_+}{2\ell}\right), \tag{A22}$$

with

$$A_\pm(r) \equiv \sqrt{\frac{4r^2+\ell^2\beta_\pm^2}{\beta_+^2-\beta_-^2}}. \tag{A23}$$

This geometry is obtained through identifications generated by the Killing vector

$$\mathbf{k} = \frac{\beta_+}{2}J_{21} + \frac{\beta_-}{2}J_{30}. \tag{A24}$$

This Killing vector is spacelike,

$$\mathbf{k}^2 = \frac{\beta_+^2}{4}[(X_1)^2+(X_2)^2] - \frac{\beta_-^2}{4}[(X_0)^2+(X_3)^2] = r^2 > 0. \tag{A25}$$

Exponentiating (A25) yields the identification matrix

$$H = \begin{pmatrix} \cos(\pi\beta_-) & 0 & 0 & -\sin(\pi\beta_-) \\ 0 & \cos(\pi\beta_+) & -\sin(\pi\beta_+) & 0 \\ 0 & \sin(\pi\beta_+) & \cos(\pi\beta_+) & 0 \\ \sin(\pi\beta_-) & 0 & 0 & \cos(\pi\beta_-) \end{pmatrix}. \tag{A26}$$

Using the coordinates (t, r, θ), the chordal distance $\sigma(x, x')$ [Eq. (3.6)] for the nonextremal NS reads

$$\sigma(x,x') = -\sqrt{\frac{\beta_-^2\ell^2+4r^2}{\beta_+^2-\beta_-^2}}\sqrt{\frac{\beta_-^2\ell^2+4r'^2}{\beta_+^2-\beta_-^2}}\cos\left(\frac{\beta_+\ell(\theta-\theta')+\beta_-(t-t')}{2\ell}\right) + \sqrt{\frac{\beta_+^2\ell^2+4r^2}{\beta_+^2-\beta_-^2}}\sqrt{\frac{\beta_+^2\ell^2+4r'^2}{\beta_+^2-\beta_-^2}}\cos\left(\frac{\beta_-\ell(\theta-\theta')+\beta_+(t-t')}{2\ell}\right) - \ell^2. \tag{A27}$$

The embedding (A22) breaks down for $\beta_+ = |\beta_-|$, which corresponds to the extremal case $M\ell = -|J|$. This means that the Killing vector for the identification that gives rise to the extremal NS cannot be obtained by just taking the limit $\beta_+ = |\beta_-|$ in (A25) and the matrix H needs to be recalculated for this case as well—we give it in the next subsection.

Note that $H(\beta_+, \beta_-)$ remains unchanged if either β_+ or β_- are shifted by even integer numbers. In addition, if n and m are two integers such that $n(\beta_+ - \beta_-) = 2m$, then

$$\begin{aligned} H^n(\beta_+,\beta_-) &= H(n\beta_+, n\beta_-) = H(n\beta_- + 2m, n\beta_-) \\ &= H(n\beta_-, n\beta_-), \end{aligned} \tag{A28}$$

which is the form of the naive extremal limit. As we see in Sec. III B, this feature leads to a singularity in the RSET and to a breakdown of the perturbative regime for the system.

4. Extremal naked singularity

Although the line-element of the extremal NS coincides with the line-element in Eq. (A21) when taking the extremal limit $M\ell = -|J|$, the extremal NS space-time cannot be obtained by taking the limit $\beta_+ = |\beta_-| = 2\beta$ in the embedding (A22), Killing vector (A25) or the identification matrix (A26). In fact, the extremal metric

$$ds^2 = -\left(\frac{r^2}{\ell^2}+2\beta^2\right)dt^2 + \frac{\ell^2 r^2 dr^2}{(r^2+\ell^2\beta^2)^2} - 2\gamma\ell\beta^2 dt d\theta + r^2 d\theta^2, \tag{A29}$$

with $-\infty < t < \infty, 0 < r < \infty, 0 \le \theta < 2\pi$ (periodic), is obtained via the embedding

$$\begin{aligned} X^0 &= \frac{\ell\left(\left(\frac{1}{B(r)}-(v-1)B(r)\right)\sin(\beta u)+\left(-(v+1)B(r)-\frac{1}{B(r)}\right)\cos(\beta u)\right)}{2\sqrt{2}}, \\ X^1 &= \frac{\ell\left(\left(-(v-1)B(r)-\frac{1}{B(r)}\right)\sin(\beta u)+\left((v+1)B(r)-\frac{1}{B(r)}\right)\cos(\beta u)\right)}{2\sqrt{2}}, \\ X^2 &= \frac{\ell\left(\left((v+1)B(r)-\frac{1}{B(r)}\right)\sin(\beta u)+\left((v-1)B(r)+\frac{1}{B(r)}\right)\cos(\beta u)\right)}{2\sqrt{2}}, \\ X^3 &= \frac{\ell\left(\left(-(v+1)B(r)-\frac{1}{B(r)}\right)\sin(\beta u)+\left((v-1)B(r)-\frac{1}{B(r)}\right)\cos(\beta u)\right)}{2\sqrt{2}}. \end{aligned} \tag{A30}$$

Here $\beta \equiv \sqrt{-M/2} > 0$ and the angular momentum is $J = -\gamma M\ell$ with $\gamma = \pm 1$, where

$$B(r) \equiv \sqrt{\frac{r^2+\ell^2\beta^2}{\ell^2\beta}}, \qquad u \equiv \theta + \frac{\gamma t}{\ell}, \qquad v \equiv \theta - \frac{\gamma t}{\ell}. \tag{A31}$$

This extremal NS is obtained through identifications generated by the Killing vector

$$\mathbf{k} = \beta(J_{03} - J_{12}) - \frac{1}{2}(J_{01} + J_{03} + J_{12} - J_{23}). \tag{A32}$$

The identification matrix in this case is given by

$$H = e^{2\pi\mathbf{k}} = \begin{pmatrix} \cos(2\pi\beta) + \pi\sin(2\pi\beta) & -\pi\cos(2\pi\beta) & \pi\sin(2\pi\beta) & \pi\cos(2\pi\beta) - \sin(2\pi\beta) \\ -\pi\cos(2\pi\beta) & \cos(2\pi\beta) - \pi\sin(2\pi\beta) & -\pi\cos(2\pi\beta) - \sin(2\pi\beta) & \pi\sin(2\pi\beta) \\ -\pi\sin(2\pi\beta) & \pi\cos(2\pi\beta) + \sin(2\pi\beta) & \cos(2\pi\beta) - \pi\sin(2\pi\beta) & -\pi\cos(2\pi\beta) \\ \sin(2\pi\beta) - \pi\cos(2\pi\beta) & -\pi\sin(2\pi\beta) & -\pi\cos(2\pi\beta) & \cos(2\pi\beta) + \pi\sin(2\pi\beta) \end{pmatrix}, \tag{A33}$$

and the nth power of H is obtained replacing π by $n\pi$ in the above expression.

For the extremal NS, the chordal distance $\sigma(x, x')$ [Eq. (3.6)] is given by

$$\sigma(x,x') = \frac{\ell B(r)B(r')}{2}(\ell(\theta-\theta') + \gamma(t'-t))\sin\left(\frac{\beta(\ell(\theta-\theta')+\gamma(t-t'))}{\ell}\right) + \frac{\ell^2(B(r)^2 + B(r')^2)}{2B(r)B(r')}\cos\left(\frac{\beta(\ell(\theta-\theta')+\gamma(t-t'))}{\ell}\right) - 1. \tag{A34}$$

APPENDIX B: TWO-POINT FUNCTION IN CAdS$_3$

In this Appendix we derive the anti-commutator in CAdS$_3$, Eq. (3.5). Let us consider the line element in the covering space of AdS$_3$ in coordinates $\rho \in [0, \pi/2]$, $\theta \in (0, 2\pi]$, $\tau \in \mathbb{R}$ [28]:

$$ds^2 = \ell^2 \sec^2\rho(-d\tau^2 + d\rho^2 + \sin^2\rho d\theta^2). \tag{B1}$$

The transformation between these coordinates in AdS$_3$ and those in Eq. (2.7) in $\mathbb{R}^{(2,2)}$ is [28]:

$$X^0 = \ell\frac{\cos\tau}{\cos\rho}, \qquad X^1 = \ell\tan\rho\cos\theta,$$
$$X^2 = \ell\tan\rho\sin\theta, \qquad X^3 = \ell\frac{\sin\tau}{\cos\rho}. \tag{B2}$$

This transformation allows us to write the function σ in Eq. (3.6) in the AdS$_3$ coordinates of Eq. (B1) as

$$\sigma(x,x') = \ell^2(\cos(\Delta\tau)\ \sec\rho\sec\rho' - 1 - \tan\rho\tan\rho'\cos\Delta\theta). \tag{B3}$$

The metric Eq. (B1) is manifestly conformal to half of the Einstein Universe $\mathbb{R}\times S^2$ with a conformal factor $\Omega(x) = \ell/\cos\rho$, and, therefore (see, e.g., Eq. (3.154) [47]), $G_A^+(x,x') = \sqrt{\cos\rho\cos\rho'}G_E^+(x,x')/\ell$, where G_A^+ is the Wightman function in AdS$_3$ and G_E^+ is the Wightman function in the Einstein universe. By using this fact and explicitly calculating G_E^+, Appendix A [28] finds

$$G_A^+(x,x') = \lim_{\epsilon\to 0^+}\frac{1}{4\sqrt{2}\pi\ell}(\cos(\Delta\tau - i\epsilon)\ \sec\rho\sec\rho' - 1 - \tan\rho\tan\rho'\cos\Delta\theta)^{-1/2}, \tag{B4}$$

where $\Delta\tau \equiv \tau - \tau'$ and $\Delta\theta \equiv \theta - \theta'$, for a quantum state which corresponds to imposing transparent b.c.; the '$i\epsilon$' corresponds to the Feynman prescription. Now, by using

$$\cos(\Delta\tau - i\epsilon) \approx \cos(\Delta\tau) + i\sin(\Delta\tau)\epsilon, \qquad \epsilon\to 0^+, \tag{B5}$$

$$\lim_{\epsilon\to 0^+}(x \pm i\epsilon)^{-1/2} = |x|^{-1/2}e^{\mp i\pi\Theta(-x)/2}, \qquad x\in\mathbb{R}, \tag{B6}$$

together with Eqs. (3.3) and (B3), it readily follows that the anticommutator corresponding to Eq. (B4) is given by Eq. (3.5).

APPENDIX C: TWO-POINT FUNCTION IN STATIC BTZ NAKED SINGULARITY VIA MODE SUMS

In Sec. III A, we gave the two-point function on a static BTZ NS space-time as derived by applying the method of images on the two-point function in AdS$_3$. Specifically, the two-point function on a static BTZ NS is given by Eq. (3.11) with $N = 1/\sqrt{-M}$. In this Appendix, we are going to rederive that expression by instead using mode sums over homogeneous solutions of the field equation, Eq. (3.2). This alternative derivation will enable us to clarify the boundary conditions used in obtaining the two-point function.

We start with the homogeneous field Eq. (3.2) and write a field mode solution as

$$\phi_{m\omega}(x) = N_{m\omega} e^{-i\omega t + im\theta} R_{m\omega}(r), \tag{C1}$$

where $N_{m\omega}$ is a normalization constant, $\omega \in \mathbb{C}$ and $m \in \mathbb{Z}$. The radial function $R_{m\omega}(r)$ is found to satisfy the ordinary differential equation

$$\left(\frac{1}{r}\frac{d}{dr}\left(r(r^2-M)\frac{d}{dr}\right) - \frac{m^2}{r^2} + \frac{\omega^2}{r^2-M} + \frac{3}{4}\right) R_{m\omega}(r) = 0, \tag{C2}$$

where $r \in (0,\infty)$. We need to choose boundary conditions for the solutions of this radial equation at the singularity "$r = 0$" and at the AdS boundary $r = \infty$.

Let us now define normalize quantities as: $\bar{r} \equiv r/\sqrt{-M} \in (0,\infty)$, $\bar{\omega} \equiv \omega/\sqrt{-M}$ and $\bar{m} \equiv m/\sqrt{-M}$, where we remind the reader that $M < 0$ for a static NS. From now on we restrict ourselves to the case that $M = -1/N^2$, with $N \in \mathbb{Z}^+$, so that, in particular, $\bar{m} = m \cdot N \in \mathbb{Z}$.

The solutions of Eq. (C2) can be expressed in terms of associated Legendre functions. In particular, we choose the following two linearly independent solutions:

$$\begin{aligned} {}_1R_{m\omega}(\bar{r}) &\equiv (1+\bar{r}^2)^{-1/4} P^{-\bar{m}}_{-1/2+\bar{\omega}}\left(\frac{1}{\sqrt{1+\bar{r}^2}}\right), \\ {}_2R_{m\omega}(\bar{r}) &\equiv (1+\bar{r}^2)^{-1/4} P^{\bar{m}}_{-1/2+\bar{\omega}}\left(-\frac{1}{\sqrt{1+\bar{r}^2}}\right). \end{aligned} \tag{C3}$$

It can be easily checked that the functions in Eq. (C3) satisfy Eq. (C2). In what follows, it will be convenient to use the coordinate $\rho \in (0,\pi/2)$ defined via $\cos\rho \equiv (1+\bar{r}^2)^{-1/2}$. In terms of this new coordinate, the solutions read

$$\begin{aligned} {}_1R_{m\omega}(\rho) &= \sqrt{\cos\rho} P^{-\bar{m}}_{-1/2+\bar{\omega}}(\cos\rho), \\ {}_2R_{m\omega}(\rho) &= \sqrt{\cos\rho} P^{\bar{m}}_{-1/2+\bar{\omega}}(-\cos\rho). \end{aligned} \tag{C4}$$

Let us now turn to their boundary conditions. They behave as ${}_1R_{m\omega} = O(\bar{r}^{|\bar{m}|})$ (for which $\bar{m} \in \mathbb{Z}$ is needed) and ${}_2R_{m\omega} = O(\bar{r}^{-|\bar{m}|})$ as $\bar{r} \to 0^+$ [70]. That is, ${}_1R_{m\omega}$ is regular as $r \to 0^+$ and square integrable near $r = 0$; on the other hand, ${}_2R_{m\omega}$ is irregular as $r \to 0^+$ and is not square integrable near $r = 0$ (except for $m = 0$). Near the AdS boundary, ${}_2R_{m\omega}$ obeys transparent boundary conditions [34,51]. Therefore, ${}_1R_{m\omega}$ is the appropriate solution near the singularity $r = 0$ and ${}_2R_{m\omega}$ is the appropriate one near the AdS boundary $r = \infty$.

We now proceed to write the two-point function similarly to the way that it is done in [30,51] for the BH case. The idea is that one first Euclideanizes the space-time. The field equation becomes elliptic in the Euclidean manifold and so there is a unique Green function (under the conditions of square-integrability near the origin and transparent boundary conditions at infinity), which is the so-called Euclidean Green function. The Euclidean Green function may be constructed in the usual way that one constructs a Green function: with the radial part of the modes given by the radial solution which satisfies the desired boundary condition near $r = 0$ evaluated at the point with the smallest radius [i.e., $r_< \equiv \min(r, r')$], times the radial solution which satisfies the desired boundary condition near $r = \infty$ evaluated at the point with the largest radius [i.e., $r_> \equiv \max(r, r')$]. The Euclidean Green function is obtained as a frequency-integral of the modes constructed as per above (it is a frequency instead of a discrete sum since, in this case, the corresponding Euclidean manifold contains no conical singularity and so no periodicity is required in the Euclideanized time). One then de-Euclideanizes and obtains the Feynman Green function from the Euclidean Green function by the corresponding analytic continuation. When de-Euclideanizing, the integration contour over the purely imaginary frequencies in the Euclidean Green function is deformed to an integral over just below the real axis for $\mathrm{Re}(\omega) < 0$ and just above the real axis for $\mathrm{Re}(\omega) > 0$; we denote such contour by $\mathcal{C}$ (see, e.g., Fig. 1 in [49]). Specifically, the Feynman Green function in the static NS space-time when the field satisfies transparent boundary conditions is given by

$$\begin{aligned} G_F(x,x') = -\frac{N^2}{(2\pi)^2}\int_{\mathcal{C}} d\omega \sum_{m=-\infty}^{\infty} e^{-i\omega t + im\theta} \\ \times \frac{{}_1R_{m\omega}(\rho_<){}_2R_{m\omega}(\rho_>)}{\tan\rho \cdot W[{}_1R_{m\omega}, {}_2R_{m\omega}]}. \end{aligned} \tag{C5}$$

Here we have taken $t' = 0$ and $\theta' = 0$ without loss of generality (due to the stationarity and circular symmetry of the space-time). The factor "$\tan\rho$" is required so that the denominator is constant. The Wronskian is given by

$$\begin{aligned} W[{}_1R_{m\omega}, {}_2R_{m\omega}] &\equiv {}_1R_{m\omega}\frac{d_2R_{m\omega}}{d\rho} - {}_2R_{m\omega}\frac{d_1R_{m\omega}}{d\rho} \\ &= -\frac{2}{\pi}\cot\rho\cos\left(\pi(\bar{m}-\bar{\omega})\right). \end{aligned} \tag{C6}$$

The Feynman propagator (C5) satisfies the Green function equation (3.4).

From Eqs. (C5) and (C6) it readily follows that

$$\begin{aligned} G_F(x,x') = \frac{N}{8\pi}(\cos\rho\cos\rho')^{1/2}\int_{\mathcal{C}} d\bar{\omega} \sum_{m=-\infty}^{\infty} (-1)^{\bar{m}} e^{-i\bar{\omega}\bar{t} + im\theta} \\ \times \frac{P^{-\bar{m}}_{-1/2+\bar{\omega}}(\cos\rho_<)P^{\bar{m}}_{-1/2+\bar{\omega}}(-\cos\rho_>)}{\cos(\pi\bar{\omega})}, \end{aligned} \tag{C7}$$

where we have defined $\bar{t} \equiv t\sqrt{-M}$. We note that the only singularities in the complex-ω plane of the integrand [for $r, r' \in (0,\infty)$] in Eq. (C7) are the poles which correspond to the zeros of the denominator, i.e., $\bar{\omega} = n + 1/2$ with $n \in \mathbb{Z}$. We next wish to perform the infinite-sum and integral in Eq. (C7).

For the sum, we will mirror a similar calculation in the Appendix of [71]. We start with Eq. (8.794) of [72]. After basic operations and the use of the property

$$P_\nu^k(\cos\psi_1)P_\nu^{-k}(\cos\psi_2) = P_\nu^{-k}(\cos\psi_1)P_\nu^k(\cos\psi_2) \tag{C8}$$

for $k \in \mathbb{Z}$, $\psi_1, \psi_2 \in \mathbb{R}$, $\nu \in \mathbb{C}$, we obtain

$$\sum_{k=-\infty}^{\infty}(-1)^k P_\nu^{-k}(\cos\psi_1)P_\nu^k(\cos\psi_2)e^{ik\varphi} = P_\nu(\cos\psi_1\cos\psi_2 + \sin\psi_1\sin\psi_2\cos\varphi), \tag{C9}$$

with $\varphi \in \mathbb{R}$. We now take $\varphi \to \varphi + 2n\pi/N$ onto Eq. (C9) and take a sum over n from 0 to $N-1$.

After some more basic operations and the use of the distributional identity [71]

$$\sum_{n=0}^{N-1} e^{ik(\varphi+2n\pi/N)} = Ne^{ik\varphi}\sum_{m=-\infty}^{\infty}\delta_{k,m\cdot N}, \tag{C10}$$

we obtain the useful identity

$$\sum_{m=-\infty}^{\infty}(-1)^{m\cdot N}P_\nu^{-m\cdot N}(\cos\psi_1)P_\nu^{m\cdot N}(\cos\psi_2)e^{imN\varphi} = \frac{1}{N}\sum_{n=0}^{N-1}P_\nu\left(\cos\psi_1\cos\psi_2 + \sin\psi_1\sin\psi_2\cos\left(\varphi+\frac{2n\pi}{N}\right)\right). \tag{C11}$$

We can now apply Eq. (C11) to the infinite-sum in Eq. (C7):

$$\sum_{m=-\infty}^{\infty}(-1)^{\bar m}e^{im\theta}P_{-1/2+\bar\omega}^{-\bar m}(\cos\rho_<)P_{-1/2+\bar\omega}^{\bar m}(-\cos\rho_>) = \frac{1}{N}\sum_{k=0}^{N-1}P_{-1/2+\bar\omega}(\cos\beta_k), \tag{C12}$$

where

$$\cos\beta_k \equiv -\cos\rho\cos\rho' - \sin\rho\sin\rho'\cos\left(\frac{\theta+2k\pi}{N}\right). \tag{C13}$$

Therefore, we have, from Eqs. (C7) and (C12),

$$G_F(x,x') = \frac{1}{8\pi}(\cos\rho\cos\rho')^{1/2}\sum_{k=0}^{N-1}\int_{\mathcal{C}}d\bar\omega e^{-i\bar\omega\bar t}\frac{P_{-1/2+\bar\omega}(\cos\beta_k)}{\cos(\pi\bar\omega)}. \tag{C14}$$

In order to evaluate this contour integral we shall use the residue theorem. For this purpose, we choose to close the contour $\mathcal{C}$ in the lower ω-plane. When $t > 0$, the integral along the arc at infinite radius in the lower plane vanishes and so from now on we consider $t > 0$. Then, taking into account the poles of the integrand for $\bar\omega > 0$ (i.e., $\bar\omega = n + 1/2$ with $n \in \mathbb{Z}^+ \cup 0$) when using the residue theorem, we obtain

$$G_F(x,x') = \frac{i}{4\pi}(\cos\rho\cos\rho')^{1/2}\lim_{\epsilon\to0^+}\sum_{k=0}^{N-1}\sum_{n=0}^{\infty}e^{-i(n+1/2)(\bar t-i\epsilon)}(-1)^nP_n(\cos\beta_k), \tag{C15}$$

where we have introduced a small-ϵ prescription for convergence. In order to carry out the n-sum, we use the fact that $(-1)^nP_n(\cos\beta_k) = P_n(-\cos\beta_k)$ for $n \in \mathbb{Z}^+ \cup 0$, together with Eq. (8.921) [72], which requires that $|e^{-i(\bar t-i\epsilon)}| = e^{-\epsilon} < 1$, which is satisfied for $\epsilon > 0$. As a result, we obtain

$$G_F(x,x') = \frac{i}{4\sqrt{2}\pi}(\cos\rho\cos\rho')^{1/2}\lim_{\epsilon\to0^+}\sum_{k=0}^{N-1}\frac{1}{(\cos(\bar t-i\epsilon)+\cos\beta_k)^{1/2}}. \tag{C16}$$

By writing it in the original BTZ coordinates, it is easy to check that (restoring ℓ)

$$\frac{\cos(\bar{t}-i\epsilon)+\cos\beta_k}{\cos\rho\cos\rho'}=((N^2r^2+\ell^2)(N^2r'^2+\ell^2))^{1/2}\cos\left(\frac{t-i\epsilon}{N\ell}\right)-N^2rr'\cos\left(\frac{\theta+2k\pi}{N}\right)-\ell^2, \tag{C17}$$

Comparing with Eq. (A27), we can see that, for $k=0$ and $\epsilon=0$, the right-hand side of (C17) is equal to the world function $\sigma(x,x')$ with $M=-1/N^2$. The expression for $k\neq 0$ (and $\epsilon=0$) simply corresponds to $\sigma(x,H^kx')$.

In its turn, the ϵ-dependence can be separated out so that:

$$\frac{\cos(\bar{t}-i\epsilon)+\cos\beta_k}{\cos\rho\cos\rho'}\sim\sigma_\epsilon(x,H^kx')\equiv\sigma(x,H^kx')+\sin\bar{t}\cdot i\epsilon,\qquad \epsilon\to 0^+. \tag{C18}$$

The final expression for the Feynman Green function is thus

$$G_F(x,x')=\frac{i}{4\sqrt{2}\pi}\lim_{\epsilon\to 0^+}\sum_{n=0}^{N-1}\frac{1}{\sqrt{\sigma_\epsilon(x,H^nx')}}. \tag{C19}$$

In its turn, the final expression for the anticommutator is thus, from Eqs. (3.3) and (C19),

$$G^{(1)}_{NS}(x,x')=2\mathrm{Im}(G_F(x,x'))=\frac{1}{2\sqrt{2}\pi}\sum_{n=0}^{N-1}\frac{\Theta(\sigma(x,H^nx'))}{\sqrt{\sigma(x,H^nx')}}. \tag{C20}$$

Even though this expression has been derived assuming $t>0$, since the expression for the anticommutator $G^{(1)}(x,x')$ is the same for $t>0$ as for $t<0$, this expression is actually valid for all $t\in\mathbb{R}$. Equations (C20) and Eq. (3.11) agree while they have been derived in completely different ways: as a mode-sum here whereas using the method of images there. We note that the "sum over caustics" (or, in other words, the generalization $\theta\to\theta+2n\pi/N$ with the associated sum over n or, in other words, the "sum over images" within the method of images) has arisen naturally here from the distributional identity Eq. (C10).

[1] S. W. Hawking, Particle creation by black holes, Commun. Math. Phys. **43**, 199 (1975); Erratum, Commun. Math. Phys. **46**, 206(E) (1976).

[2] R. Penrose, The question of cosmic censorship, J. Astrophys. Astron. **20**, 233 (1999).

[3] R. Penrose, Gravitational collapse: The role of general relativity, Riv. Nuovo Cimento **1**, 257 (1969); "Golden Oldie": Gravitational Collapse: The Role of General Relativity, Gen. Relativ. Gravit. **34**, 1141 (2002).

[4] R. M. Wald, *Gravitational Collapse and Cosmic Censorship*, edited by B. R. Iyer and B. Bhawal, Black Holes, Gravitational Radiation and the Universe (Springer, Dordrecht, 1999).

[5] R. Penrose, Singularities and time-asymmetry, in *General Relativity: An Einstein Centenary Survey*, edited by S. W. Hawking and W. Israel (Cambridge University Press, Cambridge, England, 1979).

[6] C. Cardoso, J. L. Costa, K. Destounis, P. Hintz, and A. Jansen, Quasinormal Modes and Strong Cosmic Censorship, Phys. Rev. Lett. **120**, 031103 (2018).

[7] J. L. Costa, P. M. Girão, J. Natário, and J. D. Silva, On the occurrence of mass inflation for the Einstein-Maxwell-scalar field system with a cosmological constant and an exponential Price law, Commun. Math. Phys. **361**, 289 (2018).

[8] A. Ori, Inner Structure of a Charged Black Hole: An Exact Mass-Inflation Solution, Phys. Rev. Lett. **67**, 789 (1991).

[9] J. Luk and S-J. Oh, Strong cosmic censorship in spherical symmetry for two-ended asymptotically flat initial data I. The interior of the black hole region, arXiv:1702.05715.

[10] M. Dafermos, The interior of charged black holes and the problem of uniqueness in general relativity, Commun. Appl. Math. **58**, 445 (2005).

[11] E. Poisson and W. Israel, Inner-Horizon Instability and Mass Inflation in Black Holes, Phys. Rev. Lett. **63**, 1663 (1989).

[12] M. Dafermos and J. Luk, The interior of dynamical vacuum black holes I: The C^0-stability of the Kerr Cauchy horizon, arXiv:1710.01722.

[13] A. Ori, Structure of the Singularity Inside a Realistic Rotating Black Hole, Phys. Rev. Lett. **68**, 2117 (1992).

[14] L. Lehner and F. Pretorius, Black Strings, Low Viscosity Fluids, and Violation of Cosmic Censorship, Phys. Rev. Lett. **105**, 101102 (2010).

[15] J. E. Santos and B. Way, Neutral Black Rings in Five Dimensions Are Unstable, Phys. Rev. Lett. **114**, 221101 (2015).

[16] R. Gregory and R. Laflamme, Black Strings and p-Branes Are Unstable, Phys. Rev. Lett. **70**, 2837 (1993).

[17] J. Sorce and R. M. Wald, Gedanken experiments to destroy a black hole II: Kerr-Newman black holes cannot be overcharged or over-spun, Phys. Rev. D **96**, 104014 (2017).

[18] T. Crisford and J. E. Santos, Violating the Weak Cosmic Censorship Conjecture in Four-Dimensional Anti-de Sitter Space, Phys. Rev. Lett. **118**, 181101 (2017).

[19] N. D. Birrell and P. C. W. Davies, On falling through a black hole into another universe, Nature (London) **272**, 35 (1978).
[20] A. C. Ottewill and E. Winstanley, The renormalized stress tensor in Kerr space-time: General results, Phys. Rev. D **62**, 084018 (2000).
[21] W. A. Hiscock, Quantum-mechanical instability of the Kerr-Newman black-hole interior, Phys. Rev. D **21**, 2057 (1980).
[22] A. Lanir, A. Ori, N. Zilberman, O. Sela, A. Maline, and A. Levi, Analysis of quantum effects inside spherical charged black holes, Phys. Rev. D **99**, 061502 (2019).
[23] J. W. York, Jr., Black hole in thermal equilibrium with a scalar field: the back-reaction, Phys. Rev. D **31**, 775 (1985).
[24] A. Fabbri and J. Navarro-Salas, *Modeling Black Hole Evaporation* (Imperial College Press/World Scientific, London, 2005).
[25] M. Bañados, C. Teitelboim, and J. Zanelli, The Black Hole in Three-Dimensional Space-Time, Phys. Rev. Lett. **69**, 1849 (1992).
[26] M. Bañados, M. Henneaux, C. Teitelboim, and J. Zanelli, Geometry of the $(2+1)$ black hole, Phys. Rev. D **48**, 1506 (1993); Erratum, Phys. Rev. D **88**, 069902(E) (2013).
[27] O. Mišković and J. Zanelli, Negative spectrum of the $2+1$ black hole, Phys. Rev. D **79**, 105011 (2009).
[28] G. Lifschytz and M. Ortiz, Scalar field quantization on the $(2+1)$-dimensional black hole background, Phys. Rev. D **49**, 1929 (1994).
[29] C. Martínez and J. Zanelli, Back reaction of a conformal field on a three-dimensional black hole, Phys. Rev. D **55**, 3642 (1997).
[30] K. Shiraishi and T. Maki, Vacuum polarization around a three-dimensional black hole, Classical Quantum Gravity **11**, 695 (1994).
[31] M. Casals, A. Fabbri, C. Martínez, and J. Zanelli, Quantum dress for a naked singularity, Phys. Lett. B **760**, 244 (2016).
[32] A. R. Steif, The Quantum stress tensor in the three-dimensional black hole, Phys. Rev. D **49**, R585 (1994).
[33] M. Casals, A. Fabbri, C. Martínez, and J. Zanelli, Quantum Backreaction on Three-Dimensional Black Holes and Naked Singularities, Phys. Rev. Lett. **118**, 131102 (2017).
[34] S. J. Avis, C. J. Isham, and D. Storey, Quantum field theory in anti-de Sitter space-time, Phys. Rev. D **18**, 3565 (1978).
[35] J. S. F. Chan, K. C. K. Chan, and R. B. Mann, Interior structure of a charged spinning black hole in $(2+1)$-dimensions, Phys. Rev. D **54**, 1535 (1996).
[36] V. Husain, Radiation collapse and gravitational waves in three dimensions, Phys. Rev. D **50**, R2361 (1994).
[37] P. R. Brady and C. M. Chambers, Nonlinear instability of Kerr type Cauchy horizons, Phys. Rev. D **51**, 4177 (1995).
[38] S. Carroll, *Spacetime and Geometry: An Introduction to General Relativity* (Addison Wesley, San Francisco, 2004).
[39] N. Cruz, C. Martínez, and L. Peña, Geodesic structure of the $(2+1)$ black hole, Classical Quantum Gravity **11**, 2731 (1994).
[40] A. A. Starobinsky, Amplification of waves during reflection from a rotating "black hole", Zh. Eksp. Teor. Fiz. **64**, 48 (1973) [Sov. Phys. JETP **37**, 28 (1973)].
[41] Ya. B. Zel'dovich, Generation of waves by a rotating body, ZhETF Pisma Redaktsiiu **14**, 270 (1971) [JETP Lett. **14**, 180 (1971)].
[42] E. Winstanley, On classical superradiance in Kerr-Newman–anti-de Sitter black holes, Phys. Rev. D **64**, 104010 (2001).
[43] L. Ortiz, No superradiance for the scalar field in the BTZ black hole with reflexive boundary conditions, Phys. Rev. D **86**, 047703 (2012).
[44] C. Dappiaggi, H. R. C. Ferreira, and C. A. R. Herdeiro, Superradiance in the BTZ black hole with Robin boundary conditions, Phys. Lett. B **778**, 146 (2018).
[45] C. Martínez, C. Teitelboim, and J. Zanelli, Charged rotating black hole in three spacetime dimensions, Phys. Rev. D **61**, 104013 (2000).
[46] C. Martínez and J. Zanelli, Conformally dressed black hole in $(2+1)$-dimensions, Phys. Rev. D **54**, 3830 (1996).
[47] N. Birrell and P. Davies, *Quantum Fields in Curved Space* (Cambridge University Press, Cambridge, England, 1984).
[48] S. M. Christensen, Regularization, renormalization, and covariant geodesic point separation, Phys. Rev. D **17**, 946 (1978).
[49] B. S. DeWitt, *Dynamical Theory of Groups and Fields* (Gordon and Breach, New York, 1965).
[50] K. Shiraishi and T. Maki, Quantum fluctuation of stress tensor and black holes in three dimensions, Phys. Rev. D **49**, 5286 (1994).
[51] K. Shiraishi and T. Maki, Vacuum polarization near asymptotically anti-de Sitter black holes in odd dimensions, Classical Quantum Gravity **11**, 1687 (1994).
[52] Y. Décanini and A. Folacci, Off-diagonal coefficients of the DeWitt-Schwinger and Hadamard representations of the Feynman propagator, Phys. Rev. D **73**, 044027 (2006).
[53] E. W. Hobson, On a type of spherical harmonics of unrestricted degree, order, and argument, Phil. Trans. (A) **187**, 443 (1896); H. Bateman, *Higher Transcendental Functions* (McGraw-Hill Book Company, New York, 1953), Vol. I.
[54] T. Souradeep and V. Sahni, Quantum effects near a point mass in $(2+1)$-Dimensional gravity, Phys. Rev. D **46**, 1616 (1992).
[55] J. Cheeger and M. Taylor, On the diffraction of waves by conical singularities I, Commun. Pure Appl. Math. **35**, 275 (1982); On the diffraction of waves by conical singularities II, Commun. Pure Appl. Math. **35**, 487 (1982).
[56] M. Casals, A. Fabbri, C. Martínez, and J. Zanelli, Quantum fields as cosmic censors in $(2+1)$-dimensions, Int. J. Mod. Phys. D **27**, 1843011 (2018).
[57] V. P. Frolov, F. D. Mazzitelli, and J. P. Paz, Quantum effects near multidimensional black holes, Phys. Rev. D **40**, 948 (1989).
[58] D. A. Kothawala, S. Shankaranarayanan, and L. Sriramkumar, Quantum gravitational corrections to the stress-energy tensor around the rotating BTZ black hole, J. High Energy Phys. 09 (2008) 095.
[59] K. Worden, Aspects of quantum field theory on low-dimensional curved space-times, Ph.D. Thesis, University of Sheffield, 2014.
[60] E. Winstanley and K. Worden (to be published).
[61] G. Dotti and R. J. Gleiser, I. F. Ranea-Sandoval, and H. Vucetich, Gravitational instabilities in Kerr spacetimes, Classical Quantum Gravity **25**, 245012 (2008).
[62] R. Balbinot and E. Poisson, Mass inflation: The semi-classical regime, Phys. Rev. Lett. **70**, 13 (1993).

[63] S. W. Hawking and H. S. Reall, Charged and rotating AdS black holes and their CFT duals, Phys. Rev. D **61**, 024014 (1999).

[64] N. Iizuka, A. Ishibashi, and K. Maeda, A rotating hairy AdS_3 black hole with the metric having only one Killing vector field, J. High Energy Phys. 08 (2015) 112.

[65] R. Emparan, A. Fabbri, and N. Kaloper, Quantum black holes as holograms in AdS braneworlds, J. High Energy Phys. 08 (2002) 043.

[66] R. Emparan, G. Horowitz, and R. Myers, Exact description of black holes on branes, J. High Energy Phys. 01 (2000) 007.

[67] R. Emparan, G. Horowitz, and R. Myers, Exact description of black holes on branes II. Comparison with BTZ black holes and black strings, J. High Energy Phys. 01 (2000) 021.

[68] S. DeDeo and J. R. Gott, III, An Eternal time machine in $(2+1)$-dimensional anti-de Sitter space, Phys. Rev. D **66**, 084020 (2002); Erratum, Phys. Rev. D **67**, 069902(E) (2003).

[69] H. H. Soleng, Inverse square law of gravitation in $(2+1)$ dimensional space-time as a consequence of Casimir energy, Phys. Scr. **48**, 649 (1993).

[70] F. W. J. Olver, *Asymptotics and Special Functions* (Academic Press, New York, 1974).

[71] P. C. W. Davies and V. Sahni, Quantum gravitational effects near cosmic strings, Classical Quantum Gravity **5**, 1 (1988).

[72] I. S. Gradshteyn and I. M. Ryzhik, *Table of Integrals, Series, and Products*, 7th ed. (Academic Press, New York, 2007).